Study of exclusive semileptonic and nonleptonic decays of B_c^- in a nonrelativistic quark model.

E. Hernández,[1] J. Nieves,[2] and J. M. Verde-Velasco[1]

[1] *Grupo de Física Nuclear, Departamento de Física Fundamental e IUFFyM, Facultad de Ciencias, E-37008 Salamanca, Spain.*
[2] *Departamento de Física Atómica, Molecular y Nuclear, Universidad de Granada, E-18071 Granada, Spain.*

We present results for different observables measured in semileptonic and nonleptonic decays of the B_c^- meson. The calculations have been done within the framework of a nonrelativistic constituent quark model. In order to check the sensitivity of all our results against the inter-quark interaction we use five different quark–quark potentials. We obtain form factors, decay widths and asymmetry parameters for semileptonic $B_c^- \to c\bar{c}$ and $B_c^- \to \overline{B}$ decays. In the limit of infinite heavy quark mass our model reproduces the constraints of heavy quark spin symmetry. For the actual heavy quark masses we find nonetheless large corrections to that limiting situation for some form factors. We also analyze exclusive nonleptonic two–meson decay channels within the factorization approximation.

PACS numbers: 12.39.Hg,12.39.Jh,13.20.Fc,13.20.He

I. INTRODUCTION

Since its discovery at Fermilab by the CDF Collaboration [1] the B_c meson has drawn a lot of attention. Unlike other heavy mesons it is composed of two heavy quarks of different flavor (b, c) and, being below the B–D threshold, it can only decay through weak interactions making an ideal system to study weak decays of heavy quarks.

It is known [2] that one can not apply heavy quark symmetry (HQS) to hadrons containing two heavy quarks: the kinetic energy term, needed in those systems to regulate infrared divergences, breaks heavy flavor symmetry. Still, there is a symmetry that survives: heavy quark spin symmetry (HQSS). This symmetry amounts to the decoupling of the two heavy quark spins since the spin–spin interaction vanishes for infinite heavy quark masses. Using HQSS Jenkins *et al.* [2] were able to obtain, in the infinite heavy quark mass limit, relations between different form factors for semileptonic B_c decays into pseudoscalar and vector mesons. Contrary to the heavy-light meson case where standard HQS applies, no determination of corrections in inverse powers of the heavy quark masses has been worked out in this case. So one can only test any model calculation against HQSS predictions in the infinite heavy quark mass limit.

With both quarks being heavy, a nonrelativistic treatment of the B_c meson should provide reliable results. Besides a nonrelativistic model will comply with the constraints imposed by HQSS as the spin–spin interaction vanish in the infinity heavy quark mass limit. In this paper we will study, within the framework of a nonrelativistic quark model, exclusive semileptonic and nonleptonic decays of the B_c^- meson driven by a $b \to c$ or $\bar{c} \to \bar{d}$, $\bar{s}$ transitions at the quark level. We will not consider semileptonic processes driven by the quark $b \to u$ transition. Our experience with this kind of processes, like the analogous $B \to \pi$ semileptonic decay [3], shows that the nonrelativistic model without any improvements underestimates the decay width for two reasons: first at high q^2 transfers one might need to include the exchange of a B^* meson, and second the model underestimates the form factors at low q^2 or high three–momentum transfers. We will concentrate thus on semileptonic $B_c^- \to c\bar{c}$ and $B_c^- \to \overline{B}$ transitions. As for two–meson nonleptonic decay we will only consider channels with a least a $c\bar{c}$ or B final meson. In the first case we will include channels with final D mesons for which there is a contribution coming from an effective $b \to d$, s transition. As later explained this is not the main contribution to the decay amplitude and besides the momentum transfer in those cases is neither too high nor too low so that the problems mentioned above are avoided.

The observables studied here have been analyzed before in the context of different models like the relativistic constituent quark model [4, 5, 6], the quasi-potential approach to the relativistic quark model [7, 8], the instantaneous nonrelativistic approach to the Bethe–Salpeter equation [9, 10, 11], the Bethe–Salpeter equation [12, 13], the three point sum rules of QCD and nonrelativistic QCD [14, 15, 16, 17], the QCD relativistic potential model [18], the relativistic constituent quark model formulated on the light front [19], the relativistic quark–meson model [20] or in models that use the Isgur, Scora, Grinstein and Wise wave functions [21] like the calculations in Refs. [22, 23, 24]. We will compare our results with those obtained in these latter references whenever is possible. Besides, we will perform an exhaustive study and compile in this work all our results for exclusive semileptonic and nonleptonic B_c^- decays, paying an special attention to the theoretical uncertainties affecting our predictions and providing reliable estimates for all of them.

In the present calculation we shall use physical masses taken from Ref. [25]. For the B_c meson mass and lifetime we shall use the central values of the recent experimental determinations by the CDF Collaboration of $m_{B_c} =$

$6285.7 \pm 5.3 \pm 1.2\,\mathrm{MeV}/c^2$ [26] and $\tau_{B_c} = (0.463^{+0.073}_{-0.065} \pm 0.036) \times 10^{-12}\,\mathrm{s}$ [27]. This new mass value is very close to the one we obtain with the different quark-quark potentials that we use in this work (see below) from where we get $m_{B_c} = 6291.6^{+12}_{-33}\,\mathrm{MeV}$.

We shall also need Cabibbo-Kobayashi-Maskawa (CKM) matrix elements and different meson decay constants. For the former we shall use the ones quoted in Ref. [4] that we reproduce in Table I. All of them are within the ranges quoted by the Particle Data Group (PDG) [25].

$\lvert V_{ud}\rvert$	$\lvert V_{us}\rvert$	$\lvert V_{cd}\rvert$	$\lvert V_{cs}\rvert$	$\lvert V_{cb}\rvert$
0.975	0.224	0.224	0.974	0.0413

TABLE I: Values for Cabibbo-Kobayashi-Maskawa matrix elements used in this work.

For the meson decay constants the used values in this work are compiled in Table II. They correspond to central values of experimental measurements or lattice determinations. The results for f_ρ and f_{K^*} have been obtained by the authors in Ref. [4] using τ lepton decay data. Our own theoretical calculation, obtained with the model described in Ref. [28], give $f_\rho = 0.189 \sim 0.227\,\mathrm{GeV}$, $f_{K^*} = 0.180 \sim 0.220\,\mathrm{GeV}$ depending on the inter-quark interaction used, results which agree with the determinations in Ref. [4]. We shall nevertheless use the latter for our calculations. For f_{η_c} we have been unable to find an experimental result or a lattice determination. There are at least two theoretical determinations that predict $f_{\eta_c} = 0.484\,\mathrm{GeV}$ [4] and $f_{\eta_c} = 0.420 \pm 0.052\,\mathrm{GeV}$ [29]. Again our own calculation gives values in the range $f_{\eta_c} = 0.485 \sim 0.500\,\mathrm{GeV}$ depending on the inter-quark interaction used. Here we will take $f_{\eta_c} = 0.490\,\mathrm{GeV}$.

f_{π^-}	f_{π^0}	f_{ρ^-,ρ^0}	f_{K^-,K^0}	$f_{K^{*-},K^{*0}}$
0.1307 [25]	0.130 [25]	0.210 [4]	0.1598 [25]	0.217 [4]

f_{η_c}	$f_{J/\Psi}$
0.490	0.405 [30]

f_{D^-}	$f_{D^{*-}}$	$f_{D_s^-}$	$f_{D_s^{*-}}$
0.2226 [31]	0.245 [32]	0.294 [33]	0.272 [32]

TABLE II: Meson decay constants in GeV used in this work.

The rest of the paper is organized as follows. In Sect. II we introduce our meson states and the potential models used to obtain the spatial part of their wave functions. In Sect. III we study the B_c meson semileptonic decays into various $c\bar{c}$ channels, both for a final light charged lepton (e, μ) and for a heavy one (τ). In Sect. IV we study different exclusive nonleptonic two–meson decay channels of the B_c^- meson with one of the final mesons being a $c\bar{c}$ one. In Sect. V we study semileptonic $B_c^- \to \overline{B}$ decays and in Sect. VI nonleptonic two–meson decays with one of the mesons having a b quark. We briefly summarize our results in Sect. VII. The paper also contains four appendices: in appendix A we give different sets of polarization vectors used in this paper, appendices B and C collect the expressions for all the matrix elements needed to evaluate the different observables analyzed, finally in appendix D we give the expressions for the helicity components of the hadron tensor to be defined below.

II. MESON STATES AND INTER-QUARK INTERACTIONS

Within a nonrelativistic constituent quark model, the state of a meson M is given by

$$\left| M, \lambda\, \vec{P} \right\rangle_{NR} = \int d^3p \sum_{\alpha_1,\alpha_2} \hat{\phi}^{(M,\lambda)}_{\alpha_1,\alpha_2}(\vec{p}) \times \frac{(-1)^{(1/2)-s_2}}{(2\pi)^{3/2}\sqrt{2E_{f_1}(\vec{p}_1)2E_{f_2}(\vec{p}_2)}} \left| q,\ \alpha_1\ \vec{p}_1 = \frac{m_{f_1}}{m_{f_1}+m_{f_2}}\vec{P} - \vec{p} \right\rangle \left| \bar{q},\ \alpha_2\ \vec{p}_2 = \frac{m_{f_2}}{m_{f_1}+m_{f_2}}\vec{P} + \vec{p} \right\rangle \tag{1}$$

where $\vec{P}$ stands for the meson three momentum and λ represents the spin projection in the meson center of mass. α_1 and α_2 represent the quantum numbers of spin s, flavor f and color c ($\alpha \equiv (s, f, c)$), of the quark and the

antiquark, while $(E_{f_1}(\vec{p}_1),\, \vec{p}_1),\ m_{f_1}$ and $(E_{f_2}(\vec{p}_2),\, \vec{p}_2),\ m_{f_2}$ are their respective four–momenta and masses. The factor $(-1)^{(1/2)-s_2}$ is included in order that the antiquark spin states have the correct relative phase[1]. The normalization of the quark and antiquark states is

$$\langle\ \alpha'\ \vec{p}\,'\,|\,\alpha\ \vec{p}\,\rangle = \delta_{\alpha',\alpha}\,(2\pi)^3\,2E_f(\vec{p})\,\delta(\vec{p}\,'-\vec{p}) \tag{2}$$

Furthermore, $\hat{\phi}^{(M,\lambda)}_{\alpha_1,\alpha_2}(\,\vec{p}\,)$ is the momentum space wave function for the relative motion of the quark-antiquark system. Its normalization is given by

$$\int d^3p\ \sum_{\alpha_1\,\alpha_2}\left(\hat{\phi}^{(M,\lambda')}_{\alpha_1,\,\alpha_2}(\,\vec{p}\,)\right)^*\hat{\phi}^{(M,\lambda)}_{\alpha_1,\,\alpha_2}(\,\vec{p}\,) = \delta_{\lambda',\,\lambda} \tag{3}$$

and, thus, the normalization of our meson states is

$$_{NR}\left\langle\ M,\lambda'\,\vec{P}\,'\,|\,M,\lambda\,\vec{P}\,\right\rangle_{NR} = \delta_{\lambda',\,\lambda}\,(2\pi)^3\,\delta(\vec{P}\,'-\vec{P}\,) \tag{4}$$

In this calculation we will need the ground state wave function for scalar (0^+), pseudoscalar(0^-), vector (1^-), axial vector (1^+), tensor (2^+) and pseudotensor (2^-) mesons. Assuming always the lowest possible value for the orbital angular momentum we will have for a meson M with scalar, pseudoscalar and vector quantum numbers:

$$\begin{aligned}
\hat{\phi}^{(M(0^+))}_{\alpha_1,\,\alpha_2}(\,\vec{p}\,) &= \frac{1}{\sqrt{3}}\,\delta_{c_1,\,c_2}\ \hat{\phi}^{(M(0^+))}_{(s_1,\,f_1),\,(s_2,\,f_2)}(\,\vec{p}\,) \\
&= \frac{1}{\sqrt{3}}\,\delta_{c_1,\,c_2}\ i\ \hat{\phi}^{(M(0^+))}_{f_1,\,f_2}(\,|\vec{p}\,|)\sum_m\ (1/2,1/2,1\,;\,s_1,s_2,-m)\ (1,1,0\,;\,m,-m,0)\ Y_{1m}(\,\vec{p}\,) \\
\hat{\phi}^{(M(0^-))}_{\alpha_1,\,\alpha_2}(\,\vec{p}\,) &= \frac{1}{\sqrt{3}}\,\delta_{c_1,\,c_2}\ \hat{\phi}^{(M(0^-))}_{(s_1,\,f_1),\,(s_2,\,f_2)}(\,\vec{p}\,) \\
&= \frac{1}{\sqrt{3}}\,\delta_{c_1,\,c_2}\ (-i)\ \hat{\phi}^{(M(0^-))}_{f_1,\,f_2}(\,|\vec{p}\,|)\ (1/2,1/2,0\,;\,s_1,s_2,0)\ Y_{00}(\,\vec{p}\,) \\
\hat{\phi}^{(M(1^-),\,\lambda)}_{\alpha_1,\,\alpha_2}(\,\vec{p}\,) &= \frac{1}{\sqrt{3}}\,\delta_{c_1,\,c_2}\ \hat{\phi}^{(M(1^-),\,\lambda)}_{(s_1,\,f_1),\,(s_2,\,f_2)}(\,\vec{p}\,) \\
&= \frac{1}{\sqrt{3}}\,\delta_{c_1,\,c_2}\ (-1)\ \hat{\phi}^{(M(1^-))}_{f_1,\,f_2}(\,|\vec{p}\,|)\ (1/2,1/2,1\,;\,s_1,s_2,\lambda)\ Y_{00}(\,\vec{p}\,)
\end{aligned} \tag{5}$$

where $(j_1,j_2,j_3\,;\,m_1,m_2,m_3)$ are Clebsch-Gordan coefficients, $Y_{lm}(\vec{p}\,)$ are spherical harmonics, and $\hat{\phi}^{(M)}_{f_1,\,f_2}(|\,\vec{p}\,|)$ is the Fourier transform of the radial coordinate space wave function.
For axial mesons we need orbital angular momentum $L=1$. In this case two values of the total quark–antiquark spin $S_{q\bar{q}}=0,1$ are possible, giving rise to the two states:

$$\begin{aligned}
\hat{\phi}^{(M(1^+,S_{q\bar{q}}=0),\,\lambda)}_{\alpha_1,\,\alpha_2}(\,\vec{p}\,) &= \frac{1}{\sqrt{3}}\,\delta_{c_1,\,c_2}\ \hat{\phi}^{(M(1^+,S_{q\bar{q}}=0),\,\lambda)}_{(s_1,\,f_1),\,(s_2,\,f_2)}(\,\vec{p}\,) \\
&= \frac{1}{\sqrt{3}}\,\delta_{c_1,\,c_2}\ (-1)\ \hat{\phi}^{(M(1^+,S_{q\bar{q}}=0))}_{f_1,\,f_2}(\,|\vec{p}\,|)\ (1/2,1/2,0;s_1,s_2,0)\ Y_{1\lambda}(\,\vec{p}\,) \\
\hat{\phi}^{(M(1^+,S_{q\bar{q}}=1),\,\lambda)}_{\alpha_1,\,\alpha_2}(\,\vec{p}\,) &= \frac{1}{\sqrt{3}}\,\delta_{c_1,\,c_2}\ \hat{\phi}^{(M(1^+,S_{q\bar{q}}=1),\,\lambda)}_{(s_1,\,f_1),\,(s_2,\,f_2)}(\,\vec{p}\,) \\
&= \frac{1}{\sqrt{3}}\,\delta_{c_1,\,c_2}\ (-1)\ \hat{\phi}^{(M(1^+,S_{q\bar{q}}=1))}_{f_1,\,f_2}(\,|\vec{p}\,|) \\
&\quad\times\sum_m\ (1/2,1/2,1;s_1,s_2,\lambda-m)\ (1,1,1;m,\lambda-m,\lambda)Y_{1m}(\,\vec{p}\,)
\end{aligned} \tag{6}$$

---

[1] Note that under charge conjugation $(\mathcal{C})$ quark and antiquark creation operators are related via $\mathcal{C}\,c^\dagger_\alpha(\vec{p}\,)\,\mathcal{C}^\dagger = (-1)^{(1/2)-s}\,d^\dagger_\alpha(\vec{p}\,)$. This implies that the antiquark states with the correct spin relative phase are not $d^\dagger_\alpha(\vec{p}\,)\,|0\rangle = |\,\bar{q},\ \alpha\ \vec{p}\,\rangle$ but are given instead by $(-1)^{(1/2)-s}\,d^\dagger_\alpha(\vec{p}\,)\,|0\rangle = (-1)^{(1/2)-s}\,|\,\bar{q},\ \alpha\ \vec{p}\,\rangle$.

Finally for tensor and pseudotensor mesons we have the wave functions:

$$\begin{aligned}
\hat{\phi}^{(M(2^+),\,\lambda)}_{\alpha_1,\,\alpha_2}(\,\vec{p}\,) &= \frac{1}{\sqrt{3}}\,\delta_{c_1,\,c_2}\;\hat{\phi}^{(M(2^+),\,\lambda)}_{(s_1,\,f_1),\,(s_2,\,f_2)}(\,\vec{p}\,) \\
&= \frac{1}{\sqrt{3}}\,\delta_{c_1,\,c_2}\;\;\hat{\phi}^{(M(2^+))}_{f_1,\,f_2}(\,|\vec{p}\,|)\;\sum_m\,(1/2,1/2,1;s_1,s_2,\lambda-m)\;(1,1,2;m,\lambda-m,\lambda)\;Y_{1m}(\,\vec{p}\,) \\
\hat{\phi}^{(\,M(2^-),\,\lambda)}_{\alpha_1,\,\alpha_2}(\,\vec{p}\,) &= \frac{1}{\sqrt{3}}\,\delta_{c_1,\,c_2}\;\hat{\phi}^{(M(2^-),\,\lambda)}_{(s_1,\,f_1),\,(s_2,\,f_2)}(\,\vec{p}\,) \\
&= \frac{1}{\sqrt{3}}\,\delta_{c_1,\,c_2}\;(-1)\;\hat{\phi}^{(M(2^-))}_{f_1,\,f_2}(\,|\vec{p}\,|)\;\sum_m\,(1/2,1/2,1;s_1,s_2,\lambda-m)\;(2,1,2;m,\lambda-m,\lambda)Y_{2m}(\,\vec{p}\,) \quad (7)
\end{aligned}$$

All phases have been introduced for later convenience.

To evaluate the coordinate space wave function we use five different inter-quark interactions, one suggested by Bhaduri and collaborators [34], and four others suggested by Silvestre-Brac and Semay [35, 36]. All of them contain a confinement term, plus Coulomb and hyperfine terms coming from one-gluon exchange, and differ from one another in the form factors used for the hyperfine terms, the power of the confining term or the use of a form factor in the one gluon exchange Coulomb potential. All free parameters in the potentials had been adjusted to reproduce the light (π, ρ, K, K^*, etc.) and heavy-light (D, D^*, B, B^*, etc.) meson spectra. These potentials also lead to good results for the charmed and bottom baryon ($\Lambda_{c,b}$, $\Sigma_{c,b}$, $\Sigma^*_{c,b}$, $\Xi_{c,b}$, $\Xi'_{c,b}$, $\Xi^*_{c,b}$, $\Omega_{c,b}$ and $\Omega^*_{c,b}$) masses [35, 37], for the semileptonic $\Lambda_b^0 \to \Lambda_c^+ l^- \bar{\nu}_l$ and $\Xi_b^0 \to \Xi_c^+ l^- \bar{\nu}_l$ decays [38], for the decay constants of pseudoscalar B, D and vector B^*, D^* mesons and the semileptonic $B \to D$ and $B \to D^*$ decays [28], for the $B \to \pi$ semileptonic decay [3] , and for the strong $\Sigma_c \to \Lambda_c\,\pi$, $\Sigma_c^* \to \Lambda_c\,\pi$ and $\Xi_c^* \to \Xi_c\,\pi$ decays [39]. Preliminary results for the spectrum of doubly heavy baryons [40] also show excellent agreement with previous Faddeev calculations and lattice results. For more details on the inter-quark interactions see Ref. [37] or the original works [34, 35, 36].

The use of different inter-quark interactions will provide us with a spread in the results that we will consider, and quote, as a theoretical error added to the value obtained with the AL1 potential or Refs. [35, 36] that we will use to get our central results. Another source of theoretical uncertainty, that we can not account for, is the use of nonrelativistic kinematics in the evaluation of the orbital wave functions and the construction of our states in Eq.(1) above. While this is a very good approximation for the B_c itself it is not that good for mesons with a light quark. That notwithstanding note that any nonrelativistic quark model has free parameters in the inter-quark interaction that are fitted to experimental data. In that sense we think that at least part of the ignored relativistic effects are included in an effective way in their fitted values.

III. SEMILEPTONIC $B_c^- \to c\bar{c}$ DECAYS

In this section we will consider the semileptonic decay of the B_c^- meson into different $c\bar{c}$ states with 0^+, 0^-, 1^+, 1^-, 2^+ and 2^- spin–parity quantum numbers. Those decays correspond to a $b \to c$ transition at the quark level which is governed by the current

$$J^{c\,b}_{\mu}(0) = J^{c\,b}_{V\,\mu}(0) - J^{c\,b}_{A\,\mu}(0) = \overline{\Psi}_c(0)\gamma_\mu(I-\gamma_5)\Psi_b(0) \tag{8}$$

with Ψ_f a quark field of a definite flavor f.

A. Form factor decomposition of hadronic matrix elements

The hadronic matrix elements involved in these processes can be parametrized in terms of a few form factors as

$$\begin{aligned}
\left\langle\, c\bar{c}\,(0^-),\,\vec{P}_{c\bar{c}}\,\middle|\,J^{c\,b}_{\mu}(0)\,\middle|\,B_c,\,\vec{P}_{B_c}\,\right\rangle &= \left\langle\, c\bar{c}\,(0^-),\,\vec{P}_{c\bar{c}}\,\middle|\quad J^{c\,b}_{V\,\mu}(0)\,\middle|\,B_c,\,\vec{P}_{B_c}\,\right\rangle = P_\mu\,F_+(q^2) + q_\mu\,F_-(q^2) \\
\left\langle\, c\bar{c}\,(1^-),\,\lambda\,\vec{P}_{c\bar{c}}\,\middle|\,J^{c\,b}_{\mu}(0)\,\middle|\,B_c,\,\vec{P}_{B_c}\,\right\rangle &= \left\langle\, c\bar{c}\,(1^-),\,\lambda\,\vec{P}_{c\bar{c}}\,\middle|\,J^{c\,b}_{V\,\mu}(0) - J^{c\,b}_{A\,\mu}(0)\,\middle|\,B_c,\,\vec{P}_{B_c}\,\right\rangle \\
&= \frac{-1}{m_{B_c}+m_{c\bar{c}}}\varepsilon_{\mu\nu\alpha\beta}\;\varepsilon^{\nu\,*}_{(\lambda)}(\,\vec{P}_{c\bar{c}}\,)\,P^\alpha\,q^\beta\,V(q^2) \\
&\quad - i\left\{\;(m_{B_c}-m_{c\bar{c}})\;\varepsilon^{*}_{(\lambda)\,\mu}(\,\vec{P}_{c\bar{c}}\,)\,A_0(q^2)\right.
\end{aligned}$$

$$
\begin{aligned}
& & -\frac{P\cdot\varepsilon^{*}_{(\lambda)}(\,\vec{P}_{c\bar{c}}\,)}{m_{B_c}+m_{c\bar{c}}}\left(P_\mu\,A_+(q^2)+q_\mu\,A_-(q^2)\right)\Big\}\\
\Big\langle\, c\bar{c}\,(2^+),\,\lambda\,\vec{P}_{c\bar{c}}\,\Big|\,J^{c\,b}_{\mu}(0)\,\Big|\,B_c,\,\vec{P}_{B_c}\,\Big\rangle &=& \Big\langle\, c\bar{c}\,(2^+),\,\lambda\,\vec{P}_{c\bar{c}}\,\Big|\,J^{c\,b}_{V\,\mu}(0)-J^{c\,b}_{A\mu}(0)\,\Big|\,B_c,\,\vec{P}_{B_c}\,\Big\rangle\\
&=& \varepsilon_{\mu\nu\alpha\beta}\;\varepsilon^{\nu\delta\,*}_{(\lambda)}(\,\vec{P}_{c\bar{c}}\,)P_\delta\,P^\alpha\,q^\beta\,T_4(q^2)\\
& & -i\Big\{\;\varepsilon^{*}_{(\lambda)\,\mu\delta}(\,\vec{P}_{c\bar{c}}\,)P^\delta\,T_1(q^2)\\
& & +P^\nu P^\delta\varepsilon^{*}_{(\lambda)\nu\delta}(\,\vec{P}_{c\bar{c}},\,)\left(P_\mu\,T_2(q^2)+q_\mu\,T_3(q^2)\right)\Big\}
\end{aligned}
\tag{9}
$$

In the above expressions $P=P_{B_c}+P_{c\bar{c}}$, $q=P_{B_c}-P_{c\bar{c}}$, being P_{B_c} and $P_{c\bar{c}}$ the meson four–momenta, m_{B_c} and $m_{c\bar{c}}$ are the meson masses, $\varepsilon^{\mu\nu\alpha\beta}$ is the fully antisymmetric tensor for which we take the convention $\varepsilon^{0123}=+1$, and $\varepsilon_{(\lambda)\mu}(\,\vec{P}\,)$ and $\varepsilon_{(\lambda)\mu\nu}(\,\vec{P}\,)$ are the polarization vector and tensor of vector and tensor mesons respectively[2]. The latter can be evaluated in terms of the former as

$$
\varepsilon^{\mu\nu}_{(\lambda)}(\,\vec{P}\,)=\sum_m(1,1,2\,;\,m,\lambda-m,\lambda)\,\varepsilon^{\mu}_{(m)}(\,\vec{P}\,)\varepsilon^{\nu}_{(\lambda-m)}(\,\vec{P}\,)
\tag{10}
$$

Different sets of $\varepsilon_{(\lambda)}(\,\vec{P}\,)$ used in this work appear in appendix A.

Besides the meson states in the Lorenz decompositions of Eq. (9) are normalized such that

$$
\Big\langle\, M,\lambda'\,\vec{P}\,'\,|\,M,\lambda\,\vec{P}\,\Big\rangle=\delta_{\lambda',\,\lambda}\,(2\pi)^3\,2\,E_M(\vec{P})\delta(\vec{P}\,'-\vec{P}\,)
\tag{11}
$$

being $E_M(\vec{P})$ the energy of the M meson with three–momentum $\vec{P}$. Note the factor $2E_M$ of difference with Eq. (4)

For the 0^+, 1^+ and 2^- cases the form factor decomposition is the same as for the 0^-, 1^- and 2^+ cases respectively, but with $-J^{c\,b}_{A\mu}(0)$ contributing where $J^{c\,b}_{V\,\mu}(0)$ contributed before and vice versa.

The different form factors in Eq.(9) are all relatively real thanks to time–reversal invariance. F_+ , F_-, V, A_0, A_+, A_- and T_1 are dimensionless, whereas T_2, T_3 and T_4 have dimension of E^{-2}. They can be easily evaluated working in the center of mass of the B_c meson and taking $\vec{q}$ in the z direction, so that $\vec{P}_{c\bar{c}}=-\vec{q}=-|\vec{q}|\vec{k}$, with $\vec{k}$ representing the unit vector in the z direction.

1. $B_c^-\to\eta_c\,l^-\,\bar{\nu}_l,\ \chi_{c0}\,l^-\,\bar{\nu}_l$ *decays*

Let us start with the B_c^- decays into pseudoscalar η_c and scalar χ_{c0} $c\bar{c}$ mesons. For $B_c^-\to\eta_c$ transitions the form factors are given by:

$$
\begin{aligned}
F_+(q^2)&=\frac{1}{2m_{B_c}}\left(V^0(|\vec{q}\,|)+\frac{V^3(|\vec{q}\,|)}{|\vec{q}\,|}\;(E_{\eta_c}(-\vec{q})-m_{B_c})\right)\\
F_-(q^2)&=\frac{1}{2m_{B_c}}\left(V^0(|\vec{q}\,|)+\frac{V^3(|\vec{q}\,|)}{|\vec{q}\,|}\;(E_{\eta_c}(-\vec{q})+m_{B_c})\right)
\end{aligned}
\tag{12}
$$

whereas for $B_c\to\chi_{c0}$ transitions we have:

$$
\begin{aligned}
F_+(q^2)&=\frac{-1}{2m_{B_c}}\left(A^0(|\vec{q}\,|)+\frac{A^3(|\vec{q}\,|)}{|\vec{q}\,|}\;(E_{\chi_{c0}}(-\vec{q})-m_{B_c})\right)\\
F_-(q^2)&=\frac{-1}{2m_{B_c}}\left(A^0(|\vec{q}\,|)+\frac{A^3(|\vec{q}\,|)}{|\vec{q}\,|}\;(E_{\chi_{c0}}(-\vec{q})+m_{B_c})\right)
\end{aligned}
\tag{13}
$$

with $V^\mu(|\vec{q}\,|)$ and $A^\mu(|\vec{q}\,|)$ $(\mu=0,3)$ calculated in our model as

$$
\begin{aligned}
V^\mu(|\vec{q}\,|)&=\Big\langle\,\eta_c,\ -|\vec{q}\,|\,\vec{k}\,\Big|\,J^{c\,b\ \mu}_{V}(0)\,\Big|\,B_c^-,\,\vec{0}\Big\rangle=\sqrt{2m_{B_c}2E_{\eta_c}(-\vec{q})}\ \ {}_{NR}\Big\langle\,\eta_c,\ -|\vec{q}\,|\,\vec{k}\,\Big|\,J^{c\,b\ \mu}_{V}(0)\,\Big|\,B_c^-,\,\vec{0}\Big\rangle_{NR}\\
A^\mu(|\vec{q}\,|)&=\Big\langle\,\chi_{c0},\ -|\vec{q}\,|\,\vec{k}\,\Big|\,J^{c\,b\ \mu}_{A}(0)\,\Big|\,B_c^-,\,\vec{0}\Big\rangle=\sqrt{2m_{B_c}2E_{\chi_{c0}}(-\vec{q})}\ \ {}_{NR}\Big\langle\,\chi_{c0},\ -|\vec{q}\,|\,\vec{k}\,\Big|\,J^{c\,b\ \mu}_{A}(0)\,\Big|\,B_c^-,\,\vec{0}\Big\rangle_{NR}
\end{aligned}
\tag{14}
$$

[2] Note we have taken λ to be the third component of the meson spin measured in the meson center of mass.

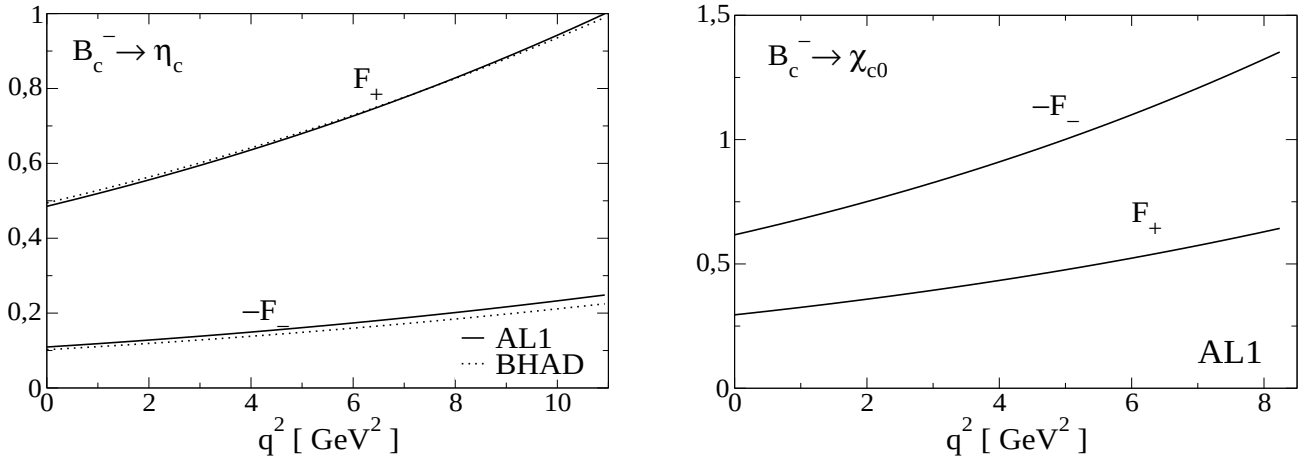

FIG. 1: F_+ and F_- form factors for $B_c^- \to \eta_c$ and $B_c^- \to \chi_{c0}$ semileptonic decay evaluated with the AL1 potential of Refs. [35, 36]. In the first case, and for comparison, we also show with dotted lines the results obtained with the Bhaduri (BHAD) potential of Ref. [34].

which expressions are given in appendix B.

In Fig. 1 we show our results for the F_+ and F_- form factors for the semileptonic $B_c^- \to \eta_c$, χ_{c0} transitions. The minimum q^2 value depends on the actual final lepton and it is given, neglecting neutrino masses, by the lepton mass as $q^2_{min} = m_l^2$. The form factors have been evaluated using the AL1 potential of Refs. [35, 36]. For decays into η_c, and for the sake of comparison, we also show the results obtained with the potential developed by Bhaduri and collaborators in Ref. [34] (BHAD). As seen in the figures the differences between the form factors evaluated with the two inter-quark interactions are smaller than 10%.

In Table III we show F_+ and F_- evaluated at $q^2_{\rm min}$ and $q^2_{\rm max}$ for a final light lepton ($l = e$, μ) and compare them to the ones obtained by Ivanov *et al.* in Ref. [5], and, when available, by Ebert *et al.* in Ref. [7]. For the $B_c \to \eta_c$ transition we also show the corresponding values for the F_0 form factor defined as

$$F_0(q^2) = F_+(q^2) + \frac{q^2}{m^2_{B_c} - m^2_{\eta_c}}\ F_-(q^2) \tag{15}$$

Our results for the η_c case are in excellent agreement with the ones obtained by Ebert *et al.*. Compared to the results by Ivanov *et al.* we find large discrepancies for F_-.

$B_c^- \to \eta_c\, l^-\bar\nu_l$	$q^2_{\rm min}$	$q^2_{\rm max}$
F_+		
This work	$0.49^{+0.01}$	$1.00_{-0.01}$
[5]	0.61	1.14
[7]	0.47	1.07
F_-		
This work	$-0.11^{+0.01}_{-0.01}$	$-0.25^{+0.03}$
[5]	-0.32	-0.61
F_0		
This work	$0.49^{+0.01}$	$0.91^{+0.01}$
[7]	0.47	0.92

$B_c^- \to \chi_{c0}\, l^-\bar\nu_l$	$q^2_{\rm min}$	$q^2_{\rm max}$
F_+		
This work	$0.30^{+0.01}$	$0.64^{+0.01}_{-0.01}$
[5]	0.40	0.65
F_-		
This work	$-0.62^{+0.01}_{-0.03}$	$-1.35^{+0.05}$
[5]	-1.00	-1.63

TABLE III: F_+ and F_- evaluated at $q^2_{\rm min}$ and $q^2_{\rm max}$ compared to the ones obtained by Ivanov *et al.* [5] and Ebert *et al.* Ref. [7]. Our central values have been obtained with the AL1 potential. For the η_c channel we also show F_0 (see text for definition). Here l stands for $l = e$, μ.

2. $B_c^- \to J/\Psi\, l\, \bar{\nu}_l,\ h_c\, l\, \bar{\nu}_l,\ \chi_{c1}\, l\, \bar{\nu}_l$ decays

Let us now see the form factors for the semileptonic B_c^- decays into vector J/Ψ and axial vector h_c ($S_{q\bar{q}}=0$) and χ_{c1} ($S_{q\bar{q}}=1$) $c\bar{c}$ mesons. For the decay into J/Ψ the form factors can be evaluated in terms of matrix elements as:

$$\begin{aligned}
V(q^2) &= \frac{i}{\sqrt{2}}\,\frac{m_{B_c}+m_{J/\Psi}}{m_{B_c}\,|\vec{q}|}\,V^1_{\lambda=-1}(|\vec{q}|)\\
A_+(q^2) &= i\,\frac{m_{B_c}+m_{J/\Psi}}{2m_{B_c}}\,\frac{m_{J/\Psi}}{|\vec{q}|\,m_{B_c}}\Big\{-A^0_{\lambda=0}(|\vec{q}|)+\frac{m_{B_c}-E_{J/\Psi}(-\vec{q})}{|\vec{q}|}\,A^3_{\lambda=0}(|\vec{q}|)\\
&\qquad -\sqrt{2}\,\frac{m_{B_c}E_{J/\Psi}(-\vec{q})-m^2_{J/\Psi}}{|\vec{q}|\,m_{J/\Psi}}\,A^1_{\lambda=-1}(|\vec{q}|)\Big\}\\
A_-(q^2) &= -i\,\frac{m_{B_c}+m_{J/\Psi}}{2m_{B_c}}\,\frac{m_{J/\Psi}}{|\vec{q}|\,m_{B_c}}\Big\{A^0_{\lambda=0}(|\vec{q}|)+\frac{m_{B_c}+E_{J/\Psi}(-\vec{q})}{|\vec{q}|}\,A^3_{\lambda=0}(|\vec{q}|)\\
&\qquad -\sqrt{2}\,\frac{m_{B_c}E_{J/\Psi}(-\vec{q})+m^2_{J/\Psi}}{|\vec{q}|\,m_{J/\Psi}}\,A^1_{\lambda=-1}(|\vec{q}|)\Big\}\\
A_0(q^2) &= -i\sqrt{2}\,\frac{1}{m_{B_c}-m_{J/\Psi}}\,A^1_{\lambda=-1}(|\vec{q}|)
\end{aligned}\tag{16}$$

with $V^\mu_\lambda(|\vec{q}|)$ and $A^\mu_\lambda(|\vec{q}|)$ calculated in our model as

$$\begin{aligned}
V^\mu_\lambda(|\vec{q}|) &= \Big\langle J/\Psi,\ \lambda\ -|\vec{q}|\,\vec{k}\ \Big|\ J_V^{c\,b\ \mu}(0)\ \Big|\ B_c^-,\,\vec{0}\Big\rangle\\
&= \sqrt{2m_{B_c}2E_{J/\Psi}(-\vec{q})}\ {}_{NR}\Big\langle J/\Psi,\ \lambda\ -|\vec{q}|\,\vec{k}\ \Big|\ J_V^{c\,b\ \mu}(0)\ \Big|\ B_c^-,\,\vec{0}\Big\rangle_{NR}\\
A^\mu_\lambda(|\vec{q}|) &= \Big\langle J/\Psi,\ \lambda\ -|\vec{q}|\,\vec{k}\ \Big|\ J_A^{c\,b\ \mu}(0)\ \Big|\ B_c^-,\,\vec{0}\Big\rangle\\
&= \sqrt{2m_{B_c}2E_{J/\Psi}(-\vec{q})}\ {}_{NR}\Big\langle J/\Psi,\ \lambda\ -|\vec{q}|\,\vec{k}\ \Big|\ J_A^{c\,b\ \mu}(0)\ \Big|\ B_c^-,\,\vec{0}\Big\rangle_{NR}
\end{aligned}\tag{17}$$

which expressions are given in appendix B.

The form factors corresponding to transitions to the χ_{c1} and h_c axial vector mesons are obtained from the expressions in Eq.(16) by just changing

$$V^\mu_\lambda(|\vec{q}|) \longleftrightarrow -A^\mu_\lambda(|\vec{q}|)\tag{18}$$

and using the appropriate mass for the final meson. Obviously in Eq. (17) J/Ψ has to be replaced by χ_{c_1} or h_c.

In Table IV we show the result for the different form factors evaluated at $q^2_{\rm min}$ and $q^2_{\rm max}$ for the case where the final lepton is light ($l=e,\,\mu$). For the decay into J/Ψ we also show the combination of form factors[3]:

$$\widetilde{A}_0(q^2) = \frac{m_{B_c}-m_{J/\Psi}}{2m_{J/\Psi}}\left(A_0(q^2)-A_+(q^2)\right)-\frac{q^2}{2m_{J/\Psi}\,(m_{B_c}+m_{J/\Psi})}\,A_-(q^2)\tag{19}$$

Our results for the $B_c \to J/\Psi$ decay channel are in agreement with the ones obtained by Ebert *et al.*. They also agree reasonably well, with the exception of A_-, with the ones obtained by Ivanov *et al.*. For the other two cases the discrepancies are in general large.

All the form factors are depicted in Figs. 2 and 3

[3] This combination is called A_0 by the authors of Ref. [7]

$B_c^- \to J/\Psi\, l^-\bar{\nu}_l$	$q^2_{\rm min}$	$q^2_{\rm max}$	$B_c^- \to h_c\, l^-\bar{\nu}_l$	$q^2_{\rm min}$	$q^2_{\rm max}$	$B_c^- \to \chi_{c1}\, l^-\bar{\nu}_l$	$q^2_{\rm min}$	$q^2_{\rm max}$
V			V			V		
This work	$-0.61_{-0.03}$	$-1.26^{+0.01}$	This work	$-0.040_{-0.003}$	$-0.078_{-0.003}$	This work	$0.92^{+0.04}_{-0.02}$	$1.86_{-0.12}$
[5]	-0.83^*	-1.53^*	[5]	$-0.25^{\ *}$	-0.365^*	[5]	1.18^*	1.81^*
[7]	-0.49	-1.34						
A_+			A_+			A_+		
This work	$0.56^{+0.03}$	$1.13^{+0.01}$	This work	$-0.85^{+0.01}_{-0.05}$	$-1.90^{+0.06}$	This work	$-0.44_{-0.03}$	$-0.78^{+0.04}$
[5]	0.54	0.97	[5]	-1.08	-1.80	[5]	-0.39	-0.50
[7]	0.73	1.33						
A_-			A_-			A_-		
This work	$-0.60_{-0.03}$	$-1.24_{-0.01}$	This work	$0.12^{+0.01}_{-0.02}$	$0.36_{-0.06}$	This work	$0.96^{+0.04}_{-0.01}$	$1.97_{-0.13}$
[5]	-0.95	-1.76	[5]	0.52	0.89	[5]	1.52	2.36
A_0			A_0			A_0		
This work	$1.44^{+0.08}$	$2.58^{+0.01}_{-0.02}$	This work	$0.28^{+0.02}$	$0.52^{+0.02}$	This work	$-0.50_{-0.02}$	$-0.32_{-0.02}$
[5]	1.64	2.50	[5]	0.44	0.54	[5]	-0.064	0.46
[7]	1.47	2.59						
$\widetilde{A}_0$								
This work	$0.45^{+0.03}$	$0.96_{-0.01}$						
[7]	0.40	1.06						

TABLE IV: V, A_+, A_- and A_0 form factors evaluated at $q^2_{\rm min}$ and $q^2_{\rm max}$ compared to the ones obtained by Ivanov *et al.* [5] and Ebert *et al.* Ref. [7]. Our central values have been evaluated with the AL1 potential. For the J/Ψ channel we also show $\widetilde{A}_0$ (see text for definition). Here l stands for $l = e$, μ. The asterisk to the right of a number means we have changed its sign to account for the different choice of $\varepsilon^{\,0\,1\,2\,3}$ in Ref. [5].

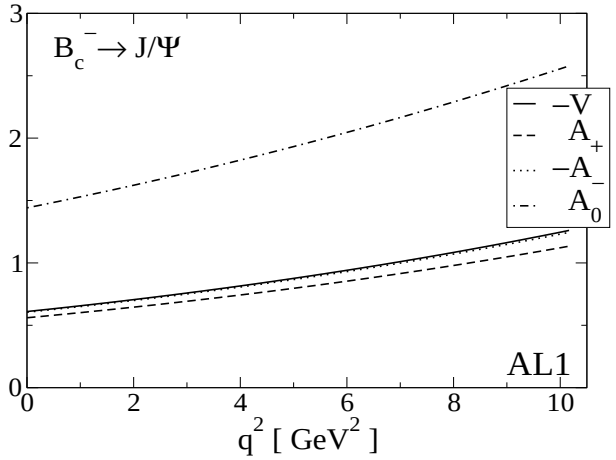

FIG. 2: V (solid line), A_+ (dashed line), A_- (dotted line) and A_0 (dashed-dotted line) form factors for the $B_c^- \to J/\Psi$ semileptonic decay evaluated with the AL1 potential.

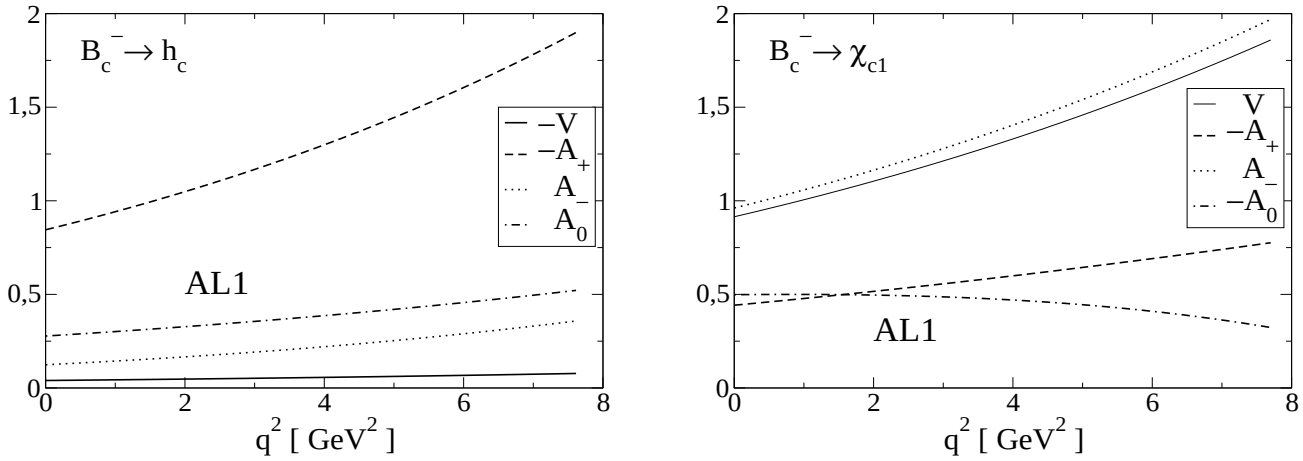

FIG. 3: V (solid line), A_+ (dashed line), A_- (dotted line) and A_0 (dashed-dotted line) form factors for $B_c^- \to h_c$ and $B_c^- \to \chi_{c1}$ semileptonic decay evaluated with the AL1 potential.

3. $B_c^- \to \Psi(3836)\, l\, \bar{\nu}_l,\ \chi_{c2}\, l\, \bar{\nu}_l$, decays

Finally let us see the form factors for the B_c^- decays into tensor χ_{c2} and pseudotensor $\Psi(3836)$ [4] mesons. For the decay into χ_{c2} the form factors can be evaluated in terms of matrix elements as:

$$
\begin{aligned}
T_1(q^2) &= -i\,\frac{2m_{\chi_{c2}}}{m_{B_c}|\vec{q}|}\,A^1_{T\lambda=+1}(|\vec{q}|) \\
T_2(q^2) &= i\,\frac{1}{2m^3_{B_c}}\Bigg\{-\sqrt{\frac{3}{2}}\,\frac{m^2_{\chi_{c2}}}{|\vec{q}|^2}\,A^0_{T\lambda=0}(|\vec{q}|)-\sqrt{\frac{3}{2}}\,\frac{m^2_{\chi_{c2}}}{|\vec{q}|^3}\,(E_{\chi_{c2}}(-\vec{q})-m_{B_c})\,A^3_{T\lambda=0}(|\vec{q}|) \\
&\qquad +\frac{2m_{\chi_{c2}}}{|\vec{q}|}\left(1-\frac{E_{\chi_{c2}}(-\vec{q})}{|\vec{q}|^2}\,(E_{\chi_{c2}}(-\vec{q})-m_{B_c})\right)A^1_{T\lambda=+1}(|\vec{q}|)\Bigg\} \\
T_3(q^2) &= i\,\frac{1}{2m^3_{B_c}}\Bigg\{-\sqrt{\frac{3}{2}}\,\frac{m^2_{\chi_{c2}}}{|\vec{q}|^2}\,A^0_{T\lambda=0}(|\vec{q}|)-\sqrt{\frac{3}{2}}\,\frac{m^2_{\chi_{c2}}}{|\vec{q}|^3}\,(E_{\chi_{c2}}(-\vec{q})+m_{B_c})\,A^3_{T\lambda=0}(|\vec{q}|) \\
&\qquad +\frac{2m_{\chi_{c2}}}{|\vec{q}|}\left(1-\frac{E_{\chi_{c2}}(-\vec{q})}{|\vec{q}|^2}\,(E_{\chi_{c2}}(-\vec{q})+m_{B_c})\right)A^1_{T\lambda=+1}(|\vec{q}|)\Bigg\} \\
T_4(q^2) &= i\,\frac{m_{\chi_{c2}}}{m^2_{B_c}|\vec{q}|^2}\,V^1_{T\lambda=+1}(|\vec{q}|)
\end{aligned}
\tag{20}
$$

with $V^\mu_{T\lambda}(|\vec{q}|)$ and $A^\mu_{T\lambda}(|\vec{q}|)$ calculated in our model as

$$
\begin{aligned}
V^\mu_{T\lambda}(|\vec{q}|) &= \left\langle \chi_{c2},\ \lambda\ -|\vec{q}|\,\vec{k}\ \middle|\ J_V^{c\,b\ \mu}(0)\ \middle|\ B_c^-,\,\vec{0}\right\rangle \\
&= \sqrt{2m_{B_c}2E_{\chi_{c2}}(-\vec{q})}\ {}_{NR}\left\langle \chi_{c2},\ \lambda\ -|\vec{q}|\,\vec{k}\ \middle|\ J_V^{c\,b\ \mu}(0)\ \middle|\ B_c^-,\,\vec{0}\right\rangle_{NR} \\
A^\mu_{T\lambda}(|\vec{q}|) &= \left\langle \chi_{c2},\ \lambda\ -|\vec{q}|\,\vec{k}\ \middle|\ J_A^{c\,b\ \mu}(0)\ \middle|\ B_c^-,\,\vec{0}\right\rangle \\
&= \sqrt{2m_{B_c}2E_{\chi_{c2}}(-\vec{q})}\ {}_{NR}\left\langle \chi_{c2},\ \lambda\ -|\vec{q}|\,\vec{k}\ \middle|\ J_A^{c\,b\ \mu}(0)\ \middle|\ B_c^-,\,\vec{0}\right\rangle_{NR}
\end{aligned}
\tag{21}
$$

[4] Note that while the $\Psi(3836)$ was still quoted in the particle listings of the former Review of Particle Physics [25], it has been excluded from the more recent one [33]. We shall nevertheles keep it in our study to illustrate the results to be expected for a ground state pseudotensor particle.

which expressions are given in appendix B.

The form factors corresponding to transitions to $\Psi(3836)$ are obtained from the expressions in Eq.(20) by just changing

$$V^{\mu}_{T\lambda}(|\vec{q}|) \longleftrightarrow -A^{\mu}_{T\lambda}(|\vec{q}|) \tag{22}$$

and using the appropriate mass for the final meson. Besides in Eq. (21) χ_{c2} has to be replaced by $\Psi(3836)$.

The results for the different form factors appear in Fig. 4. In Table V we show T_1, T_2, T_3 and T_4 evaluated at q^2_{min}

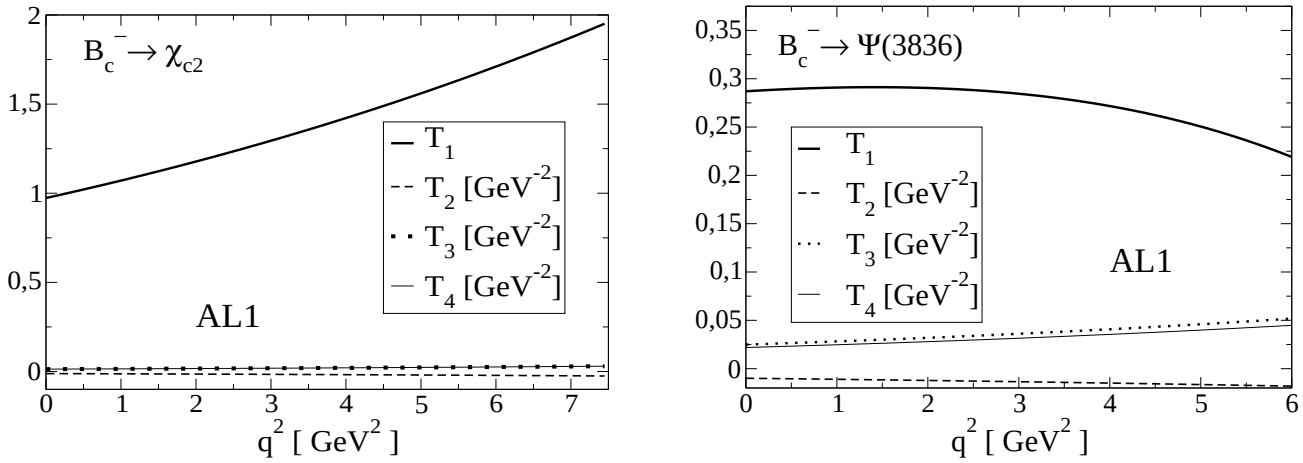

FIG. 4: T_1 (bold solid line), T_2 (dashed line), T_3 (dotted line) and T_4 (thin solid line) form factors for $B_c^- \to \chi_{c2}$ and $B_c^- \to \Psi(3836)$ semileptonic decay evaluated with the AL1 potential.

and q^2_{max} for the case of a final light lepton, and compare them to the values obtained by Ivanov *et al.* [5]. For the $B_c^- \to \chi_{c2}$ transition we find a reasonable agreement between the two calculations. For $B_c^- \to \Psi(3836)$ there is also a reasonable agreement for the absolute values of the form factors but we disagree for some of the signs.

$B_c^- \to \chi_{c2}\, l^- \bar{\nu}_l$	$q^2_{\rm min}$	$q^2_{\rm max}$
T_1		
This work	$0.97^{+0.08}_{-0.01}$	$1.95_{-0.06}$
[5]	1.22	1.69
T_2 $[GeV^{-2}]$		
This work	$-0.012_{-0.001}$	$-0.025^{+0.001}$
[5]	-0.011	-0.018
T_3 $[GeV^{-2}]$		
This work	$0.013^{+0.001}$	$0.030_{-0.001}$
[5]	0.025	0.040
T_4 $[GeV^{-2}]$		
This work	$0.013^{+0.001}$	$0.030_{-0.001}$
[5]	0.021^*	0.033^*

$B_c^- \to \Psi(3836)\, l^- \bar{\nu}_l$	$q^2_{\rm min}$	$q^2_{\rm max}$
T_1		
This work	$0.29_{-0.02}$	$0.22_{-0.01}$
[5]	0.052	0.35
T_2 $[GeV^{-2}]$		
This work	$-0.010^{+0.006}$	$-0.018^{+0.001}$
[5]	0.0071	0.0090
T_3 $[GeV^{-2}]$		
This work	$0.025_{-0.002}$	$0.052_{-0.004}$
[5]	-0.036	-0.052
T_4 $[GeV^{-2}]$		
This work	$0.022_{-0.001}$	$0.045_{-0.003}$
[5]	-0.026^*	-0.038^*

TABLE V: Values for T_1, T_2, T_3 and T_4 evaluated at $q^2_{\rm min}$ and $q^2_{\rm max}$ compared to the ones obtained by Ivanov *et al.* [5]. Here l stands for $l = e$, μ. Asterisk as in Table IV

B. Decay width

For a B_c at rest the double differential decay width with respect to q^2 and x_l, being x_l the cosine of the angle between the final meson momentum and the momentum of the final charged lepton measured in the lepton–neutrino center of mass frame (CMF), is given by[5]

$$\frac{d^2\Gamma}{dq^2 dx_l} = \frac{G_F^2}{64 m_{B_c}^2}\,\frac{|V_{bc}|^2}{8\pi^3}\,\frac{\lambda^{1/2}(q^2, m_{B_c}^2, m_{c\bar{c}}^2)}{2m_{B_c}}\,\frac{q^2 - m_l^2}{q^2}\;\mathcal{H}_{\alpha\,\beta}(P_{B_c}, P_{c\bar{c}})\;\mathcal{L}^{\alpha\,\beta}(p_l, p_\nu) \tag{23}$$

where $G_F = 1.16637(1)\times 10^{-5}\mathrm{GeV}^{-2}$ [25] is the Fermi constant, $\lambda(a,b,c) = (a+b-c)^2 - 4ab$, m_l is the mass of the charged lepton, $\mathcal{H}_{\alpha\,\beta}$ and $\mathcal{L}^{\alpha\,\beta}$ are the hadron and lepton tensors, and $P_{B_c},\ P_{c\bar{c}},\ p_l,\ p_\nu$ are the meson and lepton four–momenta. The lepton tensor is[6]

$$\mathcal{L}^{\alpha\,\beta}(p_l, p_\nu) = 8\left(p_l^\alpha p_\nu^\beta + p_l^\beta p_\nu^\alpha - g^{\alpha\beta} p_l\cdot p_\nu \mp i\,\varepsilon^{\alpha\,\beta\,\sigma\,\rho} p_{l\,\sigma} p_{\nu\,\rho}\right) \tag{24}$$

As for the hadron tensor it is given by

$$\mathcal{H}_{\alpha\,\beta}(P_{B_c}, P_{c\bar{c}}) \;=\; \sum_\lambda\; h_{(\lambda)\,\alpha}(P_{B_c}, P_{c\bar{c}})\, h^*_{(\lambda)\,\beta}(P_{B_c}, P_{c\bar{c}}) \tag{25}$$

with

$$h_{(\lambda)\,\alpha}(P_{B_c}, P_{c\bar{c}}) = \left\langle c\bar{c},\ \lambda\,\vec{P}_{c\bar{c}}|J_\alpha^{cb}(0)|B_c,\ \vec{P}_{B_c}\right\rangle \tag{26}$$

The quantity

$$\mathcal{H}_{\alpha\,\beta}(P_{B_c}, P_{c\bar{c}})\;\mathcal{L}^{\alpha\,\beta}(p_l, p_\nu) \tag{27}$$

is a scalar and to evaluate it we can choose $\vec{P}_{c\bar{c}}$ along the negative z-axis. This implies also that the CMF of the final leptons moves in the positive z-direction. Furthermore we shall follow Ref. [5] and introduce helicity components for the hadron and lepton tensors. For that purpose we rewrite

$$\mathcal{H}_{\alpha\,\beta}(P_{B_c}, P_{c\bar{c}})\;\mathcal{L}^{\alpha\,\beta}(p_l, p_\nu) = \mathcal{H}^{\sigma\,\rho}(P_{B_c}, P_{c\bar{c}})\;g_{\sigma\alpha}\,g_{\rho\beta}\;\mathcal{L}^{\alpha\,\beta}(p_l, p_\nu) \tag{28}$$

and use [41]

$$g_{\mu\nu} = \sum_{r=t,\pm1,0} g_{rr}\;\varepsilon_{(r)\,\mu}(q)\,\varepsilon^*_{(r)\,\nu}(q) \quad ; \quad g_{tt} = 1, g_{\pm1,0} = -1 \tag{29}$$

with $\varepsilon^\mu_{(t)}(q) = q^\mu/q^2$ and where the $\varepsilon_{(r)}(q)$, $r = \pm1,\,0$ are the polarization vectors for an on–shell vector particle with four–momentum q and helicity r. Defining helicity components for the hadron and lepton tensors as

$$\begin{aligned}\mathcal{H}_{r\,s}(P_{B_c}, P_{c\bar{c}}) \;&=\; \varepsilon^*_{(r)\,\sigma}(q)\,\mathcal{H}^{\sigma\,\rho}(P_{B_c}, P_{c\bar{c}})\,\varepsilon_{(s)\,\rho}(q)\\ \mathcal{L}_{r\,s}(p_l, p_\nu) \;&=\; \varepsilon_{(r)\,\alpha}(q)\,\mathcal{L}^{\alpha\,\beta}(p_l, p_\nu)\,\varepsilon^*_{(s)\,\beta}(q)\end{aligned} \tag{30}$$

we have that

$$\mathcal{H}_{\alpha\,\beta}(P_{B_c}, P_{c\bar{c}})\;\mathcal{L}^{\alpha\,\beta}(p_l, p_\nu) = \sum_{r=t,\pm1,0}\;\sum_{s=t,\pm1,0}\; g_{rr}\,g_{ss}\;\mathcal{H}_{r\,s}(P_{B_c}, P_{c\bar{c}})\;\mathcal{L}_{r\,s}(p_l, p_\nu) \tag{31}$$

Let us start with the lepton tensor. We can take advantage of the fact that the Wigner rotation relating the original frame and the CMF of the final leptons is the identity to evaluate the lepton tensor helicity components in this latter reference system

$$\mathcal{L}_{r\,s}(p_l, p_\nu) \;=\; \varepsilon_{(r)\,\alpha}(q)\,\mathcal{L}^{\alpha\,\beta}(p_l, p_\nu)\,\varepsilon^*_{(s)\,\beta}(q) = \varepsilon_{(r)\,\alpha}(\widetilde{q})\,\mathcal{L}^{\alpha,\beta}(\widetilde{p}_l, \widetilde{p}_\nu)\,\varepsilon^*_{(s)\,\beta}(\widetilde{q}) \tag{32}$$

---

[5] We shall neglect neutrino masses in the calculation.

[6] The $\mp$ signs correspond respectively to decays into $l^-\bar{\nu}_l$ (for B_c^- decays) and $l^+\nu_l$ (for B_c^+ decays)

were the tilde stands for momenta measured in the final leptons CMF. For the purpose of evaluation we can use[7]

$$\begin{aligned}\widetilde{p}_l^{\,\alpha} &= (E_l(|\widetilde{p}_l|), -|\widetilde{p}_l|\,\sqrt{1-x_l^2}, 0, -|\widetilde{p}_l|\,x_l)\\ \widetilde{p}_\nu^{\,\alpha} &= (|\widetilde{p}_l|, |\widetilde{p}_l|\,\sqrt{1-x_l^2}, 0, |\widetilde{p}_l|\,x_l)\end{aligned} \tag{33}$$

with $|\widetilde{p}_l|$ the modulus of the lepton three-momentum measured in the leptons CMF.

The only helicity components that we shall need are the following.

$$\begin{aligned}\mathcal{L}_{t\,t}(p_l,p_\nu) &= 4\frac{m_l^2(q^2-m_l^2)}{q^2}\\ \mathcal{L}_{t\,0}(p_l,p_\nu) &= \mathcal{L}_{0\,t}(p_l,p_\nu) = -4x_l\frac{m_l^2(q^2-m_l^2)}{q^2}\\ \mathcal{L}_{+1\,+1}(p_l,p_\nu) &= (q^2-m_l^2)\,\left(4(1\pm x_l) - 2(1-x_l^2)\frac{q^2-m_l^2}{q^2}\right)\\ \mathcal{L}_{-1\,-1}(p_l,p_\nu) &= (q^2-m_l^2)\,\left(4(1\mp x_l) - 2(1-x_l^2)\frac{q^2-m_l^2}{q^2}\right)\\ \mathcal{L}_{0\,0}(p_l,p_\nu) &= 4(q^2-m_l^2)\,\left(1 - x_l^2\frac{q^2-m_l^2}{q^2}\right)\end{aligned} \tag{34}$$

As for the hadron tensor it is convenient to introduce helicity amplitudes defined as

$$h_{(\lambda)\,r}(P_{B_c},P_{c\bar{c}}) = \varepsilon^*_{(r)\,\alpha}(q)\;h^\alpha_{(\lambda)}(P_{B_c},P_{c\bar{c}}) \quad , \quad r=t,\,\pm1,\,0 \tag{35}$$

in terms of which

$$\mathcal{H}_{r\,s}(P_{B_c},P_{c\bar{c}}) = \sum_\lambda h_{(\lambda)\,r}(P_{B_c},P_{c\bar{c}})\,h^*_{(\lambda)\,s}(P_{B_c},P_{c\bar{c}}) \tag{36}$$

We now give the expressions for the helicity amplitudes evaluated in the original frame.

- Case $0^-\to 0^-,0^+$.

$$\begin{aligned}h_t(P_{B_c},P_{c\bar{c}}) &= \frac{m^2_{B_c}-m^2_{c\bar{c}}}{\sqrt{q^2}}\,F_+(q^2) + \sqrt{q^2}\,F_-(q^2)\\ h_0(P_{B_c},P_{c\bar{c}}) &= \frac{\lambda^{1/2}(q^2,m^2_{B_c},m^2_{c\bar{c}})}{\sqrt{q^2}}\,F_+(q^2)\\ h_{+1}(P_{B_c},P_{c\bar{c}}) &= h_{-1}(P_{B_c},P_{c\bar{c}}) = 0\end{aligned} \tag{37}$$

- Case $0^-\to 1^-,1^+$.

$$\begin{aligned}h_{(\lambda)\,t}(P_{B_c},P_{c\bar{c}}) &= i\delta_{\lambda\,0}\,\frac{\lambda^{1/2}(q^2,m^2_{B_c},m^2_{c\bar{c}})}{2m_{c\bar{c}}\sqrt{q^2}}\,\left((m_{B_c}-m_{c\bar{c}})\,\big(A_0(q^2)-A_+(q^2)\big) - \frac{q^2}{m_{B_c}+m_{c\bar{c}}}A_-(q^2)\right)\\ h_{(\lambda)\,+1}(P_{B_c},P_{c\bar{c}}) &= -i\delta_{\lambda\,-1}\,\left(\frac{\lambda^{1/2}(q^2,m^2_{B_c},m^2_{c\bar{c}})}{m_{B_c}+m_{c\bar{c}}}\,V(q^2) + (m_{B_c}-m_{c\bar{c}})\,A_0(q^2)\right)\\ h_{(\lambda)\,-1}(P_{B_c},P_{c\bar{c}}) &= -i\delta_{\lambda\,+1}\,\left(-\frac{\lambda^{1/2}(q^2,m^2_{B_c},m^2_{c\bar{c}})}{m_{B_c}+m_{c\bar{c}}}\,V(q^2) + (m_{B_c}-m_{c\bar{c}})\,A_0(q^2)\right)\\ h_{(\lambda)\,0}(P_{B_c},P_{c\bar{c}}) &= i\delta_{\lambda\,0}\,\left((m_{B_c}-m_{c\bar{c}})\frac{m^2_{B_c}-q^2-m^2_{c\bar{c}}}{2m_{c\bar{c}}\sqrt{q^2}}\,A_0(q^2) - \frac{\lambda(q^2,m^2_{B_c},m^2_{c\bar{c}})}{2m_{c\bar{c}}\sqrt{q^2}}\,\frac{A_+(q^2)}{m_{B_c}+m_{c\bar{c}}}\right)\end{aligned} \tag{38}$$

---

[7] Note this is in accordance with the definition of x_l and the fact that we have taken $\vec{P}_{c\bar{c}}$ in the negative z direction. Furthermore there can be no dependence on the φ_l azimuthal angle so that we can take $\widetilde{\vec{p}}_l$, and then $\widetilde{\vec{p}}_\nu$, in the OXZ plane.

- Case $0^- \to 2^-, 2^+$.

$$
\begin{aligned}
h_{(\lambda)\,t}(P_{B_c}, P_{c\bar{c}}) &= -i\delta_{\lambda\,0}\sqrt{\frac{2}{3}}\,\frac{\lambda(q^2, m_{B_c}^2, m_{c\bar{c}}^2)}{4\,m_{c\bar{c}}^2\,\sqrt{q^2}}\,\left(T_1(q^2) + (m_{B_c}^2 - m_{c\bar{c}}^2)\,T_2(q^2) + q^2\,T_3(q^2)\right) \\
h_{(\lambda)\,+1}(P_{B_c}, P_{c\bar{c}}) &= i\delta_{\lambda\,-1}\,\frac{1}{\sqrt{2}}\,\frac{\lambda^{1/2}(q^2, m_{B_c}^2, m_{c\bar{c}}^2)}{2\,m_{c\bar{c}}}\,\left(T_1(q^2) - \lambda^{1/2}(q^2, m_{B_c}^2, m_{c\bar{c}}^2)\,T_4(q^2)\right) \\
h_{(\lambda)\,-1}(P_{B_c}, P_{c\bar{c}}) &= i\delta_{\lambda\,+1}\,\frac{1}{\sqrt{2}}\,\frac{\lambda^{1/2}(q^2, m_{B_c}^2, m_{c\bar{c}}^2)}{2\,m_{c\bar{c}}}\,\left(T_1(q^2) + \lambda^{1/2}(q^2, m_{B_c}^2, m_{c\bar{c}}^2)\,T_4(q^2)\right) \\
h_{(\lambda)\,0}(P_{B_c}, P_{c\bar{c}}) &= -i\delta_{\lambda\,0}\sqrt{\frac{2}{3}}\,\frac{\lambda^{1/2}(q^2, m_{B_c}^2, m_{c\bar{c}}^2)}{4\,m_{c\bar{c}}^2\,\sqrt{q^2}}\,\left((m_{B_c}^2 - q^2 - m_{c\bar{c}}^2)\,T_1(q^2) + \lambda(q^2, m_{B_c}^2, m_{c\bar{c}}^2)\,T_2(q^2)\right)
\end{aligned}
\tag{39}
$$

We see that the helicity amplitudes, and thus the helicity components of the hadron tensor, only depend on q^2. The expressions for the latter are collected in appendix D.

We can now define the combinations [5]

$$
\begin{aligned}
H_U &= \mathcal{H}_{+1\,+1} + \mathcal{H}_{-1\,-1} \\
H_L &= \mathcal{H}_{0\,0} \\
H_P &= \mathcal{H}_{+1\,+1} - \mathcal{H}_{-1\,-1} \\
H_S &= 3\,\mathcal{H}_{t\,t} \\
H_{SL} &= \mathcal{H}_{t\,0} \\
\widetilde{H}_J &= \frac{m_l^2}{2\,q^2}\,H_J \quad ; \quad J = U, L, S, SL
\end{aligned}
\tag{40}
$$

with U, L, P, S, SL representing respectively unpolarized–transverse, longitudinal, parity–odd, scalar and scalar–longitudinal interference.

Finally the double differential decay width is written in terms of the above defined combinations as

$$
\begin{aligned}
\frac{d^2\Gamma}{dq^2 dx_l} &= \frac{G_F^2}{8\pi^3}\,|V_{bc}|^2\,\frac{(q^2 - m_l^2)^2}{12 m_{B_c}^2 q^2}\,\frac{\lambda^{1/2}(q^2, m_{B_c}^2, m_{c\bar{c}}^2)}{2 m_{B_c}}\,\Big\{\,\frac{3}{8}(1 + x_l^2)\,H_U + \frac{3}{4}(1 - x_l^2)\,H_L \pm \frac{3}{4}x_l H_P \\
&\qquad + \frac{3}{4}(1 - x_l^2)\widetilde{H}_U + \frac{3}{2}x_l^2\,\widetilde{H}_L + \frac{1}{2}\widetilde{H}_S + 3x_l\widetilde{H}_{SL}\Big\}
\end{aligned}
\tag{41}
$$

Note that for antiparticle decay H_P has the opposite sign to the case of particle decay while all other hadron tensor helicity components combinations defined in Eq.(40) do not change (See appendix C for details). The sign change of H_P compensates the extra sign coming from the lepton tensor. This means that in fact the double differential decay width is the same for B_c^- or B_c^+ decay.

Integrating over x_l we obtain the differential decay width

$$
\frac{d\Gamma}{dq^2} = \frac{G_F^2}{8\pi^3}\,|V_{bc}|^2\,\frac{(q^2 - m_l^2)^2}{12 m_{B_c}^2 q^2}\,\frac{\lambda^{1/2}(q^2, m_{B_c}^2, m_{c\bar{c}}^2)}{2 m_{B_c}}\,\Big\{\,H_U + H_L + \widetilde{H}_U + \widetilde{H}_L + \widetilde{H}_S\Big\}
\tag{42}
$$

from where, integrating over q^2, we obtain the total decay width that we write, following Ref. [5], as

$$
\Gamma = \Gamma_U + \Gamma_L + \widetilde{\Gamma}_U + \widetilde{\Gamma}_L + \widetilde{\Gamma}_S
\tag{43}
$$

with Γ_J and $\widetilde{\Gamma}_J$ partial helicity widths defined as

$$
\Gamma_J = \int dq^2 \frac{G_F^2}{8\pi^3}\,|V_{bc}|^2\,\frac{(q^2 - m_l^2)^2}{12 m_{B_c}^2 q^2}\,\frac{\lambda^{1/2}(q^2, m_{B_c}^2, m_{c\bar{c}}^2)}{2 m_{B_c}}\,H_J
\tag{44}
$$

and similarly for $\widetilde{\Gamma}_J$ in terms of $\widetilde{H}_J$.

$B_c^- \to$	Γ_U	$\widetilde{\Gamma}_U$	Γ_L	$\widetilde{\Gamma}_L$	Γ_P	$\widetilde{\Gamma}_S$	$\widetilde{\Gamma}_{SL}$
$\eta_c\, e^-\bar{\nu}_e$	0	0	$6.95^{+0.31}$	$0.13^{+0.01}\ 10^{-5}$	0	$0.44^{+0.03}\ 10^{-5}$	$0.14^{+0.01}\ 10^{-5}$
$\eta_c\, \mu^-\bar{\nu}_\mu$	0	0	$6.80^{+0.31}$	$0.28^{+0.02}\ 10^{-1}$	0	$0.10^{+0.01}$	$0.31^{+0.01}\ 10^{-1}$
$\eta_c\, \tau^-\bar{\nu}_\tau$	0	0	$0.71^{+0.02}$	$0.17^{+0.01}$	0	$1.58^{+0.04}$	$0.29^{+0.01}$
$\chi_{c0}\, e^-\bar{\nu}_e$	0	0	$1.55^{+0.14}_{-0.02}$	$0.37^{+0.05}\ 10^{-6}$	0	$0.11^{+0.01}\ 10^{-5}$	$0.37^{+0.05}\ 10^{-6}$
$\chi_{c0}\, \mu^-\bar{\nu}_\mu$	0	0	$1.51^{+0.13}_{-0.02}$	$0.75^{+0.09}\ 10^{-2}$	0	$0.23^{+0.02}\ 10^{-1}$	$0.75^{+0.09}\ 10^{-2}$
$\chi_{c0}\, \tau^-\bar{\nu}_\tau$	0	0	$0.80^{+0.04}_{-0.02}\ 10^{-1}$	$0.23^{+0.01}_{-0.01}\ 10^{-1}$	0	$0.84^{+0.07}\ 10^{-1}$	$0.25^{+0.02}\ 10^{-1}$
$J/\Psi\, e^-\bar{\nu}_e$	$11.5^{+0.6}$	$0.32^{+0.02}\ 10^{-6}$	$10.4^{+0.6}$	$0.12^{+0.01}\ 10^{-5}$	$-5.48_{-0.24}$	$0.32^{+0.03}\ 10^{-5}$	$0.11^{+0.01}\ 10^{-5}$
$J/\Psi\, \mu^-\bar{\nu}_\mu$	$11.4^{+0.6}$	$0.13^{+0.01}\ 10^{-1}$	$10.2^{+0.7}$	$0.28^{+0.03}\ 10^{-1}$	$-5.45_{-0.24}$	$0.68^{+0.07}\ 10^{-1}$	$0.25^{+0.02}\ 10^{-1}$
$J/\Psi\, \tau^-\bar{\nu}_\tau$	$2.78^{+0.10}_{-0.01}$	$0.59^{+0.02}$	$1.74^{+0.07}_{-0.01}$	$0.39^{+0.02}$	$-1.10_{-0.03}$	$0.36^{+0.02}$	$0.21^{+0.01}$
$\chi_{c1}\, e^-\bar{\nu}_e$	$0.90^{+0.05}_{-0.03}$	$0.43^{+0.03}_{-0.01}\ 10^{-7}$	$0.35^{+0.03}\ 10^{-1}$	$0.28^{+0.03}\ 10^{-8}$	$-0.75^{+0.02}_{-0.04}$	$0.57^{+0.07}\ 10^{-8}$	$0.22^{+0.02}\ 10^{-8}$
$\chi_{c1}\, \mu^-\bar{\nu}_\mu$	$0.89^{+0.05}_{-0.03}$	$0.18^{+0.01}_{-0.01}\ 10^{-2}$	$0.35^{+0.03}\ 10^{-1}$	$0.77^{+0.08}\ 10^{-4}$	$-0.75^{+0.02}_{-0.04}$	$0.11^{+0.01}\ 10^{-3}$	$0.49^{+0.05}\ 10^{-4}$
$\chi_{c1}\, \tau^-\bar{\nu}_\tau$	$0.75^{+0.02}\ 10^{-1}$	$0.21^{+0.01}\ 10^{-1}$	$0.46^{+0.04}\ 10^{-2}$	$0.12^{+0.01}\ 10^{-2}$	$-0.64_{-0.03}\ 10^{-1}$	$0.23^{+0.02}\ 10^{-3}$	$0.28^{+0.02}\ 10^{-3}$
$h_c\, e^-\bar{\nu}_e$	$0.16^{+0.02}$	$0.57^{+0.07}\ 10^{-8}$	$2.23^{+0.12}$	$0.72^{+0.09}\ 10^{-6}$	$-0.26_{-0.03}\ 10^{-1}$	$0.23^{+0.03}\ 10^{-5}$	$0.74^{+0.09}\ 10^{-6}$
$h_c\, \mu^-\bar{\nu}_\mu$	$0.16^{+0.02}$	$0.24^{+0.03}\ 10^{-3}$	$2.16^{+0.21}_{-0.01}$	$0.14^{+0.01}\ 10^{-1}$	$-0.26_{-0.03}\ 10^{-1}$	$0.45^{+0.05}_{-0.01}\ 10^{-1}$	$0.14^{+0.02}\ 10^{-1}$
$h_c\, \tau^-\bar{\nu}_\tau$	$0.23^{+0.02}\ 10^{-1}$	$0.60^{+0.06}\ 10^{-2}$	$0.67^{+0.05}\ 10^{-1}$	$0.20^{+0.01}\ 10^{-1}$	$-0.27_{-0.03}\ 10^{-2}$	$0.97^{+0.05}_{-0.03}\ 10^{-1}$	$0.26^{+0.02}_{-0.01}\ 10^{-1}$
$\chi_{c2}\, e^-\bar{\nu}_e$	$0.71^{+0.03}_{-0.03}$	$0.37^{+0.02}_{-0.02}\ 10^{-7}$	$1.17^{+0.08}_{-0.05}$	$0.31^{+0.03}_{-0.01}\ 10^{-6}$	$-0.35^{+0.01}_{-0.02}$	$0.88^{+0.09}_{-0.03}\ 10^{-6}$	$0.30^{+0.03}_{-0.01}\ 10^{-6}$
$\chi_{c2}\, \mu^-\bar{\nu}_\mu$	$0.71^{+0.02}_{-0.03}$	$0.15^{+0.01}\ 10^{-2}$	$1.14^{+0.07}_{-0.05}$	$0.62^{+0.06}_{-0.02}\ 10^{-2}$	$-0.34^{+0.01}_{-0.02}$	$0.16^{+0.02}\ 10^{-1}$	$0.57^{+0.06}_{-0.02}\ 10^{-2}$
$\chi_{c2}\, \tau^-\bar{\nu}_\tau$	$0.49^{+0.01}_{-0.03}\ 10^{-1}$	$0.15_{-0.01}\ 10^{-1}$	$0.43^{+0.01}_{-0.02}\ 10^{-1}$	$0.13_{-0.01}\ 10^{-1}$	$-0.18^{+0.01}\ 10^{-1}$	$0.12_{-0.01}\ 10^{-1}$	$0.70^{+0.02}_{-0.04}\ 10^{-2}$
$\Psi(3836)\, e^-\bar{\nu}_e$	$0.58_{-0.07}\ 10^{-1}$	$0.47_{-0.06}\ 10^{-8}$	$0.33^{+0.01}_{-0.02}\ 10^{-2}$	$0.68^{+0.04}_{-0.04}\ 10^{-9}$	$-0.48^{+0.05}\ 10^{-1}$	$0.17^{+0.01}_{-0.01}\ 10^{-8}$	$0.60^{+0.03}_{-0.04}\ 10^{-9}$
$\Psi(3836)\, \mu^-\bar{\nu}_\mu$	$0.57_{-0.06}\ 10^{-1}$	$0.19_{-0.02}\ 10^{-3}$	$0.32^{+0.01}_{-0.02}\ 10^{-2}$	$0.15_{-0.01}\ 10^{-4}$	$-0.48^{+0.06}\ 10^{-1}$	$0.28^{+0.02}_{-0.02}\ 10^{-4}$	$0.11^{+0.01}\ 10^{-4}$
$\Psi(3836)\, \tau^-\bar{\nu}_\tau$	$0.78_{-0.09}\ 10^{-3}$	$0.28_{-0.03}\ 10^{-3}$	$0.74_{-0.06}\ 10^{-4}$	$0.25_{-0.02}\ 10^{-4}$	$-0.69^{+0.08}\ 10^{-3}$	$0.54_{-0.04}\ 10^{-5}$	$0.65_{-0.05}\ 10^{-5}$

TABLE VI: Partial helicity widths in units of $10^{-15}\,$GeV for B_c^- decays. Central values have been evaluated with the AL1 potential.

Another quantity of interest is the forward-backward asymmetry of the charged lepton measured in the leptons CMF. This asymmetry is defined as[8]

$$A_{FB} = \frac{\Gamma_{x_l>0} - \Gamma_{x_l<0}}{\Gamma_{x_l>0} + \Gamma_{x_l<0}} \tag{45}$$

and it is given in terms or partial helicity widths as

$$= \frac{3}{4}\,\frac{\pm\Gamma_P + 4\,\widetilde{\Gamma}_{SL}}{\Gamma_U + \Gamma_L + \widetilde{\Gamma}_U + \widetilde{\Gamma}_L + \widetilde{\Gamma}_S} \tag{46}$$

being the same for a negative charged lepton l^- (B_c^- decay) than for a positive charged one l^+ (B_c^+ decay), as Γ_P for antiparticle decay has the opposite sign as for particle decay.

Finally for the decay channel $B_c \to J/\Psi\, l\bar{\nu}_l$ with the J/Ψ decaying into $\mu^-\mu^+$ we can evaluate the differential cross section

$$\frac{d\Gamma_{B_c\to\mu^-\mu^+(J/\Psi)\,l\bar{\nu}_l}}{dx_\mu} = \left(1 + \frac{\sqrt{1-4m_\mu^2/m_{J/\Psi}^2}\left(\Gamma_U + \widetilde{\Gamma}_U - 2(\Gamma_L + \widetilde{\Gamma}_L + \widetilde{\Gamma}_S)\right)}{\left(2 - \sqrt{1-4m_\mu^2/m_{J/\Psi}^2}\right)\left(\Gamma_U + \widetilde{\Gamma}_U\right) + 2\left(\Gamma_L + \widetilde{\Gamma}_L + \widetilde{\Gamma}_S\right)}\, x_\mu^2\right)$$

[8] The forward direction is determined by the momentum of the final meson that we have chosen in the negative z-direction.

		$A_{FB}(e)$	$A_{FB}(\mu)$	$A_{FB}(\tau)$	$\alpha^*(e)$	$\alpha^*(\mu)$	$\alpha^*(\tau)$
$B_c \to \eta_c$							
	This work	$0.60^{+0.01}\ 10^{-6}$	$0.13^{+0.01}\ 10^{-1}$	0.35			
	[5]	$0.953\ 10^{-6}$		0.36			
$B_c \to \chi_{c0}$							
	This work	$0.72^{+0.02}\ 10^{-6}$	$0.15\ 10^{-1}$	0.40			
	[5]	$1.31\ 10^{-6}$		0.39			
$B_c \to J/\Psi$							
	This work	-0.19	$-0.18_{-0.01}$	$-0.35^{+0.02}\ 10^{-1}$	$-0.29_{-0.01}$	-0.29	-0.19
	[5]	-0.21		$-0.48\ 10^{-1}$	-0.34		-0.24
$B_c \to \chi_{c1}$							
	This work	$-0.60_{-0.01}$	$-0.60_{-0.01}$	-0.46			
	[5]	0.19		0.34			
$B_c \to h_c$							
	This work	$-0.83_{-0.05}\ 10^{-2}$	$0.97^{+0.01}_{-0.05}\ 10^{-2}$	0.35			
	[5]	$-3.6\ 10^{-2}$		0.31			
$B_c \to \chi_{c2}$							
	This work	-0.14	-0.13	$0.55^{+0.02}\ 10^{-1}$			
	[5]	-0.16		$0.44\ 10^{-1}$			
$B_c \to \Psi(3836)$							
	This work	-0.59	-0.59	-0.42			
	[5]	0.21		0.41			

TABLE VII: Asymmetry parameters in semileptonic $B_c \to c\bar{c}$ decays. Our central values have been evaluated with the AL1 potential. We also show the results obtained by Ivanov *et al.* [5].

$$\times \frac{\Gamma_{J/\Psi\to\mu^-\mu^+}}{\Gamma_{J/\Psi}} \frac{1}{1+2m_\mu^2/m_{J/\Psi}^2}\Bigg[\frac{3}{4}\left(\Gamma_L+\widetilde{\Gamma}_L+\widetilde{\Gamma}_S\right) + \frac{3}{8}\left(2-\sqrt{1-4m_\mu^2/m_{J/\Psi}^2}\ \right)\left(\Gamma_U+\widetilde{\Gamma}_U\right)\Bigg] \tag{47}$$

where x_μ is the cosine of the polar angle for the final $\mu^-\mu^+$ pair, relative to the momentum of the decaying J/Ψ, measured in the $\mu^-\mu^+$ CMF, $\Gamma_{J/\Psi\to\mu^-\mu^+}$ is the J/Ψ decay width into the $\mu^-\mu^+$ channel, and $\Gamma_{J/\Psi}$ is the total J/Ψ decay width. The asymmetry parameter

$$\alpha^* = \frac{\sqrt{1-4m_\mu^2/m_{J/\Psi}^2}\left(\Gamma_U+\widetilde{\Gamma}_U-2(\Gamma_L+\widetilde{\Gamma}_L+\widetilde{\Gamma}_S)\right)}{\left(2-\sqrt{1-4m_\mu^2/m_{J/\Psi}^2}\ \right)\left(\Gamma_U+\widetilde{\Gamma}_U\right)+2\left(\Gamma_L+\widetilde{\Gamma}_L+\widetilde{\Gamma}_S\right)} \tag{48}$$

governs the muons angular distribution in their CMF.

1. *Results*

In Table VI we give our results for the partial helicity widths corresponding to B_c^- decays. For B_c^+ decay the "P" column changes sign while all others remain the same. The central values have been evaluated with the AL1 potential and the theoretical errors quoted reflect the dependence of the results on the inter-quark potential.

In Table VII we show the asymmetry parameters. Our values for α^* compare well with the results obtained in Ref. [5]. The same is true for the forward–backward asymmetry with some exceptions: most notably we get opposite signs for $B_c \to \chi_{c1}$ and $B_c \to \Psi(3836)$.

In Fig. 5 we show the differential decay width $d\Gamma/dq^2$ for the decay channels $\eta_c l^- \bar{\nu}_l$ and $\chi_{c0} l^- \bar{\nu}_l$ for the case where the final lepton is a light one $l = e, \mu$[9] or a heavy one $l = \tau$. We show the results obtained with the AL1 and BHAD

[9] We show the distribution corresponding to a final electron. The distribution for a final muon differs from the former only for q^2 around m_μ^2

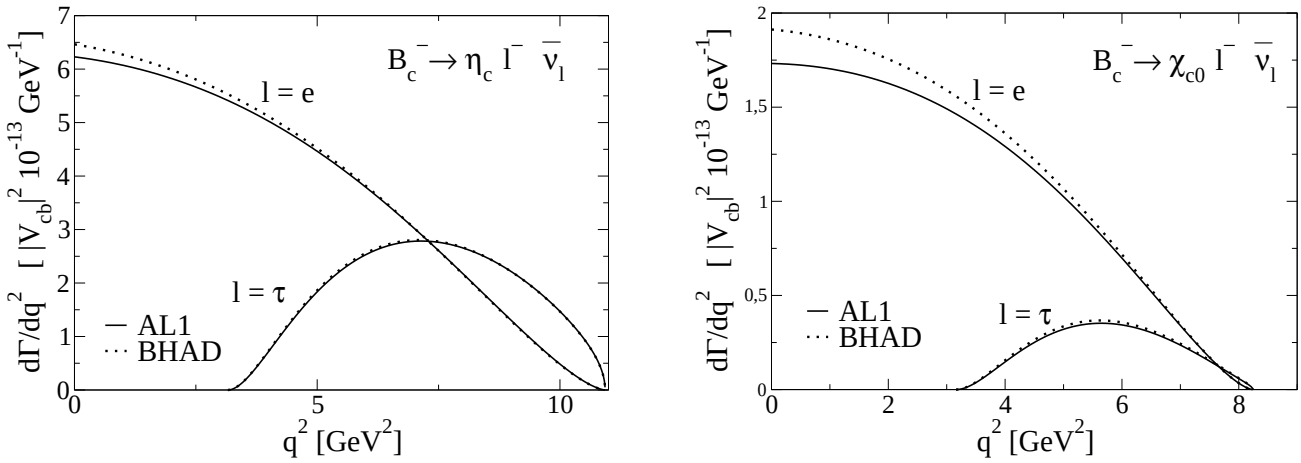

FIG. 5: Differential decay width for the $B_c^- \to \eta_c l^- \bar{\nu}_l$ and $B_c^- \to \chi_{c0} l^- \bar{\nu}_l$ processes obtained with the AL1 potential. For comparison, we also show with dotted lines the results obtained with the Bhaduri (BHAD) potential. The distribution for a final muon is not explicitly shown. It differs appreciably from the corresponding to a final electron only for q^2 around m_μ^2.

	Γ [10^{-15} GeV]									
	This work	[5]	[7]	[9, 10]	[12]	[13]	[14]	[18]	[19]	[22]
$B_c^- \to \eta_c\, l^-\, \bar{\nu}_l$	$6.95^{+0.29}$	10.7	5.9	14.2	11.1	8.31	11 ± 1	2.1 (6.9)	8.6	10
$B_c^- \to \eta_c\, \tau^-\, \bar{\nu}_\tau$	$2.46^{+0.07}$	3.52							3.3 ± 0.9	
$B_c^- \to \chi_{c0}\, l^-\, \bar{\nu}_l$	$1.55^{+0.14}_{-0.02}$	2.52		1.69						
$B_c^- \to \chi_{c0}\, \tau^-\, \bar{\nu}_\tau$	$0.19^{+0.01}$	0.26		0.25						
$B_c^- \to J/\Psi\, l^-\, \bar{\nu}_l$	$21.9^{+1.2}$	28.2	17.7	34.4	30.2	20.3	28 ± 5	21.6 (48.3)	17.2	42
$B_c^- \to J/\Psi\, \tau^-\, \bar{\nu}_\tau$	$5.86^{+0.23}_{-0.03}$	7.82							7 ± 2	
$B_c^- \to \chi_{c1}\, l^-\, \bar{\nu}_l$	$0.94^{+0.05}_{-0.03}$	1.40		2.21						
$B_c^- \to \chi_{c1}\, \tau^-\, \bar{\nu}_\tau$	0.10	0.17		0.35						
$B_c^- \to h_c\, l^-\, \bar{\nu}_l$	$2.40^{+0.23}_{-0.01}$	4.42		2.51						
$B_c^- \to h_c\, \tau^-\, \bar{\nu}_\tau$	$0.21^{+0.01}$	0.38		0.36						
$B_c^- \to \chi_{c2}\, l^-\, \bar{\nu}_l$	$1.89^{+0.11}_{-0.08}$	2.92		2.73						
$B_c^- \to \chi_{c2}\, \tau^-\, \bar{\nu}_\tau$	$0.13^{+0.01}_{-0.01}$	0.20		0.42						
$B_c^- \to \Psi(3836)\, l^-\, \bar{\nu}_l$	$0.062_{-0.008}$	0.13								
$B_c^- \to \Psi(3836)\, \tau^-\, \bar{\nu}_\tau$	$0.0012_{-0.0002}$	0.0031								

TABLE VIII: Decay widths in units of 10^{-15} GeV for semileptonic $B_c^- \to c\bar{c}$ decays. Our central values have been evaluated with the AL1 potential. Here l stands for $l = e,\, \mu$.

potentials, finding no significant difference for the τ case, while for the light final lepton case the differences are around 10% at low q^2.

In Fig. 6 we show now the results for vector and tensor mesons. As before only for the case where the final lepton is light we see up to 10% differences between the calculation with the AL1 and the BHAD potentials.

Finally in Tables VIII, IX we give the total decay widths and corresponding branching ratios for the different transitions. The branching ratios evaluated by Ivanov *et al.* [4], where they have used the new B_c mass determination by the CDF Collaboration [26], are in reasonable agreement with our results. Discrepancies are larger for the decay widths in Table VIII where they use the larger mass value $m_{B_c} = 6400\,\text{MeV}$ quoted by the PDG [25].

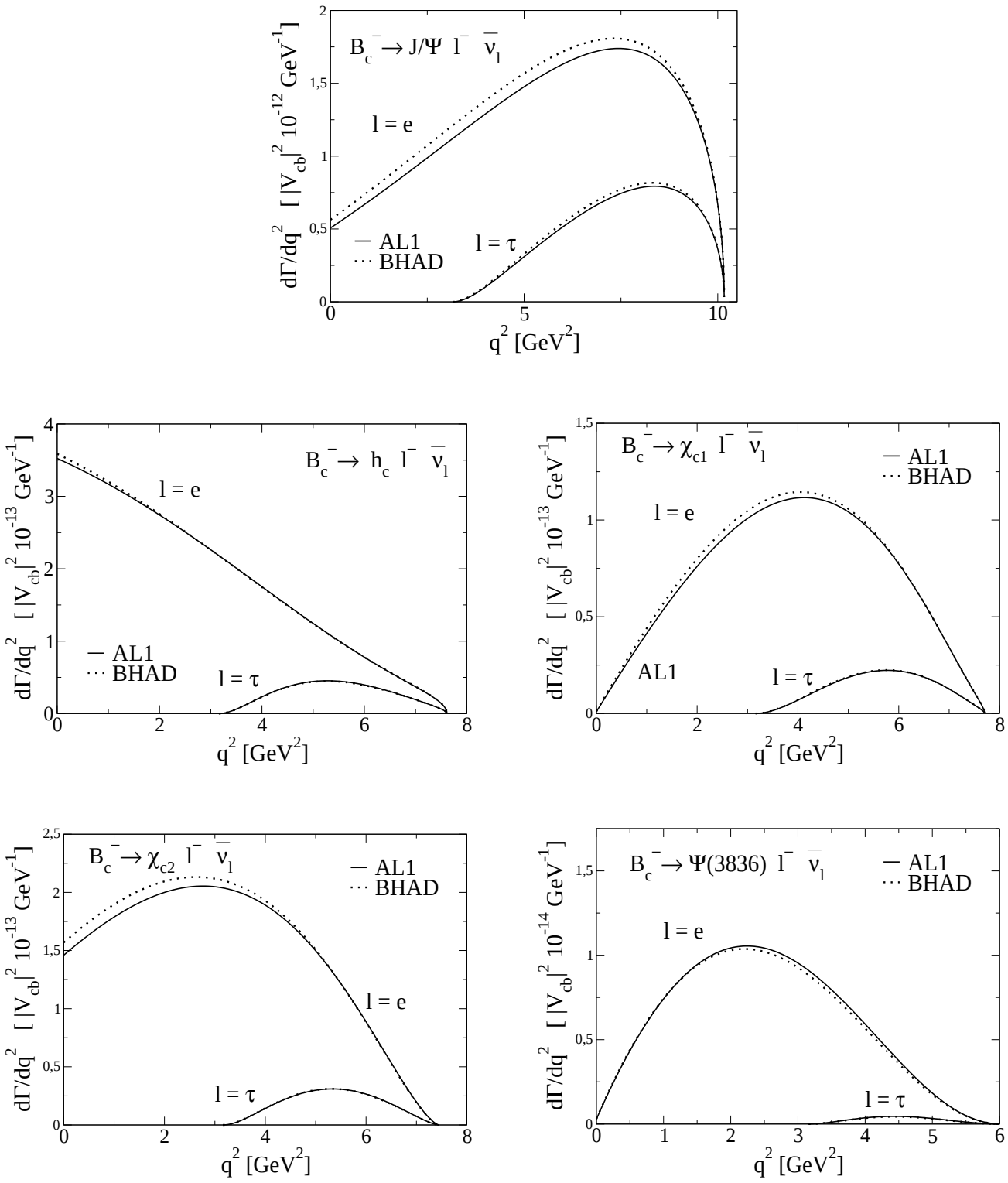

FIG. 6: Differential decay width for the $B_c^- \to J/\Psi l^- \bar{\nu}_l$, $B_c^- \to h_c l^- \bar{\nu}_l$, $B_c^- \to \chi_{c1} l^- \bar{\nu}_l$, $B_c^- \to \chi_{c2} l^- \bar{\nu}_l$ and $B_c^- \to \Psi(3836) l^- \bar{\nu}_l$ decay channels obtained with the AL1 potential (solid lines) and the Bhaduri (BHAD) potential (dotted lines) . The distribution for a final muon is not explicitly shown. It differs appreciably from the corresponding to a final electron only for q^2 around m_μ^2.

B.R. (%)

	This work	[4]	[7]	[9, 10, 11]	[12]	[15, 16]	[18]	[19]	[20]
$B_c^- \to \eta_c\, l^-\, \bar{\nu}_l$	$0.48^{+0.02}$	0.81	0.42	0.97	0.76	0.75	0.15	0.59	0.51
$B_c^- \to \eta_c\, \tau^-\, \bar{\nu}_\tau$	$0.17^{+0.01}$	0.22				0.23		0.20	
$B_c^- \to \chi_{c0}\, l^-\, \bar{\nu}_l$	$0.11^{+0.01}$	0.17		0.12					
$B_c^- \to \chi_{c0}\, \tau^-\, \bar{\nu}_\tau$	$0.013^{+0.001}$	0.013		0.017					
$B_c^- \to J/\Psi\, l^-\, \bar{\nu}_l$	$1.54^{+0.06}$	2.07	1.23	2.35	2.01	1.9	1.47	1.20	1.44
$B_c^- \to J/\Psi\, \tau^-\, \bar{\nu}_\tau$	$0.41^{+0.02}$	0.49				0.48		0.34	
$B_c^- \to \chi_{c1}\, l^-\, \bar{\nu}_l$	$0.066^{+0.003}_{-0.002}$	0.092		0.15					
$B_c^- \to \chi_{c1}\, \tau^-\, \bar{\nu}_\tau$	$0.0072^{+0.0002}_{-0.0003}$	0.0089		0.024					
$B_c^- \to h_c\, l^-\, \bar{\nu}_l$	$0.17^{+0.02}$	0.27		0.17					
$B_c^- \to h_c\, \tau^-\, \bar{\nu}_\tau$	$0.015^{+0.001}$	0.017		0.024					
$B_c^- \to \chi_{c2}\, l^-\, \bar{\nu}_l$	$0.13^{+0.01}$	0.17		0.19					
$B_c^- \to \chi_{c2}\, \tau^-\, \bar{\nu}_\tau$	$0.0093^{+0.0002}_{-0.0005}$	0.0082		0.029					
$B_c^- \to \Psi(3836)\, l^-\, \bar{\nu}_l$	$0.0043_{-0.0005}$	0.0066							
$B_c^- \to \Psi(3836)\, \tau^-\, \bar{\nu}_\tau$	$0.000083_{-0.000010}$	0.000099							

TABLE IX: Branching ratios in % for semileptonic $B_c^- \to c\bar{c}$ decays. Our central values have been evaluated with the AL1 potential. Here l stands for $l = e,\, \mu$.

C. Heavy quark spin symmetry

As mentioned in the Introduction one can not apply HQS to systems with two heavy quarks due to flavor symmetry breaking by the kinetic energy terms. The symmetry that survives for such systems is HQSS amounting to the decoupling of the two heavy quark spins. Using HQSS Jenkins *et al.* [2] obtained relations between different form factors for semileptonic B_c decays into ground state vector and pseudoscalar mesons. Let us check the agreement of our calculations with their results. For that purpose let us re-write the general form factor decompositions in Eq. (9) introducing the four vectors v and k such that

$$P_{B_c} = m_{B_c}\, v \quad ; \quad P_{c\bar{c}} = m_{c\bar{c}}\, v + k \tag{49}$$

v is the four-velocity of the initial B_c meson whereas k is a residual momentum. In terms of those we have

$$P = P_{B_c} + P_{c\bar{c}} = (m_{B_c} + m_{c\bar{c}})\, v + k \quad ; \quad q = P_{B_c} - P_{c\bar{c}} = (m_{B_c} - m_{c\bar{c}})\, v - k \tag{50}$$

and we can write for the $\eta_c\,(c\bar{c}\,(0^-))$ final state case

$$\begin{aligned}
\left\langle \eta_c,\, \vec{P}_{\eta_c} \,\middle|\, J_\mu^{c\,b}(0) \,\middle|\, B_c^-,\, \vec{P}_{B_c} \right\rangle &= \left\langle \eta_c,\, \vec{P}_{\eta_c} \,\middle|\, J_{V\,\mu}^{c\,b}(0) \,\middle|\, B_c^-,\, \vec{P}_{B_c} \right\rangle \\
&= \left((m_{B_c} + m_{\eta_c})\, F_+(q^2) + (m_{B_c} - m_{\eta_c})\, F_-(q^2) \right)\, v_\mu + (F_+(q^2) - F_-(q^2))\, k_\mu \\
&= \sqrt{2m_{B_c} 2m_{\eta_c}} \left(\Sigma_1^{(0^-)}(q^2)\, v_\mu + \overline{\Sigma}_2^{(0^-)}(q^2)\, k_\mu \right)
\end{aligned} \tag{51}$$

where we have introduced the new form factors

$$\begin{aligned}
\Sigma_1^{(0^-)}(q^2) &= \frac{1}{\sqrt{2m_{B_c} 2m_{\eta_c}}} \left((m_{B_c} + m_{\eta_c})\, F_+(q^2) + (m_{B_c} - m_{\eta_c})\, F_-(q^2) \right) \\
\overline{\Sigma}_2^{(0^-)}(q^2) &= \frac{1}{\sqrt{2m_{B_c} 2m_{\eta_c}}} \left(F_+(q^2) - F_-(q^2) \right)
\end{aligned} \tag{52}$$

Similarly for the $J/\Psi\,(c\bar{c}\,(1^-))$ final state case we have

$$\left\langle J/\Psi,\, \lambda\, \vec{P}_{J/\Psi} \,\middle|\, J_\mu^{c\,b}(0) \,\middle|\, B_c^-,\, \vec{P}_{B_c} \right\rangle = \left\langle J/\Psi,\, \lambda\, \vec{P}_{J/\Psi} \,\middle|\, J_{V\,\mu}^{c\,b}(0) - J_{A\mu}^{c\,b}(0) \,\middle|\, B_c^-,\, \vec{P}_{B_c} \right\rangle$$

$$
\begin{aligned}
&= \frac{2m_{B_c}}{m_{B_c}+m_{J/\Psi}}\varepsilon_{\mu\nu\alpha\beta}\,\varepsilon^{\nu *}_{(\lambda)}(\,\vec{P}_{J/\Psi}\,)\,v^{\alpha}\,k^{\beta}\,V(q^2)\\
&\quad - i\Big\{\,(m_{B_c}-m_{J/\Psi})\,\varepsilon^{*}_{(\lambda)\,\mu}(\,\vec{P}_{J/\Psi}\,)\,A_0(q^2)\\
&\qquad + \frac{m_{B_c}}{m_{J/\Psi}}k\cdot\varepsilon^{*}_{(\lambda)}(\,\vec{P}_{J/\Psi}\,)\Big(\,\frac{A_+(q^2)}{m_{B_c}+m_{J/\Psi}}\left((m_{B_c}+m_{J/\Psi})\,v_\mu+k_\mu\right)\\
&\qquad\qquad + \frac{A_-(q^2)}{m_{B_c}+m_{J/\Psi}}\left((m_{B_c}-m_{J/\Psi})\,v_\mu-k_\mu\right)\Big)\Big\}\\
&= -\sqrt{2m_{B_c}2m_{J/\Psi}}\,\varepsilon_{\mu\nu\alpha\beta}\,\varepsilon^{\nu *}_{(\lambda)}(\,\vec{P}_{J/\Psi}\,)\,v^{\alpha}\,k^{\beta}\,\overline{\Sigma}_2^{\prime(1^-)}(q^2)\\
&\quad -i\sqrt{2m_{B_c}2m_{J/\Psi}}\Big\{\,\varepsilon^{*}_{(\lambda)\,\mu}(\,\vec{P}_{J/\Psi}\,)\,\Sigma_1^{(1^-)}(q^2)\\
&\qquad\qquad + \Big(k\cdot\varepsilon^{*}_{(\lambda)}(\,\vec{P}_{J/\Psi}\,)\Big)\,\overline{\Sigma}_2^{(1^-)}(q^2)\,v_\mu\\
&\qquad\qquad + \Big(k\cdot\varepsilon^{*}_{(\lambda)}(\,\vec{P}_{J/\Psi}\,)\Big)\,\overline{\Sigma}_3^{(1^-)}(q^2)\,k_\mu\Big\}
\end{aligned}
\tag{53}
$$

with

$$
\begin{aligned}
\Sigma_1^{(1^-)}(q^2) &= \frac{1}{\sqrt{2m_{B_c}2m_{J/\Psi}}}\,\left(m_{B_c}-m_{J/\Psi}\right)\,A_0(q^2)\\
\overline{\Sigma}_2^{(1^-)}(q^2) &= \frac{1}{\sqrt{2m_{B_c}2m_{J/\Psi}}}\,\frac{m_{B_c}}{m_{J/\Psi}}\,\left(A_+(q^2)+\frac{m_{B_c}-m_{J/\Psi}}{m_{B_c}+m_{J/\Psi}}\,A_-(q^2)\right)\\
\overline{\Sigma}_2^{\prime(1^-)}(q^2) &= \frac{1}{\sqrt{2m_{B_c}2m_{J/\Psi}}}\,\frac{-2m_{B_c}}{m_{B_c}+m_{J/\Psi}}\,V(q^2)\\
\overline{\Sigma}_3^{(1^-)}(q^2) &= \frac{1}{\sqrt{2m_{B_c}2m_{J/\Psi}}}\,\frac{m_{B_c}}{m_{J/\Psi}}\,\frac{1}{m_{B_c}+m_{J/\Psi}}\,\left(A_+(q^2)-A_-(q^2)\right)
\end{aligned}
\tag{54}
$$

$\Sigma_1^{(0^-)}$ and $\Sigma_1^{(1^-)}$ are dimensionless, $\overline{\Sigma}_2^{(0^-)}$, $\overline{\Sigma}_2^{(1^-)}$, $\overline{\Sigma}_2^{\prime(1^-)}$ have dimensions of E^{-1}, and $\overline{\Sigma}_3^{(1^-)}$ has dimensions of E^{-2}.

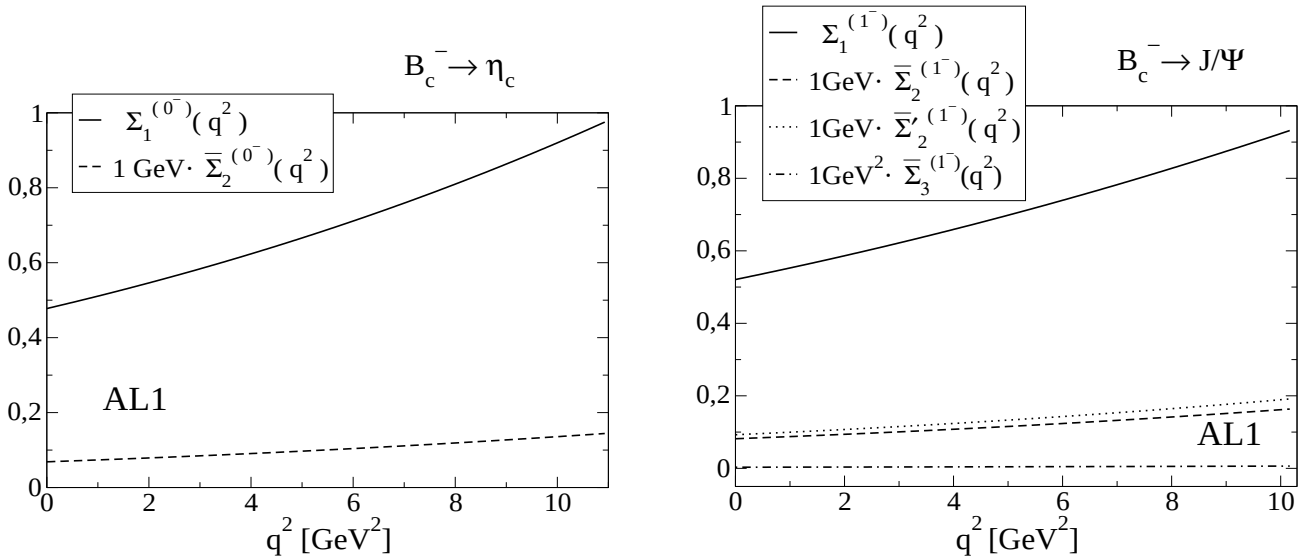

FIG. 7: $\Sigma_1^{(0^-)}$ (solid line) and $\overline{\Sigma}_2^{(0^-)}$ (dashed line) of the $B_c^- \to \eta_c$, and $\Sigma_1^{(1^-)}$ (solid line), $\overline{\Sigma}_2^{(1^-)}$ (dashed line), $\overline{\Sigma}_2^{\prime(1^-)}$ (dotted line) and $\overline{\Sigma}_3^{(1^-)}$ (dashed–dotted line) of the $B_c^- \to J/\Psi$ semileptonic decays evaluated with the AL1 potential.

We can take the infinite heavy quark mass limit $m_b \gg m_c \gg \Lambda_{QCD}$ with the result that near zero recoil

$$\Sigma_1^{(0^-)} = \Sigma_1^{(1^-)}$$

$$\overline{\Sigma}_2^{(0^-)} = \overline{\Sigma}_2^{(1^-)} = \overline{\Sigma}_2^{\prime(1^-)} = 0$$
$$\overline{\Sigma}_3^{(1^-)} = 0 \tag{55}$$

This agrees perfectly with the result obtained in Ref. [2] using HQSS[10].

In Fig. 7 we give our results for the above quantities for the semileptonic $B_c^- \to \eta_c$ and $B_c^- \to J/\Psi$ decays for the actual heavy quark masses. Even though we are not in the infinite heavy quark mass limit we find that $\Sigma_1^{(0^-)}$ and $\Sigma_1^{(1^-)}$ dominate over the whole q^2 interval. This dominant behavior would be more so near the zero–recoil point where $k \approx 0$ and thus the contributions from the terms in $\overline{\Sigma}_2^{(0^-)}$, $\overline{\Sigma}_2^{(1^-)}$, $\overline{\Sigma}_2^{\prime(1^-)}$ and $\overline{\Sigma}_3^{(1^-)}$ are even more suppressed. Thus, even for the actual heavy quark masses we find that near zero recoil

$$\left\langle \eta_c,\, \vec{P}_{\eta_c} \,\middle|\, J_\mu^{c\,b}(0) \,\middle|\, B_c^-,\, \vec{P}_{B_c} \right\rangle \;\approx\; \sqrt{2m_{B_c} 2m_{\eta_c}}\; \Sigma_1^{(0^-)}(q^2)\, v_\mu$$
$$\left\langle J/\Psi,\, \lambda\, \vec{P}_{J/\Psi} \,\middle|\, J_\mu^{c\,b}(0) \,\middle|\, B_c^-,\, \vec{P}_{B_c} \right\rangle \;\approx\; -i\sqrt{2m_{B_c} 2m_{J/\Psi}}\; \varepsilon^*_{(\lambda)\,\mu}(\,\vec{P}_{J/\Psi}\,)\, \Sigma_1^{(1^-)}(q^2) \tag{56}$$

Besides, as seen in In Fig. 8, $\Sigma_1^{(0^-)}$ of the $B_c^- \to \eta_c$, and $\Sigma_1^{(1^-)}$ of the $B_c^- \to J/\Psi$ semileptonic decays are very close to each other over the whole q^2 interval. This implies that the result obtained in Ref. [2] near zero recoil using HQSS seems to be valid, to a very good approximation, outside the infinite heavy quark mass limit.

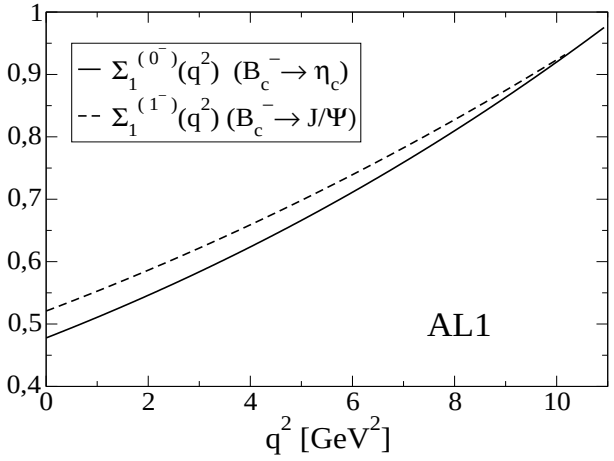

FIG. 8: $\Sigma_1^{(0^-)}$ (solid line) of the $B_c^- \to \eta_c$, and $\Sigma_1^{(1^-)}$ (dashed line) of the $B_c^- \to J/\Psi$ semileptonic decays evaluated with the AL1 potential.

IV. NONLEPTONIC $B_c^- \to c\bar{c}\; M_F^-$ TWO–MESON DECAYS.

In this section we will evaluate decay widths for nonleptonic $B_c^- \to c\bar{c}\; M_F^-$ two–meson decays where M_F^- is a pseudoscalar or vector meson. These decay modes involve a $b \to c$ transition at the quark level and they are governed, neglecting penguin operators, by the effective Hamiltonian [4, 7, 18]

$$H_{eff.} = \frac{G_F}{\sqrt{2}}\, \left\{ V_{cb} \left[c_1(\mu)\, Q_1^{cb} + c_2(\mu)\, Q_2^{cb} \right] + H.c. \right\} \tag{57}$$

where c_1, c_2 are scale–dependent Wilson coefficients, and Q_1^{cb}, Q_2^{cb} are local four–quark operators given by

$$Q_1^{cb} \;=\; \overline{\Psi}_c(0)\gamma_\mu(I-\gamma_5)\Psi_b(0) \Big[\; V_{ud}^*\, \overline{\Psi}_d(0)\gamma^\mu(I-\gamma_5)\Psi_u(0) + V_{us}^*\, \overline{\Psi}_s(0)\gamma^\mu(I-\gamma_5)\Psi_u(0)$$

[10] Note, however, the different global phases and notation used in Ref. [2].

$$
\begin{aligned}
& & +V_{cd}^{*}\,\overline{\Psi}_d(0)\gamma^\mu(I-\gamma_5)\Psi_c(0) + V_{cs}^{*}\,\overline{\Psi}_s(0)\gamma^\mu(I-\gamma_5)\Psi_c(0)\Big] \\
Q_2^{cb} &=& \overline{\Psi}_d(0)\gamma_\mu(I-\gamma_5)\Psi_b(0)\Big[\, V_{ud}^{*}\,\overline{\Psi}_c(0)\gamma^\mu(I-\gamma_5)\Psi_u(0) + V_{cd}^{*}\,\overline{\Psi}_c(0)\gamma^\mu(I-\gamma_5)\Psi_c(0)\Big] \\
& & +\overline{\Psi}_s(0)\gamma_\mu(I-\gamma_5)\Psi_b(0)\Big[V_{us}^{*}\,\overline{\Psi}_c(0)\gamma^\mu(I-\gamma_5)\Psi_u(0) + V_{cs}^{*}\,\overline{\Psi}_c(0)\gamma^\mu(I-\gamma_5)\Psi_c(0)\Big]
\end{aligned}
\tag{58}
$$

where the different V_{jk} are CKM matrix elements.

We shall work in the factorization approximation which amounts to evaluate the hadron matrix elements of the effective Hamiltonian as a product of quark–current matrix elements: one of these is the matrix element for the B_c^- transition to one of the final mesons, while the other matrix element corresponds to the transition from the vacuum to the other final meson. The latter is given by the corresponding meson decay constant. This factorization approximation is schematically represented in Fig. 9.

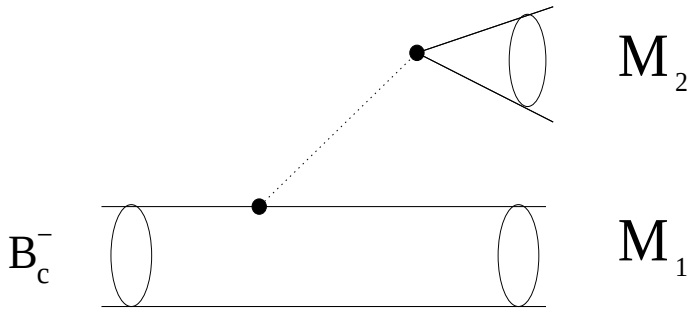

FIG. 9: Diagrammatic representation of B_c^- two–meson decay in the factorization approximation.

When writing the factorization amplitude one has to take into account the Fierz reordered contribution so that the relevant coefficients are not c_1 and c_2 but the combinations

$$
a_1(\mu) = c_1(\mu) + \frac{1}{N_C}\,c_2(\mu) \quad ; \quad a_2(\mu) = c_2(\mu) + \frac{1}{N_C}\,c_1(\mu) \tag{59}
$$

with $N_C = 3$ the number of colors. The energy scale μ appropriate in this case is $\mu \simeq m_b$ and the values for a_1 and a_2 that we use are [4]

$$
a_1 = 1.14 \quad ; \quad a_2 = -0.20 \tag{60}
$$

1. $M_F^- = \pi^-,\, \rho^-,\, K^-,\, K^{*-}$

This is the simplest case. The decay width is given by

$$
\Gamma = \frac{G_F^2}{16\pi m_{B_c}^2}\,|V_{cb}|^2\,|V_F|^2\;a_1^2\,\frac{\lambda^{1/2}(m_{B_c}^2,\,m_{c\bar{c}}^2,\,m_F^2)}{2m_{B_c}}\,\mathcal{H}_{\alpha\beta}(P_{B_c},P_{c\bar{c}})\,\widehat{\mathcal{H}}^{\alpha\beta}(P_F) \tag{61}
$$

with m_F the mass of the M_F^- final meson, and $V_F = V_{ud}$ or $V_F = V_{us}$ depending on whether $M_F^- = \pi^-,\, \rho^-$ or $M_F^- = K^-,\, K^{*-}$. $\mathcal{H}_{\alpha\beta}(P_{B_c},P_{c\bar{c}})$ is the hadron tensor for the $B_c^- \to c\bar{c}$ transition and $\widehat{\mathcal{H}}^{\alpha\beta}(P_F)$ is the hadron tensor for the vacuum $\to M_F^-$ transition. The latter is

$$
\begin{aligned}
\widehat{\mathcal{H}}^{\alpha\beta}(P_F) &=& P_F^\alpha\,P_F^\beta\,f_F^2 && M_F^- \equiv 0^-\ \text{case} \\
\widehat{\mathcal{H}}^{\alpha\beta}(P_F) &=& (P_F^\alpha\,P_F^\beta - m_F^2\,g^{\alpha\,\beta})f_F^2 && M_F^- \equiv 1^-\ \text{case}
\end{aligned}
\tag{62}
$$

	Γ [10^{-15} GeV]
$B_c^- \to \eta_c\,\pi^-$	$1.02^{+0.07}\,a_1^2$
$B_c^- \to \eta_c\,\rho^-$	$2.60^{+0.16}\,a_1^2$
$B_c^- \to \eta_c\,K^-$	$0.082^{+0.004}\,a_1^2$
$B_c^- \to \eta_c\,K^{*-}$	$0.15^{+0.01}\,a_1^2$
$B_c^- \to J/\Psi\,\pi^-$	$0.83^{+0.09}\,a_1^2$
$B_c^- \to J/\Psi\,\rho^-$	$2.61^{+0.27}\,a_1^2$
$B_c^- \to J/\Psi\,K^-$	$0.065^{+0.007}\,a_1^2$
$B_c^- \to J/\Psi\,K^{*-}$	$0.16^{+0.01}\,a_1^2$
$B_c^- \to \chi_{c0}\,\pi^-$	$0.28^{+0.03}\,a_1^2$
$B_c^- \to \chi_{c0}\,\rho^-$	$0.73^{+0.07}\,a_1^2$
$B_c^- \to \chi_{c0}\,K^-$	$0.022^{+0.003}\,a_1^2$
$B_c^- \to \chi_{c0}\,K^{*-}$	$0.041^{+0.005}\,a_1^2$
$B_c^- \to \chi_{c1}\,\pi^-$	$0.0015^{+0.0002}\,a_1^2$
$B_c^- \to \chi_{c1}\,\rho^-$	$0.11^{+0.01}\,a_1^2$
$B_c^- \to \chi_{c1}\,K^-$	$0.00012^{+0.00001}\,a_1^2$
$B_c^- \to \chi_{c1}\,K^{*-}$	$0.0080^{+0.0007}_{-0.0002}\,a_1^2$
$B_c^- \to h_c\,\pi^-$	$0.58^{+0.07}\,a_1^2$
$B_c^- \to h_c\,\rho^-$	$1.41^{+0.17}\,a_1^2$
$B_c^- \to h_c\,K^-$	$0.045^{+0.006}\,a_1^2$
$B_c^- \to h_c\,K^{*-}$	$0.078^{+0.009}\,a_1^2$
$B_c^- \to \chi_{c2}\,\pi^-$	$0.24^{+0.02}\,a_1^2$
$B_c^- \to \chi_{c2}\,\rho^-$	$0.71^{+0.07}_{-0.03}\,a_1^2$
$B_c^- \to \chi_{c2}\,K^-$	$0.018^{+0.002}\,a_1^2$
$B_c^- \to \chi_{c2}\,K^{*-}$	$0.041^{+0.004}_{-0.001}\,a_1^2$
$B_c^- \to \Psi(3836)\,\pi^-$	$0.00045^{+0.00003}_{-0.00003}\,a_1^2$
$B_c^- \to \Psi(3836)\,\rho^-$	$0.021^{+0.001}_{-0.002}\,a_1^2$
$B_c^- \to \Psi(3836)\,K^-$	$0.000034^{+0.000002}_{-0.000002}\,a_1^2$
$B_c^- \to \Psi(3836)\,K^{*-}$	$0.0015_{-0.0002}\,a_1^2$

TABLE X: Decay widths in units of 10^{-15} GeV, and for general values of the Wilson coefficient a_1, for exclusive nonleptonic decays of the B_c^- meson. Our central values have been obtained with the AL1 potential.

with f_F being the M_F^- decay constant.

Similarly to the semileptonic case, the product $\mathcal{H}_{\alpha\beta}(P_{B_c}, P_{c\bar{c}})\ \widehat{\mathcal{H}}^{\alpha\beta}(P_F)$ can now be easily written in terms of helicity amplitudes for the $B_c^- \to c\bar{c}$ transition so that the width is given as [4]

$$\Gamma = \frac{G_F^2}{16\pi m_{B_c}^2}\,|V_{cb}|^2\,|V_F|^2\ a_1^2\ \frac{\lambda^{1/2}(m_{B_c}^2,\,m_{c\bar{c}}^2,\,m_F^2)}{2m_{B_c}}\,m_F^2\,f_F^2\,\mathcal{H}_{tt}^{B_c^-\to c\bar{c}}(m_F^2) \qquad M_F^- \equiv 0^-\ \text{case}$$

$$\Gamma = \frac{G_F^2}{16\pi m_{B_c}^2}\,|V_{cb}|^2\,|V_F|^2\ a_1^2\ \frac{\lambda^{1/2}(m_{B_c}^2,\,m_{c\bar{c}}^2,\,m_F^2)}{2m_{B_c}}\,m_F^2\,f_F^2$$
$$\times\left(\mathcal{H}_{+1+1}^{B_c^-\to c\bar{c}}(m_F^2)+\mathcal{H}_{-1-1}^{B_c^-\to c\bar{c}}(m_F^2)+\mathcal{H}_{00}^{B_c^-\to c\bar{c}}(m_F^2)\right) \qquad M_F^- \equiv 1^-\ \text{case} \qquad (63)$$

with the different $\mathcal{H}_{rr}$ evaluated at $q^2 = m_F^2$. In Table X we show the decay widths for a general value of the Wilson coefficient a_1, whereas in Table XI we give the corresponding branching ratios evaluated with $a_1 = 1.14$. Our results for a final η_c or J/ψ are in good agreement with the ones obtained by Ebert *et al.* [7], El-Hady *et al.* [12] and Anisimov *et al.* [19], but they are a factor 2 smaller than the results by Ivanov *et al.* [4] and Kiselev [16]. Large discrepancies with Ivanov's results show up for the other transitions.

2. $M_F^- = D^-,\, D^{*-},\, D_s^-,\, D_s^{*-}$

In this subsection we shall evaluate the nonleptonic two–meson $B_c^- \to \eta_c D^-$, $\eta_c D^{*-}$, $J/\Psi D^-$, $J/\Psi\, D^{*-}$ and $B_c^- \to \eta_c D_s^-$, $\eta_c D_s^{*-}$, $J/\Psi D_s^-$, $J/\Psi\, D_s^{*-}$ decay widths. In these cases there are two different contributions in the factorization

B.R. (%)

	This work	[4]	[7]	[9, 10, 11]	[12]	[16, 17]	[18]	[19]	[23]
$B_c^- \to \eta_c\,\pi^-$	$0.094^{+0.006}$	0.19	0.083	0.18	0.14	0.20	0.025	0.13	
$B_c^- \to \eta_c\,\rho^-$	$0.24^{+0.01}$	0.45	0.20	0.49	0.33	0.42	0.067	0.30	
$B_c^- \to \eta_c\,K^-$	$0.0075^{+0.0005}$	0.015	0.006	0.014	0.011	0.013	0.002	0.013	
$B_c^- \to \eta_c\,K^{*-}$	$0.013^{+0.001}$	0.025	0.011	0.025	0.018	0.020	0.004	0.021	
$B_c^- \to J/\Psi\,\pi^-$	$0.076^{+0.008}$	0.17	0.060	0.18	0.11	0.13	0.13	0.073	
$B_c^- \to J/\Psi\,\rho^-$	$0.24^{+0.02}$	0.49	0.16	0.53	0.31	0.40	0.37	0.21	
$B_c^- \to J/\Psi\,K^-$	$0.0060^{+0.0006}$	0.013	0.005	0.014	0.008	0.011	0.007	0.007	
$B_c^- \to J/\Psi\,K^{*-}$	$0.014^{+0.002}$	0.028	0.010	0.029	0.018	0.022	0.020	0.016	
$B_c^- \to \chi_{c0}\,\pi^-$	$0.026^{+0.003}$	0.055		0.028		0.98			
$B_c^- \to \chi_{c0}\,\rho^-$	$0.067^{+0.006}_{-0.001}$	0.13		0.072		3.29			
$B_c^- \to \chi_{c0}\,K^-$	$0.0020^{+0.0002}$	0.0042		0.00021					
$B_c^- \to \chi_{c0}\,K^{*-}$	$0.0037^{+0.0005}$	0.0070		0.00039					
$B_c^- \to \chi_{c1}\,\pi^-$	$0.00014^{+0.00001}$	0.0068		0.007		0.0089			
$B_c^- \to \chi_{c1}\,\rho^-$	$0.010^{+0.001}_{-0.001}$	0.029		0.029		0.46			
$B_c^- \to \chi_{c1}\,K^-$	$1.1^{+0.1}\,10^{-5}$	$5.1\,10^{-4}$		$5.2\,10^{-5}$					
$B_c^- \to \chi_{c1}\,K^{*-}$	$0.00073^{+0.00007}_{-0.00002}$	0.0018		0.00018					
$B_c^- \to h_c\,\pi^-$	$0.053^{+0.007}$	0.11		0.05		1.60			
$B_c^- \to h_c\,\rho^-$	$0.13^{+0.01}$	0.25		0.12		5.33			
$B_c^- \to h_c\,K^-$	$0.0041^{+0.0006}$	0.0083		0.00038					
$B_c^- \to h_c\,K^{*-}$	$0.0071^{+0.0008}$	0.013		0.00068					
$B_c^- \to \chi_{c2}\,\pi^-$	$0.022^{+0.002}$	0.046		0.025		0.79			0.0076
$B_c^- \to \chi_{c2}\,\rho^-$	$0.065^{+0.006}_{-0.002}$	0.12		0.051		3.20			0.023
$B_c^- \to \chi_{c2}\,K^-$	$0.0017^{+0.0001}$	0.0034		0.00018					0.00056
$B_c^- \to \chi_{c2}\,K^{*-}$	$0.0038^{+0.0003}_{-0.0002}$	0.0065		0.00031					0.0013
$B_c^- \to \Psi(3836)\,\pi^-$	$4.1^{+0.03}_{-0.02}\,10^{-5}$	0.0017				0.030			
$B_c^- \to \Psi(3836)\,\rho^-$	$0.0020_{-0.0003}$	0.0055				0.98			
$B_c^- \to \Psi(3836)\,K^-$	$3.1^{+0.2}_{-0.2}\,10^{-6}$	0.00012							
$B_c^- \to \Psi(3836)\,K^{*-}$	$0.00014_{-0.00002}$	0.00032							

TABLE XI: Branching ratios in % for exclusive nonleptonic decays of the B_c^- meson. Our central values have been obtained with the AL1 potential.

approximation. Following the same steps that lead to Eq.(63) we shall get

$$\Gamma = \frac{G_F^2}{16\pi m_{B_c}^2}\,|V_{cb}|^2\,|V_F|^2\,\frac{\lambda^{1/2}(m_{B_c}^2,\,m_{c\bar{c}}^2,\,m_F^2)}{2m_{B_c}}\;\mathcal{H}\mathcal{H} \tag{64}$$

where now $V_F = V_{cd}$ for $M_F^- = D^-, D^{*-}$ and $V_F = V_{cs}$ for $M_F^- = D_s^-, D_s^{*-}$. The quantity $\mathcal{H}\mathcal{H}$ incorporates all information on the hadron matrix elements and depends on the transition as [4][11]

$$\begin{aligned}
\mathcal{H}\mathcal{H}^{B_c^-\to\eta_c D^-} &= \left|a_1\,h_t^{B_c^-\to\eta_c}(m_{D^-}^2)\,m_{D^-}\,f_{D^-} + a_2\,h_t^{B_c^-\to D^-}(m_{\eta_c}^2)\,m_{\eta_c}\,f_{\eta_c}\right|^2\\
\mathcal{H}\mathcal{H}^{B_c^-\to\eta_c D^{*-}} &= \left|-a_1\,h_0^{B_c^-\to\eta_c}(m_{D^{*-}}^2)\,m_{D^{*-}}\,f_{D^{*-}} + a_2\,i\,h_{(0)\,t}^{B_c^-\to D^{*-}}(m_{\eta_c}^2)\,m_{\eta_c}\,f_{\eta_c}\right|^2\\
\mathcal{H}\mathcal{H}^{B_c^-\to J/\Psi D^-} &= \left|a_1\,i\,h_{(0)\,t}^{B_c^-\to J/\Psi}(m_{D^-}^2)\,m_{D^-}\,f_{D^-} - a_2\;h_0^{B_c^-\to D^-}(m_{J/\Psi}^2)\,m_{J/\Psi}\,f_{J/\Psi}\right|^2\\
\mathcal{H}\mathcal{H}^{B_c^-\to J/\Psi D^{*-}} &= \sum_{r=+1,\,-1,\,0}\left|a_1\;h_{(r)\,r}^{B_c^-\to J/\Psi}(m_{D^{*-}}^2)\,m_{D^{*-}}\,f_{D^{*-}} + a_2\;h_{(r)\,r}^{B_c^-\to D^{*-}}(m_{J/\Psi}^2)\,m_{J/\Psi}\,f_{J/\Psi}\right|^2
\end{aligned} \tag{65}$$

and similarly for D_s^-, D_s^{*-}. Note that the helicity amplitudes corresponding to $B_c^- \to D^-$, D^{*-}, D_s^-, D_s^{*-} have been evaluated from the matrix elements for the effective current operators $\overline{\Psi}_{d,s}(0)\gamma^\mu(I-\gamma_5)\Psi_b(0)$ in Eq. (58). While in

[11] Note the different phases used in Ref. [4].

practice this is a $b \to d$, s transition, the momentum transfer ($m_{\eta_c^2}$ or $m^2_{J/\Psi}$) is neither too high, so that one has to include a B_c^* resonance, nor too low, so as to have too high three-momentum transfers[12]. Besides the contribution is weighed by the much smaller a_2 Wilson coefficient. In Table XII we give the decay widths for general values of the Wilson coefficients a_1 and a_2, and in Table XIII we show the branching ratios. We are in reasonable agreement with the results by Ivanov *et al.* [4], El-Hady *et al.* [12] and Kiselev [16]. For decays with a final D_s^-, D_s^{*-} the agreement is also reasonable with the results by Colangelo *et al.* [18] and Anisimov *et al.* [19].

	Γ [10^{-15} GeV]
$B_c^- \to \eta_c\, D^-$	$(0.438^{+0.010} a_1 + 0.236^{+0.030}_{-0.023} a_2)^2$
$B_c^- \to \eta_c\, D^{*-}$	$(-0.390_{-0.009} a_1 - 0.136^{+0.015}_{-0.022} a_2)^2$
$B_c^- \to J/\Psi\, D^-$	$(-0.328_{-0.012} a_1 - 0.156^{+0.016}_{-0.019} a_2)^2$
$B_c^- \to J/\Psi\, D^{*-}$	$(-0.195_{-0.008} a_1 - 0.066^{+0.006}_{-0.011} a_2)^2$
	$+(-0.390_{-0.018} a_1 - 0.209^{+0.019}_{-0.032} a_2)^2$
	$+(0.447_{-0.016} a_1 + 0.167^{+0.016}_{-0.027} a_2)^2$
$B_c^- \to \eta_c\, D_s^-$	$(2.54^{+0.05} a_1 + 1.93^{+0.10} a_2)^2$
$B_c^- \to \eta_c\, D_s^{*-}$	$(-1.84_{-0.04} a_1 - 1.17^{+0.02}_{-0.14} a_2)^2$
$B_c^- \to J/\Psi\, D_s^-$	$(-1.85^{+0.01}_{-0.06} a_1 - 1.23_{-0.06} a_2)^2$
$B_c^- \to J/\Psi\, D_s^{*-}$	$(-1.01_{-0.04} a_1 - 0.60^{+0.02}_{-0.07} a_2)^2$
	$+(-2.00_{-0.06} a_1 - 1.71^{+0.03}_{-0.18} a_2)^2$
	$+(2.17_{-0.08} a_1 + 1.42^{+0.02}_{-0.16} a_2)^2$

TABLE XII: Decay widths in units of 10^{-15} GeV, and for general values of the Wilson coefficients a_1 and a_2, for exclusive nonleptonic decays of the B_c^- meson. Our central values have been obtained with the AL1 potential. For vector–vector final state we show the three different contributions corresponding to $r = +1, -1, 0$ (see Eq.(65)).

	B.R. (%)						
	This work	[4]	[9]	[12]	[16]	[18]	[19]
$B_c^- \to \eta_c\, D^-$	$0.014^{+0.001}$	0.019	0.0012	0.014	0.015	0.005	0.010
$B_c^- \to \eta_c\, D^{*-}$	$0.012^{+0.001}$	0.019	0.0010	0.013	0.010	0.002	0.0055
$B_c^- \to J/\Psi\, D^-$	$0.0083^{+0.0005}$	0.015	0.0009	0.009	0.009	0.013	0.0044
$B_c^- \to J/\Psi\, D^{*-}$	$0.031^{+0.001}$	0.045		0.028	0.028	0.019	0.010
$B_c^- \to \eta_c\, D_s^-$	$0.44^{+0.02}$	0.44	0.054	0.26	0.28	0.50	0.35
$B_c^- \to \eta_c\, D_s^{*-}$	$0.24^{+0.02}$	0.37	0.044	0.24	0.27	0.038	0.36
$B_c^- \to J/\Psi\, D_s^-$	$0.24^{+0.02}$	0.34	0.041	0.15	0.17	0.34	0.12
$B_c^- \to J/\Psi\, D_s^{*-}$	$0.68^{+0.03}$	0.97		0.55	0.67	0.59	0.62

TABLE XIII: Branching ratios in % for exclusive nonleptonic decays of the B_c^- meson. Our central values have been obtained with the AL1 potential.

V. SEMILEPTONIC $B_c^- \to \overline{B}^0, \overline{B}^{*0}, \overline{B}_s^0, \overline{B}_s^{*0}$ DECAYS

In this section we shall study the semileptonic $B_c^- \to \overline{B}^0, \overline{B}^{*0}, \overline{B}_s^0, \overline{B}_s^{*0}$ decays. With obvious changes the calculations are done as before, with the only novel thing that now it is the antiquark that suffers the transition (we have $\bar{c} \to \bar{d}$, $\bar{s}$), and thus we have to take into account the changes in the form factors according to the results in appendix C.

[12] Our experience with the $B \to \pi$ decay [3], where we have a similar $b \to u$ quark transition, shows that the naive nonrelativistic quark model gives reliable results for $q^2 \approx 9\,\mathrm{GeV}^2$.

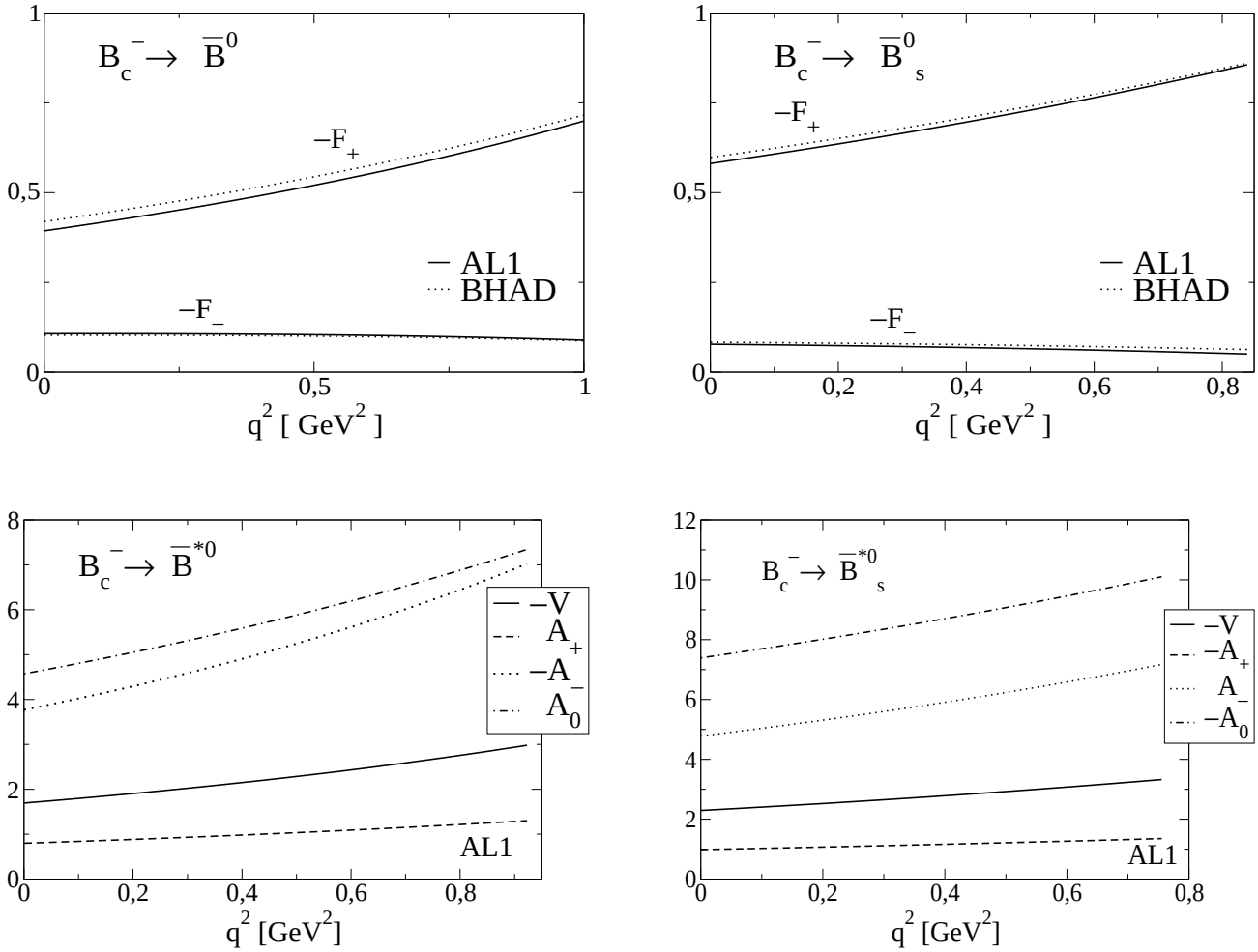

FIG. 10: F_+ and F_- form factors (solid lines) for $B_c^- \to \overline{B}^0$ and $B_c^- \to \overline{B}_s^0$ semileptonic decay, and V (solid line), A_+ (dashed line), A_- (dotted line) and A_0 (dashed–dotted line) form factors for $B_c^- \to \overline{B}^{*0}$ and $B_c^- \to \overline{B}_s^{*0}$ semileptonic decay evaluated with the AL1 potential. For the first two cases, and for comparison, we also show with dotted lines the results obtained with the Bhaduri (BHAD) potential.

A. Form factors

In Fig. 10 we show the form factors for the above transitions evaluated with the AL1 potential. For the $\overline{B}^0$ and $\overline{B}_s^0$ cases we also show the results obtained with the BHAD potential. Although they are less visible in the figures, the larger differences, of up to 25%, occur for the F_- form factor.

In Table XIV we show F_+, F_- and F_0 (defined as in Eq. (15) changing the mass of the final meson) of the $B_c^- \to \overline{B}^0$, $\overline{B}_s^0$ transitions evaluated at q^2_{min} and q^2_{max} and compare them with the results by Ivanov *et al.* [6] and Ebert *et al.* [8]. Notice that, to favor comparison, we have changed the signs of the form factors by Ebert *et al.* (they evaluate B_c^+ decay) in accordance with the results in appendix C. The agreement with the results by Ebert *et al.* is good. We also agree with Ivanov *et al.* for F_+, but get very different results for F_-. As fermion masses are very small the disagreement in the F_- form factor will have a negligible effect on the decay width.

In Table XV we show V, A_+, A_-, A_0 and $\widetilde{A}_0$ (defined as in Eq. (19) changing the mass of the final meson) of the $B_c^- \to \overline{B}^{*0}$, $\overline{B}_s^{*0}$ evaluated at q^2_{min} and q^2_{max} and compare them with the results by Ivanov *et al.* [6] and Ebert *et al.* [8]. With some exceptions the agreement with Ebert's results is bad in this case. We are also in clear disagreement with Ivanov's results.

$B_c^- \to \overline{B}^0 l^- \bar{\nu}_l$	$q^2_{\rm min}$	$q^2_{\rm max}$	$B_c^- \to \overline{B}_s^0 l^- \bar{\nu}_l$	$q^2_{\rm min}$	$q^2_{\rm max}$
F_+			F_+		
This work	$-0.39^{+0.03}_{-0.03}$	$-0.70^{+0.004}_{-0.02}$	This work	$-0.58^{+0.01}_{-0.02}$	$-0.86^{+0.01}_{-0.01}$
[6]	-0.58	-0.96	[6]	-0.61	-0.92
[8]	-0.39	-0.96	[8]	-0.50	-0.99
F_-			F_-		
This work	$-0.11^{+0.02}_{-0.03}$	$-0.09^{+0.01}_{-0.06}$	This work	$-0.08^{+0.01}_{-0.02}$	$-0.05^{+0.01}_{-0.03}$
[6]	2.14	2.98	[6]	1.83	2.35
F_0			F_0		
This work	$-0.39^{+0.03}_{-0.03}$	$-0.71^{+0.05}_{-0.02}$	This work	$-0.58_{-0.02}$	$-0.86^{+0.01}_{-0.01}$
[8]	-0.39	-0.80	[8]	-0.50	-0.86

TABLE XIV: F_+, F_- and F_0 evaluated at $q^2_{\rm min}$ and $q^2_{\rm max}$ compared to the ones obtained by Ivanov *et al.* [6] and Ebert*et al.* [8]. Our central values have been obtained with the AL1 potential. Here l stands for $l = e$, μ.

$B_c^- \to \overline{B}^{*0} l^- \bar{\nu}_l$	$q^2_{\rm min}$	$q^2_{\rm max}$	$B_c^- \to \overline{B}_s^{*0} l^- \bar{\nu}_l$	$q^2_{\rm min}$	$q^2_{\rm max}$
V			V		
This work	$-1.69^{+0.11}_{-0.09}$	$-2.98^{+0.17}_{-0.03}$	This work	$-2.29^{+0.02}_{-0.09}$	$-3.32^{+0.04}_{-0.01}$
[6]		-5.32^*	[6]		-4.91^*
[8]	-3.94	-8.91	[8]	-3.44	-6.25
A_+			A_+		
This work	$-0.80^{+0.02}_{-0.02}$	$-1.30^{+0.02}$	This work	$-0.98^{+0.01}_{-0.03}$	$-1.35^{+0.03}_{-0.02}$
[6]		0.49	[6]		0.21
[8]	-2.89	-2.83	[8]	-2.19	-2.62
A_-			A_-		
This work	$3.77^{+0.15}_{-0.17}$	$7.02_{-0.35}$	This work	$4.78^{+0.23}_{-0.01}$	$7.17^{+0.06}_{-0.18}$
[6]		18.0	[6]		15.9
A_0			A_0		
This work	$-4.57^{+0.27}_{-0.33}$	$-7.34^{+0.28}_{-0.49}$	This work	$-7.39^{+0.14}_{-0.30}$	$-10.10^{+0.22}_{-0.16}$
[6]		-5.07	[6]		-6.60
[8]	-5.08	-8.70	[8]	-6.60	-10.23
$\widetilde{A}_0$			$\widetilde{A}_0$		
This work	$-0.34^{+0.03}_{-0.03}$	$-0.60^{+0.05}_{-0.02}$	This work	$-0.51^{+0.01}_{-0.03}$	$-0.74^{+0.01}_{-0.01}$
[8]	-0.20	-1.06	[8]	-0.35	-0.91

TABLE XV: V, A_+, A_-, A_0 and $\widetilde{A}_0$ evaluated at $q^2_{\rm min}$ and $q^2_{\rm max}$ compared to the ones obtained by Ivanov *et al.* [6] and Ebert *et al.* [8]. Our central values have been obtained with the AL1 potential. Here l stands for $l = e$, μ. Asterisk as in Table IV.

B. Decay width

In Tables XVI, XVII we give respectively our results for the partial helicity widths and forward-backward asymmetries.

In Fig. 11 we show the differential decay width for the $B_c^- \to \overline{B}^0 l^- \bar{\nu}_l$, $B_c^- \to \overline{B}_s^0 l^- \bar{\nu}_l$, $B_c^- \to \overline{B}^{*0} l^- \bar{\nu}_l$ and $B_c^- \to \overline{B}_s^{*0} l^- \bar{\nu}_l$ transitions ($l = e$, μ). In Tables XVIII, XIX we give the total decay widths and branching ratios and compare them with determinations by other groups. Our results are in better agreement with the ones obtained by Ebert *et al.* [8], Colangelo *et al.* [18], Anisimov *et al.* [19] and Lu *et al.* [24].

$B_c^- \to$	Γ_U	$\widetilde{\Gamma}_U$	Γ_L	$\widetilde{\Gamma}_L$	Γ_P	$\widetilde{\Gamma}_S$	$\widetilde{\Gamma}_{SL}$
$\overline{B}^0\, e^-\bar{\nu}_e$	0	0	$0.65^{+0.07}_{-0.09}$	$0.14^{+0.02}_{-0.02}\ 10^{-5}$	0	$0.47^{+0.05}_{-0.07}\ 10^{-5}$	$0.15^{+0.01}_{-0.02}\ 10^{-5}$
$\overline{B}^0\, \mu^-\bar{\nu}_\mu$	0	0	$0.55^{+0.06}_{-0.07}$	$0.15^{+0.01}_{-0.02}\ 10^{-1}$	0	$0.64^{+0.16}_{-0.09}\ 10^{-1}$	$0.17^{+0.02}_{-0.02}\ 10^{-1}$
$\overline{B}_s^0\, e^-\bar{\nu}_e$	0	0	$15.1^{+0.7}_{-0.3}$	$0.43^{+0.02}_{-0.01}\ 10^{-4}$	0	$0.14^{+0.01}\ 10^{-3}$	$0.45^{+0.03}_{-0.01}\ 10^{-4}$
$\overline{B}_s^0\, \mu^-\bar{\nu}_\mu$	0	0	$12.4^{+0.5}_{-0.3}$	$0.40^{+0.02}_{-0.01}$	0	$1.69^{+0.08}_{-0.03}$	$0.47^{+0.02}_{-0.01}$
$\overline{B}^{*0}\, e^-\bar{\nu}_e$	$0.83^{+0.08}_{-0.11}$	$0.26^{+0.03}_{-0.04}\ 10^{-6}$	$0.76^{+0.09}_{-0.11}$	$0.10^{+0.02}_{-0.01}\ 10^{-5}$	$0.36^{+0.03}_{-0.05}$	$0.27^{+0.04}_{-0.05}\ 10^{-5}$	$0.96^{+0.15}_{-0.15}\ 10^{-6}$
$\overline{B}^{*0}\, \mu^-\bar{\nu}_\mu$	$0.79^{+0.10}_{-0.11}$	$0.97^{+0.11}_{-0.13}\ 10^{-2}$	$0.68^{+0.08}_{-0.10}$	$0.14^{+0.01}_{-0.03}\ 10^{-1}$	$0.34^{+0.02}_{-0.05}$	$0.28^{+0.04}_{-0.05}\ 10^{-1}$	$0.11^{+0.02}_{-0.02}\ 10^{-1}$
$\overline{B}_s^{*0}\, e^-\bar{\nu}_e$	$16.7^{+0.8}_{-0.7}$	$0.66^{+0.04}_{-0.03}\ 10^{-5}$	$16.8^{+1.1}_{-0.8}$	$0.33^{+0.02}_{-0.02}\ 10^{-4}$	$6.11^{+0.21}_{-0.20}$	$0.88^{+0.08}_{-0.05}\ 10^{-4}$	$0.30^{+0.03}_{-0.01}\ 10^{-4}$
$\overline{B}_s^{*0}\, \mu^-\bar{\nu}_\mu$	$15.6^{+0.8}_{-0.6}$	$0.24^{+0.02}_{-0.01}$	$14.5^{+1.0}_{-0.6}$	$0.37^{+0.02}_{-0.02}$	$5.66^{+0.18}_{-0.19}$	$0.77^{+0.06}_{-0.04}$	$0.30^{+0.02}_{-0.01}$

TABLE XVI: Partial helicity widths in units of 10^{-15} GeV for B_c^- decay. Central values have been evaluated with the AL1 potential.

	$A_{FB}(e)$	$A_{FB}(\mu)$
$B_c^- \to \overline{B}^0$	$0.67^{+0.02}\ 10^{-5}$	$0.82^{+0.01}\ 10^{-1}$
$B_c^- \to \overline{B}_s^0$	$0.89^{+0.01}\ 10^{-5}$	$0.96^{+0.01}\ 10^{-1}$
$B_c^- \to \overline{B}^{*0}$	$0.17_{-0.01}$	$0.19_{-0.01}$
$B_c^- \to \overline{B}_s^{*0}$	$0.14_{-0.01}$	$0.16^{+0.01}$

TABLE XVII: Forward-backward asymmetry. Our central values have been evaluated with the AL1 potential. We would obtain the same results for $B_c^+ \to B^0$ decays.

	Γ [10^{-15} GeV]										
	This work	[6]	[8]	[9]	[12]	[13]	[16]	[18]	[19]	[20]	[24]
$B_c^- \to \overline{B}^0\, e\, \bar{\nu}_e$	$0.65^{+0.07}_{-0.09}$	2.1	0.6	2.30	1.14	1.90	4.9	0.9(1.0)			0.59
$B_c^- \to \overline{B}^0\, \mu\, \bar{\nu}_\mu$	$0.63^{+0.07}_{-0.09}$										
$B_c^- \to \overline{B}_s^0\, e\, \bar{\nu}_e$	$15.1^{+0.7}_{-0.3}$	29	12	26.6	14.3	26.8	59	11.1(12.9)	15	12.3	11.75
$B_c^- \to \overline{B}_s^0\, \mu\, \bar{\nu}_\mu$	$14.5^{+0.6}_{-0.3}$										
$B_c^- \to \overline{B}^{*0}\, e\, \bar{\nu}_e$	$1.59^{+0.17}_{-0.22}$	2.3	1.7	3.32	3.53	2.34	8.5	2.8(3.2)			2.44
$B_c^- \to \overline{B}^{*0}\, \mu\, \bar{\nu}_\mu$	$1.52^{+0.17}_{-0.21}$										
$B_c^- \to \overline{B}_s^{*0}\, e\, \bar{\nu}_e$	$33.5^{+1.9}_{-1.5}$	37	25	44.0	50.4	34.6	65	33.5(37.0)	34	19.0	32.56
$B_c^- \to \overline{B}_s^{*0}\, \mu\, \bar{\nu}_\mu$	$31.5^{+1.8}_{-1.4}$										

TABLE XVIII: Decay widths in units of 10^{-15} GeV. Our central values have been evaluated with the AL1 potential.

C. Heavy quark spin symmetry

In Fig. 12 we give $\Sigma_1^{(0^-)}$ and $\Sigma_2^{(0^-)}$ of the $B_c^- \to \overline{B}^0$ and $B_c^- \to \overline{B}_s^0$ transitions, and $\Sigma_1^{(1^-)}$, $\overline{\Sigma}_2^{(1^-)}$, $\overline{\Sigma}_2^{\prime(1^-)}$ and $\overline{\Sigma}_3^{(1^-)}$ of the $B_c^- \to \overline{B}^{*0}$ and $B_c^- \to \overline{B}_s^{*0}$ transitions.

We can take the infinite heavy quark mass limit on our analytic expressions with the result that near zero recoil

$$\begin{aligned} \Sigma_1^{(1^-)} &= \Sigma_1^{(0^-)} \\ \overline{\Sigma}_2^{(1^-)} &= \overline{\Sigma}_2^{\prime(1^-)} = -\overline{\Sigma}_2^{(0^-)} \\ \overline{\Sigma}_3^{(1^-)} &= 0 \end{aligned} \tag{66}$$

B.R. (%)

	This work	[4]	[8]	[9]	[12]	[16]	[18]	[19]	[20]
$B_c^- \to \overline{B}^0 e\,\bar{\nu}_e$	$0.046^{+0.004}_{-0.007}$	0.071	0.042	0.16	0.078	0.34	0.06		0.048
$B_c^- \to \overline{B}^0 \mu\,\bar{\nu}_\mu$	$0.044^{+0.005}_{-0.006}$								
$B_c^- \to \overline{B}_s^0 e\,\bar{\nu}_e$	$1.06^{+0.05}_{-0.02}$	1.10	0.84	1.82	0.98	4.03	0.8	0.99	0.92
$B_c^- \to \overline{B}_s^0 \mu\,\bar{\nu}_\mu$	$1.02^{+0.04}_{-0.02}$								
$B_c^- \to \overline{B}^{*0} e\,\bar{\nu}_e$	$0.11^{+0.01}_{-0.01}$	0.063	0.12	0.23	0.24	0.58	0.19		0.051
$B_c^- \to \overline{B}^{*0} \mu\,\bar{\nu}_\mu$	$0.11^{+0.01}_{-0.02}$								
$B_c^- \to \overline{B}_s^{*0} e\,\bar{\nu}_e$	$2.35^{+0.14}_{-0.10}$	2.37	1.75	3.01	3.45	5.06	2.3	2.30	1.41
$B_c^- \to \overline{B}_s^{*0} \mu\,\bar{\nu}_\mu$	$2.22^{+0.12}_{-0.10}$								

TABLE XIX: Branching ratios in % . Our central values have been evaluated with the AL1 potential.

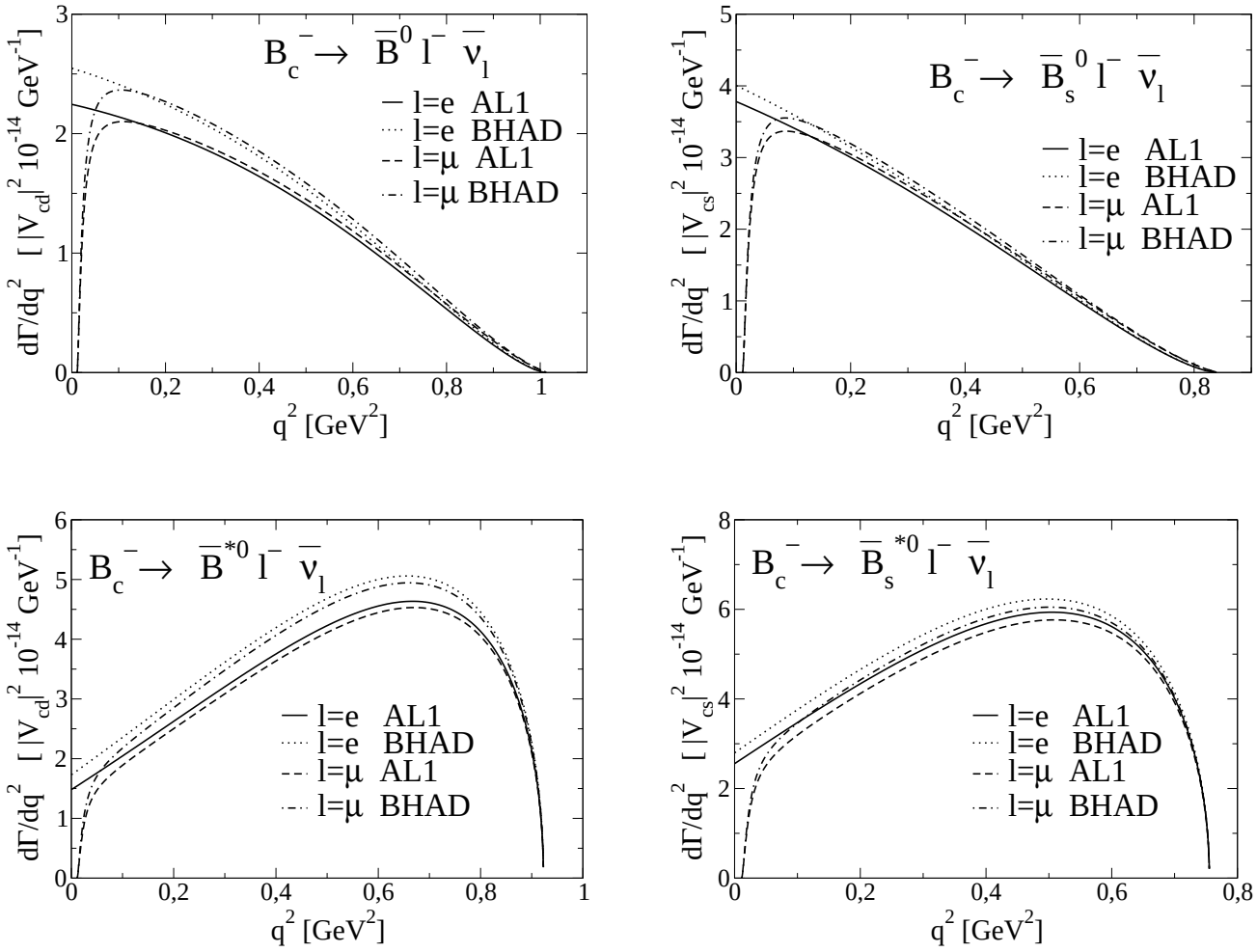

FIG. 11: Differential decay width for the for the $B_c^- \to \overline{B}^0 l^- \bar{\nu}_l$ and $B_c^- \to \overline{B}_s^0 l^- \bar{\nu}_l$, $B_c^- \to \overline{B}^{*0} l^- \bar{\nu}_l$ and $B_c^- \to \overline{B}_s^{*0} l^- \bar{\nu}_l$ ($l = e, \mu$) transitions. Solid line: results for a final e evaluated with the AL1 potential; dotted line: results for a final e evaluated with the Bhaduri (BHAD) potential; dashed line: results for a final μ evaluated with the AL1 potential; dashed–dotted line: results for a final μ evaluated with the Bhaduri (BHAD) potential.

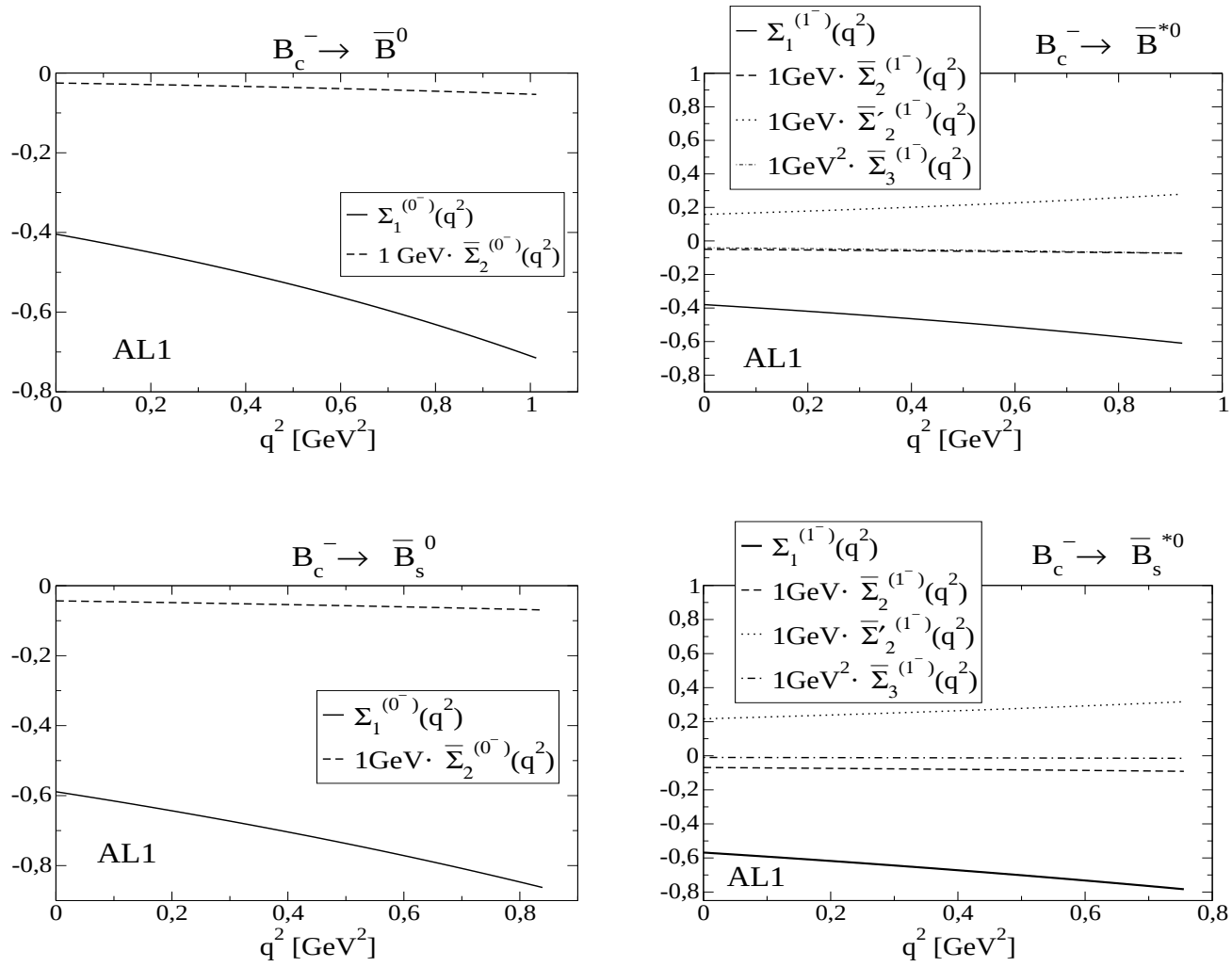

FIG. 12: $\Sigma_1^{(0^-)}$ (solid line) and $\Sigma_2^{(0^-)}$ (dashed line) of the $B_c^- \to \overline{B}^0$ and $B_c^- \to \overline{B}_s^0$ transitions, and $\Sigma_1^{(1^-)}$ (solid line), $\overline{\Sigma}_2^{(1^-)}$ (dashed line), $\overline{\Sigma}_2^{\prime(1^-)}$ (dotted line) and $\overline{\Sigma}_3^{(1^-)}$ (dashed dotted line) of the $B_c^- \to \overline{B}^{*0}$ and $B_c^- \to \overline{B}_s^{*0}$ transitions evaluated with the AL1 potential.

When compared to the results of HQSS by Jenkins *et al.* [2] we see differences. In Ref. [2] we find[13] $\overline{\Sigma}_2^{(1^-)} = \overline{\Sigma}_2^{(0^-)}$ instead. This is wrong as there is a misprint in Ref. [2] that has not been noted before: the sign of the term in v^μ in the last expression of Eqs. (2.9) and (2.10) in Ref. [2] should be a minus [42]. Also from Ref. [2] one would expect [14] $\overline{\Sigma}_2^{\prime(1^-)} = \overline{\Sigma}_2^{(0^-)}$ contradicting our result in Eq. (66) were we find $\overline{\Sigma}_2^{\prime(1^-)} = -\overline{\Sigma}_2^{(0^-)}$. Our result is a clear prediction of the quark model and comes from the extra signs that appear due to the fact that it is the antiquark that decays (See appendix C). This difference between quark and antiquark decay was not properly reflected in their published work [42].

How far are we from the infinite heavy quark mass limit?. In Fig. 13 we show $\Sigma_1^{(0^-)}$ of the semileptonic $B_c^- \to \overline{B}^0$ and $B_c^- \to \overline{B}_s^0$ transitions, and $\Sigma_1^{(1^-)}$ of the semileptonic $B_c^- \to \overline{B}^{*0}$ and $B_c^- \to \overline{B}_s^{*0}$ transitions. The differences

[13] Note the different notation and global phases used.

[14] One would have to look at Eq. (2.10) in Ref. [2], even though it refers to B_c^+ decay into D^0, D^{*0}, because that is the reaction where you have antiquark decay in their case.

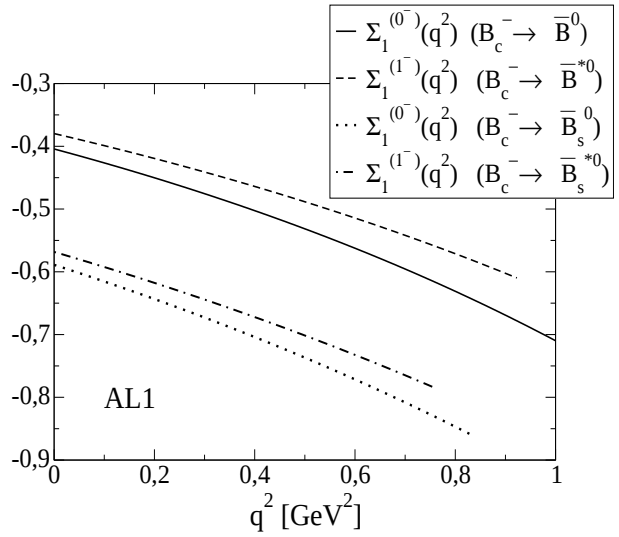

FIG. 13: $\Sigma_1^{(0^-)}$ of the semileptonic $B_c^- \to \overline{B}^0$ (solid line) and $B_c^- \to \overline{B}_s^0$ (dotted line) transitions, and $\Sigma_1^{(1^-)}$ of the semileptonic $B_c^- \to \overline{B}^{*0}$ (dashed line) and $B_c^- \to \overline{B}_s^{*0}$ (dashed–dotted line) transitions evaluated with the AL1 potential.

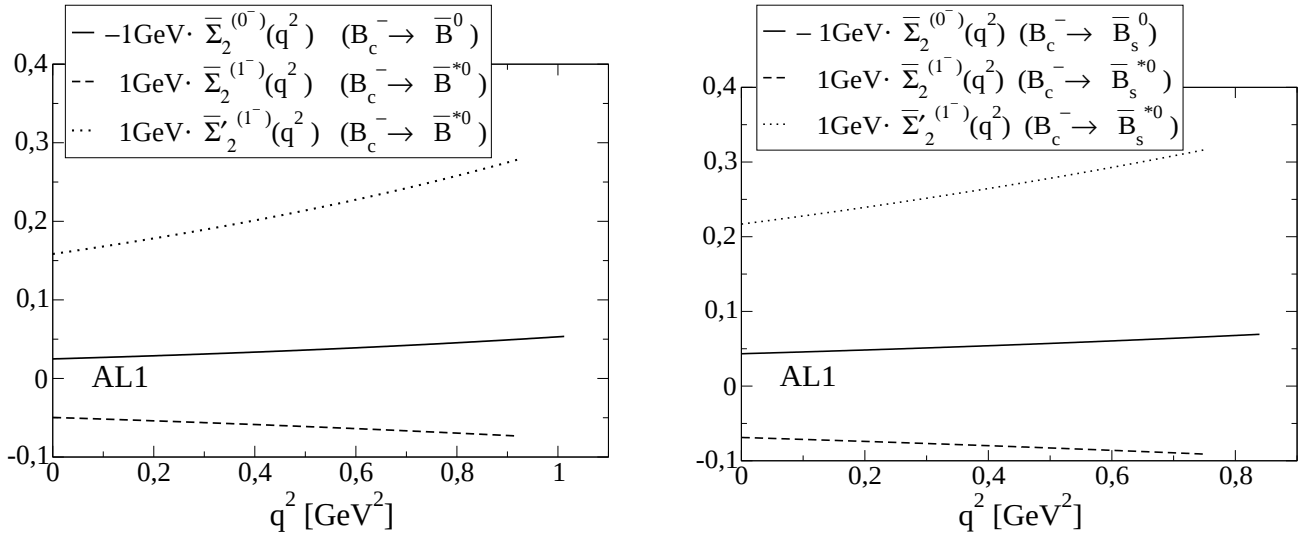

FIG. 14: $-\overline{\Sigma}_2^{(0^-)}$ (solid line) of the semileptonic $B_c^- \to \overline{B}^0$ and $B_c^- \to \overline{B}_s^0$ transitions, and $\overline{\Sigma}_2^{(1^-)}$ (dashed line), $\overline{\Sigma}_2^{\prime(1^-)}$ (dotted line) of the semileptonic $B_c^- \to \overline{B}^{*0}$ and $B_c^- \to \overline{B}_s^{*0}$ transitions evaluated with the AL1 potential.

between the corresponding $\Sigma_1^{(0^-)}$ and $\Sigma_1^{(1^-)}$ are at the level of 10%. The differences are much more significant for $\overline{\Sigma}_2^{(0^-)}$, $\overline{\Sigma}_2^{(1^-)}$ and $\overline{\Sigma}_2^{\prime(1^-)}$ that we show in Fig. 14. In each case the three curves shown would be the same in the infinite heavy quark mass limit. Clearly in this case corrections on the inverse of the heavy quark masses seem to be important.

VI. NONLEPTONIC $B_c^- \to B\,M_F$ TWO-MESON DECAYS

In this section we will evaluate decay widths for nonleptonic $B_c^- \to B\ M_F$ two–meson decays where M_F is a pseudoscalar or vector meson with no b quark content, and, at this point, B represents a meson with a b quark. These decay modes involve a $\bar{c} \to \bar{d}$ or $\bar{c} \to \bar{s}$ transition at the quark level and they are governed, neglecting penguin

operators, by the effective Hamiltonian [4, 8]

$$H_{eff.} = \frac{G_F}{\sqrt{2}} \left\{ V_{cd} \left[c_1(\mu)\, Q_1^{cd} + c_2(\mu)\, Q_2^{cd} \right] + V_{cs} \left[c_1(\mu)\, Q_1^{cs} + c_2(\mu)\, Q_2^{cs} \right] + H.c. \right\} \tag{67}$$

where c_1, c_2 are scale–dependent Wilson coefficients, and Q_1^{cd}, Q_2^{cd}, Q_1^{cs}, Q_2^{cs} are local four–quark operators given by

$$\begin{aligned}
Q_1^{cd} &= \overline{\Psi}_c(0)\gamma_\mu(I-\gamma_5)\Psi_d(0) \left[V_{ud}^*\, \overline{\Psi}_d(0)\gamma^\mu(I-\gamma_5)\Psi_u(0) + V_{us}^*\, \overline{\Psi}_s(0)\gamma^\mu(I-\gamma_5)\Psi_u(0) \right] \\
Q_2^{cd} &= \overline{\Psi}_c(0)\gamma_\mu(I-\gamma_5)\Psi_u(0) \left[V_{ud}^*\, \overline{\Psi}_d(0)\gamma^\mu(I-\gamma_5)\Psi_d(0) + V_{us}^*\, \overline{\Psi}_s(0)\gamma^\mu(I-\gamma_5)\Psi_d(0) \right] \\
Q_1^{cs} &= \overline{\Psi}_c(0)\gamma_\mu(I-\gamma_5)\Psi_s(0) \left[V_{ud}^*\, \overline{\Psi}_d(0)\gamma^\mu(I-\gamma_5)\Psi_u(0) + V_{us}^*\, \overline{\Psi}_s(0)\gamma^\mu(I-\gamma_5)\Psi_u(0) \right] \\
Q_2^{cs} &= \overline{\Psi}_c(0)\gamma_\mu(I-\gamma_5)\Psi_u(0) \left[V_{ud}^*\, \overline{\Psi}_d(0)\gamma^\mu(I-\gamma_5)\Psi_s(0) + V_{us}^*\, \overline{\Psi}_s(0)\gamma^\mu(I-\gamma_5)\Psi_s(0) \right]
\end{aligned} \tag{68}$$

We shall work again in the factorization approximation taking into account the Fierz reordered contribution so that the relevant coefficients are not c_1 and c_2 but the combinations

$$a_1(\mu) = c_1(\mu) + \frac{1}{N_C}\, c_2(\mu) \quad ; \quad a_2(\mu) = c_2(\mu) + \frac{1}{N_C}\, c_1(\mu) \tag{69}$$

The energy scale μ appropriate in this case is $\mu \simeq m_c$ and the values for a_1 and a_2 that we use are [4]

$$a_1 = 1.20 \quad ; \quad a_2 = -0.317 \tag{70}$$

1. $M_F = \pi^-,\, \rho^-,\, K^-,\, K^{*-}$

	Γ [10^{-15} GeV]		B.R. in %							
	This work		This work	[4]	[8]	[9]	[12]	[16]	[18]	[19]
$B_c^- \to \overline{B}^0\, \pi^-$	$1.10^{+0.14}_{-0.16}\, a_1^2$	$B_c^- \to \overline{B}^0\, \pi^-$	$0.11^{+0.01}_{-0.01}$	0.20	0.10	0.32	0.10	1.06	0.19	0.15
$B_c^- \to \overline{B}^0\, \rho^-$	$1.41^{+0.12}_{-0.19}\, a_1^2$	$B_c^- \to \overline{B}^0\, \rho^-$	$0.14^{+0.02}_{-0.02}$	0.20	0.13	0.59	0.28	0.96	0.15	0.19
$B_c^- \to \overline{B}^0\, K^-$	$0.098^{+0.012}_{-0.012}\, a_1^2$	$B_c^- \to \overline{B}^0\, K^-$	$0.010^{+0.001}_{-0.001}$	0.015	0.009	0.025	0.010	0.07	0.014	
$B_c^- \to \overline{B}^0\, K^{*-}$	$0.038^{+0.003}_{-0.005}\, a_1^2$	$B_c^- \to \overline{B}^0\, K^{*-}$	$0.0039^{+0.0003}_{-0.0005}$	0.0048	0.004	0.018	0.012	0.015	0.003	
$B_c^- \to \overline{B}^{*0}\, \pi^-$	$0.71^{+0.12}_{-0.11}\, a_1^2$	$B_c^- \to \overline{B}^{*0}\, \pi^-$	$0.072^{+0.012}_{-0.012}$	0.057	0.026	0.29	0.076	0.95	0.24	0.077
$B_c^- \to \overline{B}^{*0}\, \rho^-$	$5.68^{+0.55}_{-0.77}\, 1a_1^2$	$B_c^- \to \overline{B}^{*0}\, \rho^-$	$0.58^{+0.05}_{-0.08}$	0.30	0.67	1.17	0.89	2.57	0.85	0.67
$B_c^- \to \overline{B}^{*0}\, K^-$	$0.047^{+0.007}_{-0.007}\, a_1^2$	$B_c^- \to \overline{B}^{*0}\, K^-$	$0.0048^{+0.0007}_{-0.0008}$	0.0036	0.004	0.019	0.006	0.055	0.012	
$B_c^- \to \overline{B}^{*0}\, K^{*-}$	$0.29^{+0.03}_{-0.04}\, a_1^2$	$B_c^- \to \overline{B}^{*0}\, K^{*-}$	$0.030^{+0.002}_{-0.004}$	0.013	0.032	0.037	0.065	0.058	0.033	
$B_c^- \to \overline{B}_s^0\, \pi^-$	$34.7^{+2.0}_{-0.6}\, a_1^2$	$B_c^- \to \overline{B}_s^0\, \pi^-$	$3.51^{+0.19}_{-0.06}$	3.9	2.46	5.75	1.56	16.4	3.01	3.42
$B_c^- \to \overline{B}_s^0\, \rho^-$	$23.1^{+0.5}_{-0.6}\, a_1^2$	$B_c^- \to \overline{B}_s^0\, \rho^-$	$2.34^{+0.05}_{-0.06}$	2.3	1.38	4.41	3.86	7.2	1.34	2.33
$B_c^- \to \overline{B}_s^0\, K^-$	$2.87^{+0.13}_{-0.06}\, a_1^2$	$B_c^- \to \overline{B}_s^0\, K^-$	$0.29^{+0.01}_{-0.01}$	0.29	0.21	0.41	0.17	1.06	0.21	
$B_c^- \to \overline{B}_s^0\, K^{*-}$	$0.13_{-0.01}\, a_1^2$	$B_c^- \to \overline{B}_s^0\, K^{*-}$	$0.013_{-0.001}$	0.011	0.0030		0.10		0.0043	
$B_c^- \to \overline{B}_s^{*0}\, \pi^-$	$22.8^{+2.2}_{-1.0}\, a_1^2$	$B_c^- \to \overline{B}_s^{*0}\, \pi^-$	$2.34^{+0.19}_{-0.14}$	2.1	1.58	5.08	1.23	6.5	3.50	1.95
$B_c^- \to \overline{B}_s^{*0}\, \rho^-$	$132^{+5}_{-6}\, a_1^2$	$B_c^- \to \overline{B}_s^{*0}\, \rho^-$	$13.4^{+0.5}_{-0.6}$	11	10.8	14.8	16.8	20.2	10.8	12.1
$B_c^- \to \overline{B}_s^{*0}\, K^-$	$1.29^{+0.10}_{-0.06}\, a_1^2$	$B_c^- \to \overline{B}_s^{*0}\, K^-$	$0.13^{+0.01}_{-0.01}$	0.13	0.11	0.29	0.13	0.37	0.16	

TABLE XX: Decay widths in units of 10^{-15} GeV, and for general values of the Wilson coefficient a_1, and branching ratios in % for exclusive nonleptonic decays of the B_c^- meson. Our central values have been obtained with the AL1 potential.

In this case B denotes one of the $\overline{B}^0$, $\overline{B}^{*0}$, $\overline{B}_s^0$, $\overline{B}_s^{*0}$. The decay widths are

$$\Gamma = \frac{G_F^2}{16\pi m_{B_c}^2}\, |V_{cd}|^2\, |V_F|^2\, a_1^2\, \frac{\lambda^{1/2}(m_{B_c}^2,\, m_{\overline{B}^0,\, \overline{B}^{*0}}^2,\, m_F^2)}{2m_{B_c}}\, m_F^2\, f_F^2\, \mathcal{H}_{tt}^{B_c^- \to \overline{B}^0,\, \overline{B}^{*0}}(m_F^2) \qquad M_F \equiv 0^- \text{ case}$$

$$\Gamma = \frac{G_F^2}{16\pi m_{B_c}^2}\,|V_{cd}|^2\,|V_F|^2\,a_1^2\,\frac{\lambda^{1/2}(m_{B_c}^2,\,m_{\overline{B}^0,\,\overline{B}^{*0}}^2,\,m_F^2)}{2m_{B_c}}\,m_F^2\,f_F^2$$
$$\times\left(\mathcal{H}_{+1+1}^{B_c^-\to\overline{B}^0,\,\overline{B}^{*0}}(m_F^2)+\mathcal{H}_{-1-1}^{B_c^-\to\overline{B}^0,\,\overline{B}^{*0}}(m_F^2)+\mathcal{H}_{00}^{B_c^-\to\overline{B}^0,\,\overline{B}^{*0}}(m_F^2)\right)\qquad M_F\equiv 1^-\ \text{case}\quad(71)$$

and similarly for $\overline{B}_s^0$, $\overline{B}_s^{*0}$ with $|V_{cd}|\to|V_{cs}|$; $\overline{B}^0$, $\overline{B}^{*0}\to\overline{B}_s^0$, $\overline{B}_s^{*0}$. $V_F=V_{ud}$ or $V_F=V_{us}$ depending on whether $M_F=\pi^-$, ρ^- or $M_F=K^-$, K^{*-}, f_F is the decay constant of the M_F meson, and the different $\mathcal{H}_{rr}$ have been evaluated at $q^2=m_F^2$. In Table XX we show the decay widths for a general value of the Wilson coefficient a_1, and the corresponding branching ratios evaluated with $a_1=1.20$. The transition $B_c^-\to\overline{B}_s^{*0}K^{*-}$ is not allowed with the new B_c mass value from Ref. [26]. Our branching ratios for a final $\overline{B}_s^0$ or $\overline{B}_s^{*0}$ are in very good agreement with the results by Ivanov *et al.* [4], while for a final $\overline{B}^0$ or $\overline{B}^{*0}$ we are in very good agreement with the results by Ebert *et al.* [8] (with the exception of the $B_c\to\overline{B}^{*0}\pi^-$ decay).

2. $M_F=\pi^0,\,\rho^0,\,K^0,\,K^{*0}$

Here the generic name B stands for a B^- or a B^{*-} meson. The different decay widths are given by

$$\Gamma = \frac{G_F^2}{16\pi m_{B_c}^2}\,|V_{ud}|^2\,|V_F|^2\,a_2^2\,\frac{\lambda^{1/2}(m_{B_c}^2,\,m_{B^-,\,B^{*-}}^2,\,m_F^2)}{2m_{B_c}}\,m_F^2\,\widetilde{f}_F^2\,\mathcal{H}_{tt}^{B_c^-\to B^-,\,B^{*-}}(m_F^2)\qquad M_F\equiv 0^-\ \text{case}$$
$$\Gamma = \frac{G_F^2}{16\pi m_{B_c}^2}\,|V_{ud}|^2\,|V_F|^2\,a_2^2\,\frac{\lambda^{1/2}(m_{B_c}^2,\,m_{B^-,\,B^{*-}}^2,\,m_F^2)}{2m_{B_c}}\,m_F^2\,\widetilde{f}_F^2$$
$$\times\left(\mathcal{H}_{+1+1}^{B_c^-\to B^-,\,B^{*-}}(m_F^2)+\mathcal{H}_{-1-1}^{B_c^-\to B^-,\,B^{*-}}(m_F^2)+\mathcal{H}_{00}^{B_c^-\to B^-,\,B^{*-}}(m_F^2)\right)\qquad M_F\equiv 1^-\ \text{case}\quad(72)$$

where $V_F=V_{cd}$ or $V_F=V_{cs}$ depending on whether $M_F=\pi^0$, ρ^0 or $M_F=K^0$, K^{*0}, $\widetilde{f}_F=f_F$ for $M_F=K^0$, K^{*0} whereas $\widetilde{f}_F=f_F/\sqrt{2}$ for $M_F=\pi^0$, ρ^0, with f_F the M_F meson decay constant, and the different $\mathcal{H}_{rr}$ evaluated at $q^2=m_F^2$. The latter have been obtained from the matrix elements for the effective current operator $\overline{\Psi}_c(0)\gamma^\mu(I-\gamma_5)\Psi_u(0)$. The decay widths, for a general value of the Wilson coefficient a_2, and the corresponding branching ratios are shown in Table XXI. With the exception of the $B_c^-\to B^{*-}\pi^0$ case, our results are in a global good agreement with the ones by Ebert *et al.* [8].

Γ [10^{-15} GeV]

	This work
$B_c^-\to B^-\,\pi^0$	$0.54^{+0.07}_{-0.07}\,a_2^2$
$B_c^-\to B^-\,\rho^0$	$0.71^{+0.06}_{-0.10}\,a_2^2$
$B_c^-\to B^-\,K^0$	$35.3^{+4.0}_{-4.9}\,a_2^2$
$B_c^-\to B^-\,K^{*0}$	$13.1^{+0.9}_{-0.7}\,a_2^2$
$B_c\to B^{*-}\,\pi^0$	$0.35^{+0.06}_{-0.05}\,a_2^2$
$B_c\to B^{*-}\,\rho^0$	$2.84^{+0.27}_{-0.39}\,a_2^2$
$B_c\to B^{*-}\,K^0$	$16.9^{+2.4}_{-2.7}\,a_2^2$
$B_c\to B^{*-}\,K^{*0}$	$103^{+8}_{-13}\,a_2^2$

B.R. in %

	This work	[4]	[8]	[9]	[12]	[16]	[19]
$B_c^-\to B^-\,\pi^0$	$0.0038^{+0.0005}_{-0.0006}$	0.007	0.004	0.011	0.004	0.037	0.007
$B_c^-\to B^-\,\rho^0$	$0.0050^{+0.0004}_{-0.0007}$	0.0071	0.005	0.020	0.010	0.034	0.009
$B_c^-\to B^-\,K^0$	$0.25^{+0.03}_{-0.04}$	0.38	0.24	0.66	0.27	1.98	0.17
$B_c^-\to B^-\,K^{*0}$	$0.093^{+0.006}_{-0.013}$	0.11	0.09	0.47	0.32	0.43	0.095
$B_c\to B^{*-}\,\pi^0$	$0.0025^{+0.0004}_{-0.0005}$	0.0020	0.001	0.010	0.003	0.033	0.004
$B_c\to B^{*-}\,\rho^0$	$0.020^{+0.002}_{-0.003}$	0.011	0.024	0.041	0.031	0.09	0.031
$B_c\to B^{*-}\,K^0$	$0.12^{+0.02}_{-0.02}$	0.088	0.11	0.50	0.16	1.60	0.061
$B_c\to B^{*-}\,K^{*0}$	$0.73^{+0.06}_{-0.10}$	0.32	0.84	0.97	1.70	1.67	0.57

TABLE XXI: Decay widths in units of 10^{-15} GeV, and for general values of the Wilson coefficient a_2, and branching ratios in % for exclusive nonleptonic decays of the B_c^- meson. Our central values have been obtained with the AL1 potential.

VII. SUMMARY

We have made a comprehensive and exhaustive study of exclusive semileptonic and nonleptonic two–meson decays of the B_c meson within a nonrelativistic quark model. We have left out semileptonic processes involving a $b\to u$ transition at the quark level to avoid known deficiencies both at high and low q^2 transfers [3]. For similar reasons we have only considered two–meson nonleptonic decay channels that include a $c\bar{c}$ or B meson. Our model respects HQSS constraints in the infinite heavy quark mass limit but hints at sizeable corrections away from that limit for some form

factors. Unfortunately such corrections have not been worked out in perturbative QCD as they have for heavy–light mesons [43].

To check the sensitivity of our results to the inter–quark interaction we have used five different quark–quark potentials. Most observables change only at the level of a few per cent when changing the interaction. There is another source of theoretical uncertainty in the use of nonrelativistic kinematics in the evaluation of the orbital wave functions and the construction of our states in Eq.(1). While this is a very good approximation for the B_c itself it is not necessarily so for mesons with a light quark. We nevertheless think that, to a certain extent, the ignored relativistic effects are contained in an effective way in the free parameters of the inter-quark interaction, which are fitted to experimental data.

Our results for the observables analyzed are in a general good agreement (whenever comparison is possible) with the results obtained within the quasi-potential approach to the relativistic quark model of Ebert *et al.* [7, 8].

The branching ratios for the leptonic $B_c^- \to c\bar{c}$ and $B_c^- \to \overline{B}$ decays are also in reasonable agreement with the relativistic constituent quark model results of Ivanov *et al.* [4, 5].

For the nonleptonic $B_c^- \to \eta_c\, M_F^-$ and $B_c^- \to J/\Psi\, M_F^-$ two–meson decay channels with $M_F^- = \pi^-$, ρ^-, K^-, K^{*-}, we find also reasonable agreement (better for the J/Ψ channel) with the Bethe–Salpeter calculation by El-Hady *et al.* [12] and the light front calculation by Anisimov *et al.* [19], while our results are a factor of two smaller than the ones by Ivanov *et al.* [4], and Chang *et al.* [9, 10, 11], the latter obtained within the nonrelativistic approach to the Bethe–Salpeter equation. For the two–meson decay channels with χ_{c0}, χ_{c1}, h_c, χ_{c2} or $\Psi(3836)$ as the final $c\bar{c}$ meson and $M_F = \pi^-$, ρ^-, K^-, K^{*-} our results are generally a factor of two smaller than the ones of Ivanov *et al.* [4], whereas for some channels ($\chi_{c0}\,\pi^-$, $\chi_{c0}\,\rho^-$, $h_c\,\pi^-$, $h_c\,\rho^-$, $\chi_{c2}\,\pi^-$ and $\chi_{c2}\,\rho^-$,) we find very good agreement with the results by Chang *et al.* [9, 10, 11]. The disagreement with Ivanov *et al.* extend to the two-meson decay channels with a final $c\bar{c}$ and D mesons. There we find good agreement with the results by El-Hady *et al.* [12] and the ones obtained within the sum rules of QCD and nonrelativistic QCD by Kiselev [16].

As for the two–meson nonleptonic decay channels $B_c^- \to \overline{B}\, M_F$ with $M_F = \pi^-$, ρ^-, K^-, K^{*-} we are in a reasonable good agreement with the results by Anisimov *et al.* [19]. For the case of a final $\overline{B}_s^0$ or $\overline{B}_s^{*0}$ the agreement with the results by Ivanov *et al.* [4] is very good. For the $B_c^- \to B^-\, M_F$ case with $M_F = \pi^0$, ρ^0, K^0, K^{*0}, and apart from the results by Ebert *et al.* [8], we find no global agreement with other calculations, neither do they agree with each other.

From the above comparison one sees that there are different models producing sometimes very different results for the same observables. Accurate experimental data will shed light into this issue.

Acknowledgments

We thank J.G. Körner for a critical reading of our work. We also thank A.V. Manohar for discussions on the form factor decomposition in the the infinite heavy quark mass limit. This research was supported by DGI and FEDER funds, under contracts FIS2005-00810, BFM2003-00856 and FPA2004-05616, by Junta de Andalucía and Junta de Castilla y León under contracts FQM0225 and SA104/04, and it is part of the EU integrated infrastructure initiative Hadron Physics Project under contract number RII3-CT-2004-506078. J. M. V.-V. acknowledges an E.P.I.F. contract with the University of Salamanca.

APPENDIX A: $\varepsilon^\mu_{(\lambda)}(\vec{P})$ POLARIZATION VECTORS

Different sets of polarization vectors used in this paper:

$\underline{\vec{P} = \vec{0}}$

$$\text{Spin or heliciy bases} \begin{cases} \varepsilon^\mu_{(+1)}(\vec{P}) = (0, -\frac{1}{\sqrt{2}}, -\frac{i}{\sqrt{2}}, 0) \\ \varepsilon^\mu_{(-1)}(\vec{P}) = (0, \frac{1}{\sqrt{2}}, -\frac{i}{\sqrt{2}}, 0) \\ \varepsilon^\mu_{(0)}(\vec{P}) \quad = (0, 0, 0, 1) \end{cases} \tag{A1}$$

$\underline{\vec{P} = |\vec{P}|\vec{k}}$

$$\text{Spin or heliciy bases} \begin{cases} \varepsilon^{\mu}_{(+1)}(\vec{P}) = (0, -\frac{1}{\sqrt{2}}, -\frac{i}{\sqrt{2}}, 0) \\ \varepsilon^{\mu}_{(-1)}(\vec{P}) = (0, \frac{1}{\sqrt{2}}, -\frac{i}{\sqrt{2}}, 0) \\ \varepsilon^{\mu}_{(0)}(\vec{P}) \quad = (\frac{|\vec{P}|}{m}, 0, 0, \frac{E(\vec{P})}{m}) \end{cases} \tag{A2}$$

$\underline{\vec{P} = -|\vec{P}|\vec{k}}$

$$\text{Spin base} \begin{cases} \varepsilon^{\mu}_{(+1)}(\vec{P}) = (0, -\frac{1}{\sqrt{2}}, -\frac{i}{\sqrt{2}}, 0) \\ \varepsilon^{\mu}_{(-1)}(\vec{P}) = (0, \frac{1}{\sqrt{2}}, -\frac{i}{\sqrt{2}}, 0) \\ \varepsilon^{\mu}_{(0)}(\vec{P}) \quad = (-\frac{|\vec{P}|}{m}, 0, 0, \frac{E(\vec{P})}{m}) \end{cases} \qquad \text{Helicity base} \begin{cases} \varepsilon^{\mu}_{(+1)}(\vec{P}) = (0, \frac{1}{\sqrt{2}}, -\frac{i}{\sqrt{2}}, 0) \\ \varepsilon^{\mu}_{(-1)}(\vec{P}) = (0, -\frac{1}{\sqrt{2}}, -\frac{i}{\sqrt{2}}, 0) \\ \varepsilon^{\mu}_{(0)}(\vec{P}) \quad = (\frac{|\vec{P}|}{m}, 0, 0, -\frac{E(\vec{P})}{m}) \end{cases} \tag{A3}$$

APPENDIX B: EXPRESSION FOR THE $V^{\mu}(|\vec{q}|)$, $V^{\mu}_{(\lambda)}(|\vec{q}|)$, $V^{\mu}_{T(\lambda)}(|\vec{q}|)$ AND $A^{\mu}(|\vec{q}|)$, $A^{\mu}_{(\lambda)}(|\vec{q}|)$, $A^{\mu}_{T(\lambda)}(|\vec{q}|)$ MATRIX ELEMENTS

Here we give general expressions valid for transitions between a pseudoscalar meson M_I at rest with quark content $q_{f_1}\overline{q}_{f_2}$ and a final M_F meson with total angular momentum and parity $J^{\pi} = 0^-, 0^+, 1^-, 1^+, 2^-, 2^+$, three-momentum $-|\vec{q}|\vec{k}$ and quark content $q_{f_1'}\overline{q}_{f_2}$. In the transition it is the quark that changes flavor. The phases of the wave functions are the ones chosen in Eqs. (5,6,7). We generally have

$$\begin{aligned} \mathcal{V}^{\mu}(|\vec{q}|) - \mathcal{A}^{\mu}(|\vec{q}|) &= \sqrt{2m_I 2E_F(-\vec{q})}\; {}_{NR}\left\langle M_F(J^{\pi}),\, \lambda\, -|\vec{q}|\,\vec{k} \right| J^{f_1' f_1 \mu}(0) \left| M_I(0^-),\, \vec{0} \right\rangle_{NR} \\ &= \sqrt{2m_I 2E_F(-\vec{q})} \int d^3p \sum_{s_1'} \sum_{s_1, s_2} \left(\hat{\phi}^{(M_F(J^{\pi}),\lambda)}_{(s_1', f_1'),\,(s_2, f_2)}(\vec{p})\right)^* \hat{\phi}^{(M_I(0^-))}_{(s_1, f_1),\,(s_2, f_2)}(\vec{p} - \frac{m_{f_2}}{m_{f_1'} + m_{f_2}}\,|\vec{q}|\vec{k}) \\ &\quad \frac{1}{\sqrt{2E_{f_1'}\,2E_{f_1}}}\; \bar{u}_{s_1', f_1'}(-\frac{m_{f_1'}}{m_{f_1'} + m_{f_2}}|\vec{q}|\vec{k} - \vec{p})\, \gamma^{\mu}(I - \gamma_5)\, u_{s_1, f_1}(\frac{m_{f_2}}{m_{f_1'} + m_{f_2}}|\vec{q}|\vec{k} - \vec{p}) \end{aligned} \tag{B1}$$

where $\mathcal{V}^{\mu}(\mathcal{A}^{\mu})$ represent any of the $V^{\mu}\,(A^{\mu})$, $V^{\mu}_{(\lambda)}\,(A^{\mu}_{(\lambda)})$ or $V^{\mu}_{T(\lambda)}\,(A^{\mu}_{T(\lambda)})$, and where $E_{f_1'}$ and E_{f_1} are shorthand notations for $E_{f_1'}(-\frac{m_{f_1'}}{m_{f_1'}+m_{f_2}}|\vec{q}|\vec{k} - \vec{p})$ and $E_{f_1}(\frac{m_{f_2}}{m_{f_1'}+m_{f_2}}|\vec{q}|\vec{k} - \vec{p})$ respectively. Defining also $\widehat{E}_{f_1'} = E_{f_1'} + m_{f_1'}$ and $\widehat{E}_{f_1} = E_{f_1} + m_{f_1}$ we arrive at the following final expressions:

- Case $J^{\pi} = 0^-$

$$\begin{aligned} V^0(|\vec{q}|) &= \sqrt{2m_I 2E_F(-\vec{q})} \int d^3p\, \frac{1}{4\pi} \left(\hat{\phi}^{(M_F(0^-))}_{f_1',\,f_2}(|\vec{p}|)\right)^* \hat{\phi}^{(M_I(0^-))}_{f_1,\,f_2} \left(\left|\vec{p} - \frac{m_{f_2}}{m_{f_1'} + m_{f_2}}|\vec{q}|\vec{k}\right|\right) \\ &\quad \sqrt{\frac{\widehat{E}_{f_1'}\widehat{E}_{f1}}{4E_{f_1'}E_{f_1}}} \left(1 + \frac{(-\frac{m_{f_1'}}{m_{f_1'}+m_{f_2}}|\vec{q}|\vec{k} - \vec{p}) \cdot (\frac{m_{f_2}}{m_{f_1'}+m_{f_2}}|\vec{q}|\vec{k} - \vec{p})}{\widehat{E}_{f_1'}\widehat{E}_{f_1}}\right) \\ V^3(|\vec{q}|) &= \sqrt{2m_I 2E_F(-\vec{q})} \int d^3p\, \frac{1}{4\pi} \left(\hat{\phi}^{(M_F(0^-))}_{f_1',\,f_2}(|\vec{p}|)\right)^* \hat{\phi}^{(M_I(0^-))}_{f_1,\,f_2} \left(\left|\vec{p} - \frac{m_{f_2}}{m_{f_1'} + m_{f_2}}|\vec{q}|\vec{k}\right|\right) \\ &\quad \sqrt{\frac{\widehat{E}_{f_1'}\widehat{E}_{f1}}{4E_{f_1'}E_{f_1}}} \left(\frac{\frac{m_{f_2}}{m_{f_1'}+m_{f_2}}|\vec{q}| - p_z}{\widehat{E}_{f_1}} + \frac{-\frac{m_{f_1'}}{m_{f_1'}+m_{f_2}}|\vec{q}| - p_z}{\widehat{E}_{f_1'}}\right) \end{aligned} \tag{B2}$$

- Case $J^\pi = 0^+$

$$
\begin{aligned}
A^0(|\vec{q}|) \;=\; & \sqrt{2m_I 2E_F(-\vec{q})}\int d^3p\,\frac{1}{4\pi|\vec{p}|}\left(\hat{\phi}^{(M_F(0^+))}_{f_1',f_2}(|\vec{p}|)\right)^*\hat{\phi}^{(M_I(0^-))}_{f_1,f_2}\left(\left|\vec{p}-\frac{m_{f_2}}{m_{f_1'}+m_{f_2}}|\vec{q}|\vec{k}\right|\right)\\
& \sqrt{\frac{\widehat{E}_{f_1'}\widehat{E}_{f1}}{4E_{f_1'}E_{f_1}}}\left(\frac{\vec{p}\cdot(\frac{m_{f_2}}{m_{f_1'}+m_{f_2}}|\vec{q}|\vec{k}-\vec{p})}{\widehat{E}_{f_1}}+\frac{\vec{p}\cdot(-\frac{m_{f_1'}}{m_{f_1'}+m_{f_2}}|\vec{q}|\vec{k}-\vec{p})}{\widehat{E}_{f_1'}}\right)\\
A^3(|\vec{q}|) \;=\; & \sqrt{2m_I 2E_F(-\vec{q})}\int d^3p\,\frac{1}{4\pi|\vec{p}|}\left(\hat{\phi}^{(M_F(0^+))}_{f_1',f_2}(|\vec{p}|)\right)^*\hat{\phi}^{(M_I(0^-))}_{f_1,f_2}\left(\left|\vec{p}-\frac{m_{f_2}}{m_{f_1'}+m_{f_2}}|\vec{q}|\vec{k}\right|\right)\\
& \sqrt{\frac{\widehat{E}_{f_1'}\widehat{E}_{f1}}{4E_{f_1'}E_{f_1}}}\Bigg\{\,p_z\Bigg(1-\frac{(-\frac{m_{f_1'}}{m_{f_1'}+m_{f_2}}|\vec{q}|\vec{k}-\vec{p})\cdot(\frac{m_{f_2}}{m_{f_1'}+m_{f_2}}|\vec{q}|\vec{k}-\vec{p})}{\widehat{E}_{f_1'}\widehat{E}_{f_1}}\Bigg)\\
& +\frac{1}{\widehat{E}_{f_1'}\widehat{E}_{f1}}\Bigg[\quad(-\frac{m_{f_1'}}{m_{f_1'}+m_{f_2}}|\vec{q}|-p_z)\quad\vec{p}\cdot\Bigg(\quad\frac{m_{f_2}}{m_{f_1'}+m_{f_2}}|\vec{q}|\vec{k}-\vec{p}\Bigg)\\
& +(\quad\frac{m_{f_2}}{m_{f_1'}+m_{f_2}}|\vec{q}|-p_z)\quad\vec{p}\cdot\Bigg(-\frac{m_{f_1'}}{m_{f_1'}+m_{f_2}}|\vec{q}|\vec{k}-\vec{p}\Bigg)\Bigg]\Bigg\}
\end{aligned}
\tag{B3}
$$

- Case $J^\pi = 1^-$

$$
\begin{aligned}
V^{(1^-)\,1}_{\lambda=-1}(|\vec{q}|) \;=\; & \frac{-i}{\sqrt{2}}\sqrt{2m_I 2E_F(-\vec{q})}\int d^3p\,\frac{1}{4\pi}\left(\hat{\phi}^{(M_F(1^-))}_{f_1',f_2}(|\vec{p}|)\right)^*\hat{\phi}^{(M_I(0^-))}_{f_1,f_2}\left(\left|\vec{p}-\frac{m_{f_2}}{m_{f_1'}+m_{f_2}}|\vec{q}|\vec{k}\right|\right)\\
& \sqrt{\frac{\widehat{E}_{f_1'}\widehat{E}_{f1}}{4E_{f_1'}E_{f_1}}}\left(-\frac{\frac{m_{f_2}}{m_{f_1'}+m_{f_2}}|\vec{q}|-p_z}{\widehat{E}_{f_1}}+\frac{-\frac{m_{f_1'}}{m_{f_1'}+m_{f_2}}|\vec{q}|-p_z}{\widehat{E}_{f_1'}}\right)
\end{aligned}
\tag{B4}
$$

and similarly

$$
\begin{aligned}
A^{(1^-)\,0}_{\lambda=0}(|\vec{q}|) \;=\; & i\,\sqrt{2m_I 2E_F(-\vec{q})}\int d^3p\,\frac{1}{4\pi}\left(\hat{\phi}^{(M_F(1^-))}_{f_1',f_2}(|\vec{p}|)\right)^*\hat{\phi}^{(M_I(0^-))}_{f_1,f_2}\left(\left|\vec{p}-\frac{m_{f_2}}{m_{f_1'}+m_{f_2}}|\vec{q}|\vec{k}\right|\right)\\
& \sqrt{\frac{\widehat{E}_{f_1'}\widehat{E}_{f1}}{4E_{f_1'}E_{f_1}}}\left(\frac{\frac{m_{f_2}}{m_{f_1'}+m_{f_2}}|\vec{q}|-p_z}{\widehat{E}_{f_1}}+\frac{-\frac{m_{f_1'}}{m_{f_1'}+m_{f_2}}|\vec{q}|-p_z}{\widehat{E}_{f_1'}}\right)\\
A^{(1^-)\,1}_{\lambda=-1}(|\vec{q}|) \;=\; & \frac{i}{\sqrt{2}}\sqrt{2m_I 2E_F(-\vec{q})}\int d^3p\,\frac{1}{4\pi}\left(\hat{\phi}^{(M_F(1^-))}_{f_1',f_2}(|\vec{p}|)\right)^*\hat{\phi}^{(M_I(0^-))}_{f_1,f_2}\left(\left|\vec{p}-\frac{m_{f_2}}{m_{f_1'}+m_{f_2}}|\vec{q}|\vec{k}\right|\right)\\
& \sqrt{\frac{\widehat{E}_{f_1'}\widehat{E}_{f1}}{4E_{f_1'}E_{f_1}}}\left(1+\frac{2p_x^2-(-\frac{m_{f_1'}}{m_{f_1'}+m_{f_2}}|\vec{q}|\vec{k}-\vec{p})\cdot(\frac{m_{f_2}}{m_{f_1'}+m_{f_2}}|\vec{q}|\vec{k}-\vec{p})}{\widehat{E}_{f_1'}\widehat{E}_{f_1}}\right)\\
A^{(1^-)\,3}_{\lambda=0}(|\vec{q}|) \;=\; & i\sqrt{2m_I 2E_F(-\vec{q})}\int d^3p\,\frac{1}{4\pi}\left(\hat{\phi}^{(M_F(1^-))}_{f_1',f_2}(|\vec{p}|)\right)^*\hat{\phi}^{(M_I(0^-))}_{f_1,f_2}\left(\left|\vec{p}-\frac{m_{f_2}}{m_{f_1'}+m_{f_2}}|\vec{q}|\vec{k}\right|\right)\\
& \sqrt{\frac{\widehat{E}_{f_1'}\widehat{E}_{f1}}{4E_{f_1'}E_{f_1}}}\left(1+\frac{2(-\frac{m_{f_1'}}{m_{f_1'}+m_{f_2}}|\vec{q}|-p_z)\cdot(\frac{m_{f_2}}{m_{f_1'}+m_{f_2}}|\vec{q}|-p_z)}{\widehat{E}_{f_1'}\widehat{E}_{f_1}}\right.
\end{aligned}
$$

$$-\frac{(-\frac{m_{f_1'}}{m_{f_1'}+m_{f_2}}|\vec{q}|\vec{k}-\vec{p})\cdot(\frac{m_{f_2}}{m_{f_1'}+m_{f_2}}|\vec{q}|\vec{k}-\vec{p})}{\widehat{E}_{f_1'}\widehat{E}_{f_1}}\Bigg) \tag{B5}$$

- Case $J^\pi = 1^+$

$$\begin{aligned}
V_{\lambda=0}^{(1^+,S_{q\bar{q}}=0)\,0}(|\vec{q}|) &= i\sqrt{3}\sqrt{2m_I 2E_F(-\vec{q})}\int d^3p\,\frac{1}{4\pi|\vec{p}|}\left(\hat{\phi}^{(M_F(1^+,S_{q\bar{q}}=0))}_{f_1',f_2}(|\vec{p}|)\right)^*\hat{\phi}^{(M_I(0^-))}_{f_1,f_2}\left(\left|\vec{p}-\frac{m_{f_2}}{m_{f_1'}+m_{f_2}}|\vec{q}|\vec{k}\right|\right)\\
&\sqrt{\frac{\widehat{E}_{f_1'}\widehat{E}_{f1}}{4E_{f_1'}E_{f_1}}}\,p_z\left(1+\frac{(-\frac{m_{f_1'}}{m_{f_1'}+m_{f_2}}|\vec{q}|\vec{k}-\vec{p})\cdot(\frac{m_{f_2}}{m_{f_1'}+m_{f_2}}|\vec{q}|\vec{k}-\vec{p})}{\widehat{E}_{f_1'}\widehat{E}_{f_1}}\right)\\
V_{\lambda=0}^{(1^+,S_{q\bar{q}}=1)\,0}(|\vec{q}|) &= -i\sqrt{\frac{3}{2}}\sqrt{2m_I 2E_F(-\vec{q})}\int d^3p\,\frac{1}{4\pi|\vec{p}|}\left(\hat{\phi}^{(M_F(1^+,S_{q\bar{q}}=1))}_{f_1',f_2}(|\vec{p}|)\right)^*\hat{\phi}^{(M_I(0^-))}_{f_1,f_2}\left(\left|\vec{p}-\frac{m_{f_2}}{m_{f_1'}+m_{f_2}}|\vec{q}|\vec{k}\right|\right)\\
&\sqrt{\frac{\widehat{E}_{f_1'}\widehat{E}_{f1}}{4E_{f_1'}E_{f_1}}}\,\frac{|\vec{q}|(p_z^2-\vec{p}^{\,2})}{\widehat{E}_{f_1'}\widehat{E}_{f1}}\\
V_{\lambda=-1}^{(1^+,S_{q\bar{q}}=0)\,1}(|\vec{q}|) &= -i\sqrt{\frac{3}{2}}\sqrt{2m_I 2E_F(-\vec{q})}\int d^3p\,\frac{1}{4\pi|\vec{p}|}\left(\hat{\phi}^{(M_F(1^+,S_{q\bar{q}}=0))}_{f_1',f_2}(|\vec{p}|)\right)^*\hat{\phi}^{(M_I(0^-))}_{f_1,f_2}\left(\left|\vec{p}-\frac{m_{f_2}}{m_{f_1'}+m_{f_2}}|\vec{q}|\vec{k}\right|\right)\\
&\sqrt{\frac{\widehat{E}_{f_1'}\widehat{E}_{f1}}{4E_{f_1'}E_{f_1}}}\,p_x^2\left(\frac{1}{\widehat{E}_{f_1}}+\frac{1}{\widehat{E}_{f_1'}}\right)\\
V_{\lambda=-1}^{(1^+,S_{q\bar{q}}=1)\,1}(|\vec{q}|) &= i\frac{\sqrt{3}}{2}\sqrt{2m_I 2E_F(-\vec{q})}\int d^3p\,\frac{1}{4\pi|\vec{p}|}\left(\hat{\phi}^{(M_F(1^+,S_{q\bar{q}}=1))}_{f_1',f_2}(|\vec{p}|)\right)^*\hat{\phi}^{(M_I(0^-))}_{f_1,f_2}\left(\left|\vec{p}-\frac{m_{f_2}}{m_{f_1'}+m_{f_2}}|\vec{q}|\vec{k}\right|\right)\\
&\sqrt{\frac{\widehat{E}_{f_1'}\widehat{E}_{f1}}{4E_{f_1'}E_{f_1}}}\left(\frac{p_y^2+p_z^2+p_z|\vec{q}|\frac{m_{f_1'}}{m_{f_1'}+m_{f_2}}}{\widehat{E}_{f_1'}}-\frac{p_y^2+p_z^2-p_z|\vec{q}|\frac{m_{f_2}}{m_{f_1'}+m_{f_2}}}{\widehat{E}_{f_1}}\right)\\
V_{\lambda=0}^{(1^+,S_{q\bar{q}}=0)\,3}(|\vec{q}|) &= i\sqrt{3}\sqrt{2m_I 2E_F(-\vec{q})}\int d^3p\,\frac{1}{4\pi|\vec{p}|}\left(\hat{\phi}^{(M_F(1^+,S_{q\bar{q}}=0))}_{f_1',f_2}(|\vec{p}|)\right)^*\hat{\phi}^{(M_I(0^-))}_{f_1,f_2}\left(\left|\vec{p}-\frac{m_{f_2}}{m_{f_1'}+m_{f_2}}|\vec{q}|\vec{k}\right|\right)\\
&\sqrt{\frac{\widehat{E}_{f_1'}\widehat{E}_{f1}}{4E_{f_1'}E_{f_1}}}\,p_z\left(\frac{\frac{m_{f_2}}{m_{f_1'}+m_{f_2}}|\vec{q}|-p_z}{\widehat{E}_{f_1}}+\frac{-\frac{m_{f_1'}}{m_{f_1'}+m_{f_2}}|\vec{q}|-p_z}{\widehat{E}_{f_1'}}\right)\\
V_{\lambda=0}^{(1^+,S_{q\bar{q}}=1)\,3}(|\vec{q}|) &= -i\sqrt{\frac{3}{2}}\sqrt{2m_I 2E_F(-\vec{q})}\int d^3p\,\frac{1}{4\pi|\vec{p}|}\left(\hat{\phi}^{(M_F(1^+,S_{q\bar{q}}=1))}_{f_1',f_2}(|\vec{p}|)\right)^*\hat{\phi}^{(M_I(0^-))}_{f_1,f_2}\left(\left|\vec{p}-\frac{m_{f_2}}{m_{f_1'}+m_{f_2}}|\vec{q}|\vec{k}\right|\right)\\
&\sqrt{\frac{\widehat{E}_{f_1'}\widehat{E}_{f1}}{4E_{f_1'}E_{f_1}}}\,(p_x^2+p_y^2)\left(\frac{1}{\widehat{E}_{f_1}}-\frac{1}{\widehat{E}_{f_1'}}\right)
\end{aligned} \tag{B6}$$

and similarly

$$\begin{aligned}
A_{\lambda=-1}^{(1^+,S_{q\bar{q}}=0)\,1}(|\vec{q}|) &= -i\sqrt{\frac{3}{2}}\sqrt{2m_I 2E_F(-\vec{q})}\int d^3p\,\frac{1}{4\pi|\vec{p}|}\left(\hat{\phi}^{(M_F(1^+,S_{q\bar{q}}=0))}_{f_1',f_2}(|\vec{p}|)\right)^*\hat{\phi}^{(M_I(0^-))}_{f_1,f_2}\left(\left|\vec{p}-\frac{m_{f_2}}{m_{f_1'}+m_{f_2}}|\vec{q}|\vec{k}\right|\right)\\
&\sqrt{\frac{\widehat{E}_{f_1'}\widehat{E}_{f1}}{4E_{f_1'}E_{f_1}}}\,\frac{p_y^2|\vec{q}|}{\widehat{E}_{f_1}\widehat{E}_{f_1'}}
\end{aligned}$$

$$A^{(1^+,S_{q\bar{q}}=1)1}_{\lambda=-1}(|\vec{q}|) \;=\; i\frac{\sqrt{3}}{2}\sqrt{2m_I 2E_F(-\vec{q})}\;\int d^3p\;\frac{1}{4\pi|\vec{p}|}\left(\hat{\phi}^{(M_F(1^+,S_{q\bar{q}}=1))}_{f_1',f_2}(|\vec{p}|)\right)^*\hat{\phi}^{(M_I(0^-))}_{f_1,f_2}\left(\left|\vec{p}-\frac{m_{f_2}}{m_{f_1'}+m_{f_2}}|\vec{q}|\vec{k}\right|\right)$$
$$\sqrt{\frac{\widehat{E}_{f_1'}\widehat{E}_{f1}}{4E_{f_1'}E_{f_1}}}\left\{\;p_z\left(1-\frac{(-\frac{m_{f_1'}}{m_{f_1'}+m_{f_2}}|\vec{q}|\vec{k}-\vec{p})\cdot(\frac{m_{f_2}}{m_{f_1'}+m_{f_2}}|\vec{q}|\vec{k}-\vec{p})}{\widehat{E}_{f_1'}\widehat{E}_{f_1}}\right)\right.$$
$$\left.+\frac{m_{f_2}-m_{f_1'}}{m_{f_1'}+m_{f_2}}\frac{p_x^2|\vec{q}|}{\widehat{E}_{f_1'}\widehat{E}_{f1}}\right\} \tag{B7}$$

- Case $J^\pi = 2^-$

$$V^{(2^-)\,0}_{T\lambda=0}(|\vec{q}|) \;=\; i\sqrt{\frac{15}{2}}\sqrt{2m_I 2E_F(-\vec{q})}\;\int d^3p\;\frac{1}{4\pi|\vec{p}|^2}\left(\hat{\phi}^{(M_F(2^-))}_{f_1',f_2}(|\vec{p}|)\right)^*\hat{\phi}^{(M_I(0^-))}_{f_1,f_2}\left(\left|\vec{p}-\frac{m_{f_2}}{m_{f_1'}+m_{f_2}}|\vec{q}|\vec{k}\right|\right)$$
$$\sqrt{\frac{\widehat{E}_{f_1'}\widehat{E}_{f1}}{4E_{f_1'}E_{f_1}}}\;\frac{p_z\left(p_x^2+p_y^2\right)|\vec{q}|}{\widehat{E}_{f_1'}\widehat{E}_{f1}}$$
$$V^{(2^-)\,1}_{T\lambda=+1}(|\vec{q}|) \;=\; i\frac{\sqrt{5}}{2}\sqrt{2m_I 2E_F(-\vec{q})}\;\int d^3p\;\frac{1}{4\pi|\vec{p}|^2}\left(\hat{\phi}^{(M_F(2^-))}_{f_1',f_2}(|\vec{p}|)\right)^*\hat{\phi}^{(M_I(0^-))}_{f_1,f_2}\left(\left|\vec{p}-\frac{m_{f_2}}{m_{f_1'}+m_{f_2}}|\vec{q}|\vec{k}\right|\right)$$
$$\sqrt{\frac{\widehat{E}_{f_1'}\widehat{E}_{f1}}{4E_{f_1'}E_{f_1}}}\left\{\left(p_z^2-p_x^2\right)\left(\frac{-p_z-\frac{m_{f_1'}}{m_{f_1'}+m_{f_2}}|\vec{q}|}{\widehat{E}_{f_1'}}-\frac{-p_z+\frac{m_{f_2}}{m_{f_1'}+m_{f_2}}|\vec{q}|}{\widehat{E}_{f_1}}\right)\right.$$
$$\left.-p_z p_y^2\left(\frac{1}{\widehat{E}_{f_1'}}-\frac{1}{\widehat{E}_{f_1}}\right)\right\}$$
$$V^{(2^-)\,3}_{T\lambda=0}(|\vec{q}|) \;=\; i\sqrt{\frac{15}{2}}\sqrt{2m_I 2E_F(-\vec{q})}\;\int d^3p\;\frac{1}{4\pi|\vec{p}|^2}\left(\hat{\phi}^{(M_F(2^-))}_{f_1',f_2}(|\vec{p}|)\right)^*\hat{\phi}^{(M_I(0^-))}_{f_1,f_2}\left(\left|\vec{p}-\frac{m_{f_2}}{m_{f_1'}+m_{f_2}}|\vec{q}|\vec{k}\right|\right)$$
$$\sqrt{\frac{\widehat{E}_{f_1'}\widehat{E}_{f1}}{4E_{f_1'}E_{f_1}}}\;p_z\left(p_x^2+p_y^2\right)\left(\frac{1}{\widehat{E}_{f_1'}}-\frac{1}{\widehat{E}_{f_1}}\right) \tag{B8}$$

and similarly

$$A^{(2^-)\,1}_{\lambda=+1}(|\vec{q}|) \;=\; i\frac{\sqrt{5}}{2}\sqrt{2m_I 2E_F(-\vec{q})}\;\int d^3p\;\frac{1}{4\pi|\vec{p}|^2}\left(\hat{\phi}^{(M_F(2^-))}_{f_1',f_2}(|\vec{p}|)\right)^*\hat{\phi}^{(M_I(0^-))}_{f_1,f_2}\left(\left|\vec{p}-\frac{m_{f_2}}{m_{f_1'}+m_{f_2}}|\vec{q}|\vec{k}\right|\right)$$
$$\sqrt{\frac{\widehat{E}_{f_1'}\widehat{E}_{f1}}{4E_{f_1'}E_{f_1}}}\left\{\left(p_z^2-p_y^2\right)\left(1-\frac{(-\frac{m_{f_1'}}{m_{f_1'}+m_{f_2}}|\vec{q}|\vec{k}-\vec{p})\cdot(\frac{m_{f_2}}{m_{f_1'}+m_{f_2}}|\vec{q}|\vec{k}-\vec{p})}{\widehat{E}_{f_1'}\widehat{E}_{f1}}\right)\right.$$
$$\left.-p_z p_x^2|\vec{q}|\,\frac{m_{f_1'}-m_{f_2}}{m_{f_1'}+m_{f_2}}\,\frac{1}{\widehat{E}_{f_1'}\widehat{E}_{f_1}}\;\right\} \tag{B9}$$

- Case $J^\pi = 2^+$

$$V^{(2^+)\,1}_{T\lambda=+1}(|\vec{q}|) \;=\; i\frac{\sqrt{3}}{2}\sqrt{2m_I 2E_F(-\vec{q})}\;\int d^3p\;\frac{1}{4\pi|\vec{p}|}\left(\hat{\phi}^{(M_F(2^+))}_{f_1',f_2}(|\vec{p}|)\right)^*\hat{\phi}^{(M_I(0^-))}_{f_1,f_2}\left(\left|\vec{p}-\frac{m_{f_2}}{m_{f_1'}+m_{f_2}}|\vec{q}|\vec{k}\right|\right)$$

$$\sqrt{\frac{\widehat{E}_{f_1'}\widehat{E}_{f1}}{4E_{f_1'}E_{f_1}}}\left(\frac{p_y^2-p_z^2-p_z|\vec{q}|\frac{m_{f_1'}}{m_{f_1'}+m_{f_2}}}{\widehat{E}_{f_1'}}-\frac{p_y^2-p_z^2+p_z|\vec{q}|\frac{m_{f_2}}{m_{f_1'}+m_{f_2}}}{\widehat{E}_{f_1}}\right) \tag{B10}$$

and similarly

$$\begin{aligned}
A^{(2^+)\,0}_{T\lambda=0}(|\vec{q}|) &= \frac{-i}{\sqrt{2}}\sqrt{2m_I 2E_F(-\vec{q})}\int d^3p\,\frac{1}{4\pi|\vec{p}|}\left(\hat{\phi}^{(M_F(2^+))}_{f_1',\,f_2}(|\vec{p}|)\right)^*\,\hat{\phi}^{(M_I(0^-))}_{f_1,\,f_2}\left(\left|\vec{p}-\frac{m_{f_2}}{m_{f_1'}+m_{f_2}}|\vec{q}|\vec{k}\right|\right)\\
&\sqrt{\frac{\widehat{E}_{f_1'}\widehat{E}_{f1}}{4E_{f_1'}E_{f_1}}}\left(\frac{p_x^2+p_y^2-2p_z^2-2p_z|\vec{q}|\frac{m_{f_1'}}{m_{f_1'}+m_{f_2}}}{\widehat{E}_{f_1'}}+\frac{p_x^2+p_y^2-2p_z^2+2p_z|\vec{q}|\frac{m_{f_2}}{m_{f_1'}+m_{f_2}}}{\widehat{E}_{f_1}}\right)\\
A^{(2^+)\,1}_{T\lambda=+1}(|\vec{q}|) &= i\,\frac{\sqrt{3}}{2}\sqrt{2m_I 2E_F(-\vec{q})}\int d^3p\,\frac{1}{4\pi|\vec{p}|}\left(\hat{\phi}^{(M_F(2^+))}_{f_1',\,f_2}(|\vec{p}|)\right)^*\,\hat{\phi}^{(M_I(0^-))}_{f_1,\,f_2}\left(\left|\vec{p}-\frac{m_{f_2}}{m_{f_1'}+m_{f_2}}|\vec{q}|\vec{k}\right|\right)\\
&\sqrt{\frac{\widehat{E}_{f_1'}\widehat{E}_{f1}}{4E_{f_1'}E_{f_1}}}\Bigg\{\;p_z\left(1-\frac{(-\frac{m_{f_1'}}{m_{f_1'}+m_{f_2}}|\vec{q}|\vec{k}-\vec{p})\cdot(\frac{m_{f_2}}{m_{f_1'}+m_{f_2}}|\vec{q}|\vec{k}-\vec{p})}{\widehat{E}_{f_1'}\widehat{E}_{f1}}\right)\\
&+\frac{4p_zp_x^2-p_x^2|\vec{q}|\frac{m_{f_2}-m_{f_1'}}{m_{f_1'}+m_{f_2}}}{\widehat{E}_{f_1'}\widehat{E}_{f1}}\Bigg\}\\
A^{(2^+)\,3}_{T\lambda=0}(|\vec{q}|) &= -i\,\sqrt{2}\sqrt{2m_I 2E_F(-\vec{q})}\int d^3p\,\frac{1}{4\pi|\vec{p}|}\left(\hat{\phi}^{(M_F(2^+))}_{f_1',\,f_2}(|\vec{p}|)\right)^*\,\hat{\phi}^{(M_I(0^-))}_{f_1,\,f_2}\left(\left|\vec{p}-\frac{m_{f_2}}{m_{f_1'}+m_{f_2}}|\vec{q}|\vec{k}\right|\right)\\
&\sqrt{\frac{\widehat{E}_{f_1'}\widehat{E}_{f1}}{4E_{f_1'}E_{f_1}}}\Bigg\{\;p_z\left(1-\frac{(-\frac{m_{f_1'}}{m_{f_1'}+m_{f_2}}|\vec{q}|\vec{k}-\vec{p})\cdot(\frac{m_{f_2}}{m_{f_1'}+m_{f_2}}|\vec{q}|\vec{k}-\vec{p})}{\widehat{E}_{f_1'}\widehat{E}_{f1}}\right)\\
&+\frac{1}{\widehat{E}_{f_1'}\widehat{E}_{f1}}\Bigg[\;2p_z(-\frac{m_{f_1'}}{m_{f_1'}+m_{f_2}}|\vec{q}|-p_z)\cdot(\frac{m_{f_2}}{m_{f_1'}+m_{f_2}}|\vec{q}|-p_z)\\
&+\left(p_x^2+p_y^2\right)\left(-p_z+\frac{m_{f_2}-m_{f_1'}}{2(m_{f_1'}+m_{f_2})}|\vec{q}|\right)\Bigg]\;\Bigg\}
\end{aligned} \tag{B11}$$

APPENDIX C: TRANSITIONS INVOLVING ANTIQUARKS

When it is the antiquark that suffers the decay the expressions are modified as described below for a general transition between a pseudoscalar meson M_I at rest with quark content $q_{f_1}\overline{q}_{f_2}$ and a final M_F meson with total angular momentum and parity $J^\pi = 0^-, 0^+, 1^-, 1^+, 2^-, 2^+$, three-momentum $-|\vec{q}|\vec{k}$ and quark content $q_{f_1}\overline{q}_{f_2'}$. We have

$$\begin{aligned}
\mathcal{V}^\mu(|\vec{q}|)-\mathcal{A}^\mu(|\vec{q}|) &= \sqrt{2m_I 2E_F(-\vec{q})}\;{}_{NR}\left\langle M_F(J^\pi),\,\lambda\,-|\vec{q}|\,\vec{k}\right|J^{f_2\,f_2'\,\mu}(0)\left|M_I(0^-),\,\vec{0}\right\rangle_{NR}\\
&= -\sqrt{2m_I 2E_F(-\vec{q})}\int d^3p\sum_{s_2'}\sum_{s_1,s_2}\left(\hat{\phi}^{(M_F(J^\pi),\lambda)}_{(s_1,f_1),\,(s_2',f_2')}(\vec{p})\right)^*\,\hat{\phi}^{(M_I(0^-))}_{(s_1,f_1),\,(s_2,f_2)}(\vec{p}+\frac{m_{f_1}}{m_{f_1}+m_{f_2'}}|\vec{q}|\vec{k})\\
&\frac{(-1)^{s_2-s_2'}}{\sqrt{2E_{f_2'}\,2E_{f_2}}}\;\bar{v}_{s_2,f_2}(\frac{m_{f_1}}{m_{f_1}+m_{f_2'}}|\vec{q}|\vec{k}+\vec{p})\,\gamma^\mu(I-\gamma_5)\,v_{s_2',f_2'}(-\frac{m_{f_2'}}{m_{f_1}+m_{f_2'}}|\vec{q}|\vec{k}+\vec{p})
\end{aligned} \tag{C1}$$

where $\mathcal{V}^\mu(\mathcal{A}^\mu)$ represent any of the $V^\mu\,(A^\mu)$, $V^\mu_{(\lambda)}\,(A^\mu_{(\lambda)})$ or $V^\mu_{T(\lambda)}\,(A^\mu_{T(\lambda)})$, and $E_{f_2'}$, E_{f_2} are shorthand notation for $E_{f_2'}(-\frac{m_{f_2'}}{m_{f_1}+m_{f_2'}}|\vec{q}|\vec{k}+\vec{p})$, $E_{f_2}(\frac{m_{f_1}}{m_{f_1}+m_{f_2'}}|\vec{q}|\vec{k}+\vec{p})$. We can use now that

$$v_{s,f}(\vec{p}) = (-1)^{(1/2)-s}\,\mathcal{C}\,\bar{u}^T_{s,f}(\vec{p}) \quad ; \quad \bar{v}_{s,f}(\vec{p}) = -(-1)^{(1/2)-s}\,u^T_{s,f}(\vec{p})\,\mathcal{C}^\dagger \tag{C2}$$

where $\mathcal{C}$ is a matrix given in the Fermi–Dirac representation that we use by

$$\mathcal{C} = i\gamma^2\gamma^0 \tag{C3}$$

and that satisfies

$$\mathcal{C} = -\mathcal{C}^{-1} = -\mathcal{C}^\dagger = -\mathcal{C}^T \quad ; \quad \mathcal{C}\gamma^T_\mu\mathcal{C}^\dagger = -\gamma_\mu \tag{C4}$$

Using the above information and making the change of variable $\vec{p}\to-\vec{p}$ we can rewrite

$$\begin{aligned}\mathcal{V}^\mu(|\vec{q}|) - \mathcal{A}^\mu(|\vec{q}|) \;=\; \sqrt{2m_I 2E_F(-\vec{q})}\int d^3p \sum_{s_2'}\sum_{s_1,s_2}\left(\hat{\phi}^{(M_F(J^\pi),\,\lambda)}_{(s_1,f_1),\,(s_2',f_2')}(-\vec{p})\right)^*\;\hat{\phi}^{(M_I(0^-))}_{(s_1,f_1),\,(s_2,f_2)}\Bigg(-\left(\vec{p}-\frac{m_{f_1}}{m_{f_1}+m_{f_2'}}\,|\vec{q}|\vec{k}\right)\Bigg)\\ \frac{1}{\sqrt{2E_{f_2'}\,2E_{f_2}}}\;\bar{u}_{s_2',f_2'}(-\frac{m_{f_2'}}{m_{f_1}+m_{f_2'}}|\vec{q}|\vec{k}-\vec{p})\,\gamma^\mu(-I-\gamma_5)\,u_{s_2,f_2}(\frac{m_{f_1}}{m_{f_1}+m_{f_2'}}|\vec{q}|\vec{k}-\vec{p})\end{aligned} \tag{C5}$$

By comparison with the corresponding expressions involving quarks we find that, apart from the changes in the masses involved, there is an extra minus sign for the vector part, and, due to Clebsch–Gordan re-arrangements and the fact that $Y_{lm}(-\vec{p}) = (-1)^l\,Y_{lm}(\vec{p})$, a global sign given by $(-1)^{l_I+s_I-l_F-s_F}$ where l_I, $s_I\,(l_F,\,s_F)$ are the orbital and spin angular momenta of the initial (final) meson.

In any case this implies a change of sign in the relative phase between vector and axial contributions, which in its term produces a sign change in the tensor helicity components combination H_P due to the fact that $\mathcal{H}_{+1\,+1}$ goes into $\mathcal{H}_{-1\,-1}$ and vice versa. All other tensor helicity components combinations defined in Eq.(40) keep their signs.

A simple way of anticipating the above result is the following: the current for $\bar{q}_{f_2}$ decay into $\bar{q}_{f_2'}$ is

$$\overline{\Psi}_{f_2}(0)\gamma^\mu(I-\gamma_5)\Psi_{f_2'}(0) \tag{C6}$$

But for antiquarks the fields that play the similar role as the Ψ fields play for quarks are the charge conjugate ones $\Psi^{\mathcal{C}}$. In terms of the latter the above current is written as

$$\overline{\Psi}_{f_2}(0)\gamma^\mu(I-\gamma_5)\Psi_{f_2'}(0) = \overline{\Psi}^{\mathcal{C}}_{f_2'}(0)\gamma^\mu(-I-\gamma_5)\Psi^{\mathcal{C}}_{f_2}(0) \tag{C7}$$

Now this is similar to the current for quark decay but with an extra minus sign in the vector part. Whatever other changes might come from reorderings in the wave functions we will have an extra relative sign between the vector and axial part.

APPENDIX D: EXPRESIONS FOR THE HELICITY COMPONENTS OF THE HADRON TENSOR

In this appendix we give the expressions for the non–zero helicity components $\mathcal{H}_{rs}$ of the hadron tensor, as defined in Eq.(36), corresponding to a $B_c^-\to c\bar{c}$ transition. The different cases correspond to the ones discussed in the main text.

- Case $0^-\to 0^-, 0^+$

$$\begin{aligned}\mathcal{H}_{t\,t}(P_{B_c},P_{c\bar{c}}) \;&=\; \left(\frac{m^2_{B_c}-m^2_{c\bar{c}}}{\sqrt{q^2}}\,F_+(q^2)+\sqrt{q^2}\,F_-(q^2)\right)^2\\ \mathcal{H}_{t\,0}(P_{B_c},P_{c\bar{c}}) \;&=\; \mathcal{H}_{0\,t}(P_{B_c},P_{c\bar{c}}) = \lambda^{1/2}(q^2,m^2_{B_c},m^2_{c\bar{c}})\left(\frac{m^2_{B_c}-m^2_{c\bar{c}}}{q^2}\,F^2_+(q^2)+F_+(q^2)F_-(q^2)\right)\\ \mathcal{H}_{0\,0}(P_{B_c},P_{c\bar{c}}) \;&=\; \frac{\lambda(q^2,m^2_{B_c},m^2_{c\bar{c}})}{q^2}\,F^2_+(q^2)\end{aligned} \tag{D1}$$

- Case $0^- \to 1^-, 1^+$.

$$
\begin{aligned}
\mathcal{H}_{t\,t}(P_{B_c}, P_{c\bar{c}}) &= \frac{\lambda(q^2, m_{B_c}^2, m_{c\bar{c}}^2)}{4 m_{c\bar{c}}^2 q^2} \left((m_{B_c} - m_{c\bar{c}}) \left(A_0(q^2) - A_+(q^2) \right) - \frac{q^2}{m_{B_c} + m_{c\bar{c}}} A_-(q^2) \right)^2 \\
\mathcal{H}_{t\,0}(P_{B_c}, P_{c\bar{c}}) &= \mathcal{H}_{0\,t}(P_{B_c}, P_{c\bar{c}}) \\
&= \frac{\lambda^{1/2}(q^2, m_{B_c}^2, m_{c\bar{c}}^2)}{2 m_{c\bar{c}} \sqrt{q^2}} \left[(m_{B_c} - m_{c\bar{c}}) \left(A_0(q^2) - A_+(q^2) \right) - \frac{q^2}{m_{B_c} + m_{c\bar{c}}} A_-(q^2) \right] \\
&\quad \times \left[(m_{B_c} - m_{c\bar{c}}) \frac{m_{B_c}^2 - q^2 - m_{c\bar{c}}^2}{2 m_{c\bar{c}} \sqrt{q^2}} A_0(q^2) - \frac{\lambda(q^2, m_{B_c}^2, m_{c\bar{c}}^2)}{2 m_{c\bar{c}} \sqrt{q^2}} \frac{A_+(q^2)}{m_{B_c} + m_{c\bar{c}}} \right] \\
\mathcal{H}_{+1\,+1}(P_{B_c}, P_{c\bar{c}}) &= \left(\frac{\lambda^{1/2}(q^2, m_{B_c}^2, m_{c\bar{c}}^2)}{m_{B_c} + m_{c\bar{c}}} V(q^2) + (m_{B_c} - m_{c\bar{c}}) A_0(q^2) \right)^2 \\
\mathcal{H}_{-1\,-1}(P_{B_c}, P_{c\bar{c}}) &= \left(-\frac{\lambda^{1/2}(q^2, m_{B_c}^2, m_{c\bar{c}}^2)}{m_{B_c} + m_{c\bar{c}}} V(q^2) + (m_{B_c} - m_{c\bar{c}}) A_0(q^2) \right)^2 \\
\mathcal{H}_{0\,0}(P_{B_c}, P_{c\bar{c}}) &= \left((m_{B_c} - m_{c\bar{c}}) \frac{m_{B_c}^2 - q^2 - m_{c\bar{c}}^2}{2 m_{c\bar{c}} \sqrt{q^2}} A_0(q^2) - \frac{\lambda(q^2, m_{B_c}^2, m_{c\bar{c}}^2)}{2 m_{c\bar{c}} \sqrt{q^2}} \frac{A_+(q^2)}{m_{B_c} + m_{c\bar{c}}} \right)^2
\end{aligned}
\tag{D2}
$$

For a $B_c^- \to B$ transition (with B representing any of the $B = \overline{B}^0$, $\overline{B}^{*0}$, B^-, B^{*-}), where it is the $\bar{c}$ antiquark that decays, we have to change the mass of the final meson in the expressions above and take into account the changes in the form factors that derive from the discussions in appendix C.

- Case $0^- \to 2^-, 2^+$.

$$
\begin{aligned}
\mathcal{H}_{t\,t}(P_{B_c}, P_{c\bar{c}}) &= \frac{\lambda^2(q^2, m_{B_c}^2, m_{c\bar{c}}^2)}{24\, m_{c\bar{c}}^4\, q^2} \left(T_1(q^2) + (m_{B_c}^2 - m_{c\bar{c}}^2)\, T_2(q^2) + q^2\, T_3(q^2) \right)^2 \\
\mathcal{H}_{t\,0}(P_{B_c}, P_{c\bar{c}}) &= \mathcal{H}_{0\,t}(P_{B_c}, P_{c\bar{c}}) \\
&= \frac{\lambda^{3/2}(q^2, m_{B_c}^2, m_{c\bar{c}}^2)}{24\, m_{c\bar{c}}^4\, q^2} \left(T_1(q^2) + (m_{B_c}^2 - m_{c\bar{c}}^2)\, T_2(q^2) + q^2\, T_3(q^2) \right) \\
&\qquad \times \left((m_{B_c}^2 - q^2 - m_{c\bar{c}}^2)\, T_1(q^2) + \lambda(q^2, m_{B_c}^2, m_{c\bar{c}}^2)\, T_2(q^2) \right) \\
\mathcal{H}_{+1\,+1}(P_{B_c}, P_{c\bar{c}}) &= \frac{\lambda(q^2, m_{B_c}^2, m_{c\bar{c}}^2)}{8\, m_{c\bar{c}}^2} \left(T_1(q^2) - \lambda^{1/2}(q^2, m_{B_c}^2, m_{c\bar{c}}^2)\, T_4(q^2) \right)^2 \\
\mathcal{H}_{-1\,-1}(P_{B_c}, P_{c\bar{c}}) &= \frac{\lambda(q^2, m_{B_c}^2, m_{c\bar{c}}^2)}{8\, m_{c\bar{c}}^2} \left(T_1(q^2) + \lambda^{1/2}(q^2, m_{B_c}^2, m_{c\bar{c}}^2)\, T_4(q^2) \right)^2 \\
\mathcal{H}_{0\,0}(P_{B_c}, P_{c\bar{c}}) &= \frac{\lambda(q^2, m_{B_c}^2, m_{c\bar{c}}^2)}{24\, m_{c\bar{c}}^4\, q^2} \left((m_{B_c}^2 - q^2 - m_{c\bar{c}}^2)\, T_1(q^2) + \lambda(q^2, m_{B_c}^2, m_{c\bar{c}}^2)\, T_2(q^2) \right)^2
\end{aligned}
\tag{D3}
$$

[1] F. Abe *et al.* (CDF Collaboration), Phys. Rev. D 58 (1998) 112004; Phys. Rev. Lett. 81 (1998) 2432.
[2] E. Jenkins, M. Luke, A.V. Manohar, and M.J. Savage, Nucl. Phys. B390 (1993) 463.
[3] C. Albertus, J.M. Flynn, E. Hernández, J. Nieves, and J.M. Verde-Velasco, Phys. Rev. D 72 (2005) 033002.
[4] M.A. Ivanov, J.G. Körner, and P. Santorelli, Phys. Rev. D 73 (2006) 054024.
[5] M.A. Ivanov, J.G. Körner, and P. Santorelli, Phys. Rev. D 71, (2005) 094006. Erratum to be published (J.G. Körner private communication).
[6] M.A. Ivanov, J.G. Körner, and P. Santorelli, Phys. Rev. D 63 (2001) 074010.
[7] D. Ebert, R.N. Faustov, and V.O. Galkin, Phys. Rev. D 68 (2003) 094020.
[8] D. Ebert, R.N. Faustov, and V.O. Galkin, Eur. Phys. J. C 32 (2003) 29.
[9] C.H. Chang, and Y.Q. Chen, Phys. Rev. D 49 (1994) 3399.
[10] C.H. Chang, Y.Q. Chen, G.L. Wang, and H.S. Zong, Phys. Rev. D 65 (2002) 014017.

[11] C.H. Chang, Y.Q. Chen, G.L. Wang, and H.S. Zong, Commun. Theor. Phys. 35 (2001) 395.
[12] A. Abd El-Hady, J.H. Munoz, and J.P. Vary, Phys. Rev. D 62 (2000) 014019.
[13] J.-F. Liu, and K.-T. Chao, Phys. Rev. D 56 (1997) 4133.
[14] V.V. Kiselev, A.K. Likhoded, and A.I. Onishchenko, Nucl. Phys. B 569 (2000) 473.
[15] V.V. Kiselev, A.E. Kovalsky, and A.K. Likhoded, Nucl. Phys. B 585 (2000) 353.
[16] V.V. Kiselev, hep-ph/0211021.
[17] V.V. Kiselev, O.N. Pakhomova, and V.A. Saleev, J. Phys. G 28 (2002) 595.
[18] P. Colangelo, and F. De Fazio, Phys. Rev. D 61 (2000) 034012.
[19] A.Y. Anisimov, P.Y. Kulikov, I.M. Narodetsky, and K. A. Ter-Martirosian, Yad. Fiz. 62 (1999) 1868 [Phys. Atom. Nucl. 62 (1999) 1739].
[20] M.A. Nobes and R.M. Woloshyn, J. Phys. G 26 (2000) 1079.
[21] N. Isgur, D. Scora, B. Grinstein, and M.B. Wise, Phys. Rev. D 39 (1989) 799; D. Scora and N. Isgur, Phys. Rev. D 52 (1995) 2783.
[22] M. A. Sanchis-Lozano, Nucl. Phys. B 440 (1995) 251.
[23] G. Lopez Castro, H.B. Mayorga, and J.H. Muñoz, J. Phys. G 28 (2002) 2241.
[24] G. Lu, Y. Yang, and H. Li, Phys. Lett. B 341 (1995) 391.
[25] S. Eidelman *et al.* (Particle Data Group), Phys. Lett. B 592 (2004) 1.
[26] A. Abulencia *et al.* (CDF Collaboration), Phys. Rev. Lett. 96 (2006) 082002.
[27] A. Abulencia *et al.* (CDF Collaboration), Phys. Rev. Lett. 97 (2006) 012002.
[28] C. Albertus, E. Hernández, J. Nieves, and J.M. Verde-Velasco, Phys. Rev. D 71 (2005) 113006.
[29] D.S. Hwang and G.H. Kim, Z. Phys. C 76 (1997) 107.
[30] C. Caso *et al.* (Particle Data Group), Eur. Phys. J. C 3 (1998) 1.
[31] M. Artuso *et al.* (CLEO Collaboration), Phys. Rev. Lett. 95 (2005) 251801.
[32] D. Becirevic, Ph. Boucaud, J. P. Leroy, V. Lubicz, G. Martinelli, F. Mescia, and F. Rapuano, Phys. Rev. D 60 (1999) 074501.
[33] W.-M. Yao *et al.*(Particle Data Group), J. Phys. G 33 (2006) 1
[34] R. K. Bhaduri, L. E. Cohler, and Y. Nogami, Nuovo Cimento A 65 (1981) 376.
[35] B. Silvestre-Brac, Few-Body Systems 20 (1996) 1.
[36] B. Silvestre-Brac, and C. Semay, Internal Report ISN 93.6999, Grenoble, 1993.
[37] C. Albertus, J. E. Amaro,E. Hernández, and J. Nieves, Nucl. Phys. A 740 (2004) 333.
[38] C. Albertus, E. Hernández, and J. Nieves, Phys. Rev. D 71 (2005) 014012.
[39] C. Albertus, E. Hernández, J. Nieves, and J.M. Verde-Velasco, Phys. Rev. D 72 (2005) 094022.
[40] J.M. Verde-Velasco, talk given at "IVth International Conference on Quarks and Nuclear Physics (QNP06)", Madrid june 2006, to appear in the Conference Proceedings; C. Albertus, E. Hernández, J. Nieves, and J.M. Verde-Velasco, work in preparation.
[41] J.G. Körner and G.A. Schuler, Z. Phys. C 46 (1990) 93.
[42] E. Jenkins and A.V. Manohar private communication.
[43] M. Neubert, Phys. Rev. D 46 (1992) 2212.